

**Synthesis, Structure, and Reaction Pathways of C–N
containing Lanthanide Compounds**

**Synthesen, Strukturen und Reaktionswege von C–N-
haltigen Lanthanoid-Verbindungen**

DISSERTATION

der Fakultät für Chemie und Pharmazie
der Eberhard-Karls-Universität Tübingen
zur Erlangung des Grades eines Doktors
der Naturwissenschaften

2004

vorgelegt von

Radhakrishnan Srinivasan

Tag der mündlichen Prüfung:

17. Dezember 2004

Dekan:

Prof. Dr. S. Laufer

1. Berichterstatter:

Prof. Dr. H.-J. Meyer

2. Berichterstatter:

Prof. Dr. E. Schweda

Die vorliegende Arbeit wurde von Juni 2001 bis Dezember 2004 am Institut für Anorganische Chemie der Eberhard-Karls-Universität Tübingen unter der Leitung von Prof. Dr. H.-J. Meyer angefertigt.

Acknowledgements

My sincere thanks and gratitude are due to Prof Dr. Hans-Juergen Meyer for his constant guidance, motivation, suggestions, and fruitful discussions throughout this work.

I would like to express my special thanks to Dr. Jochen Glaser, Dr. Markus Ströbele, and Sonja Tragl for their help and discussions in structure solution and refinements by powder and single crystal diffraction studies.

I thank Heinz-Jürgen Kolb for the X-ray and DTA/TG measurements.

I thank Dr. Jochen Glaser and Dr. Björn Blaschkowski for their help in Squid measurements and discussions.

I thank Peter Ziegler and Marco Häberlen for their help in translating reports from English to Deutsch.

I thank all my other colleagues Katharina Gibson, Dr. Haipeng Ing, Michael Neukirch, Martina Weisser, Simone Dill, and Ruth Schmitt for the good and motivating work atmosphere.

I am thankful to DFG and Landesgraduiertenförderung of Baden-Württemberg for the scholarship provided during this work.

I also thank my parents, brother and sister and relatives for their moral support during this work.

Dedicated to my parents

Table of Contents

1. Introduction	5
2. Introduction to carbodiimides and cyanamides	7
2. 1. Different synthetic methods of carbodiimides/cyanamides.....	10
2. 2. Solid state metathesis reaction (SSM).....	12
3. Experimental techniques	14
3. 1. Physical Measurements and software packages used	14
3. 1. 1. Phase analysis.....	14
3. 1. 2. Crystal structure determination.....	14
3. 1. 3. Structure solution and refinement from powder patterns.....	14
3. 1. 4. Infrared spectra.....	15
3. 1. 5. Thermal analysis.....	15
3. 1. 6. Magnetic susceptibility studies.....	15
3. 1. 7. Graphics.....	15
3. 2. List of chemicals used	16
3. 3. Synthesis of starting materials	17
3. 3. 1. Preparation of $L_2(CN_2)$ and $Ca(CN_2)$	17
3. 3. 2. Decomposition of $L_2(CN_2)$	17
3. 3. 3. Reactivity of $L_2(CN_2)$	20
3. 3. 4. Preparation of LaX_3 with $X = Cl, Br, \text{ and } I$	20
3. 3. 5. Preparation of $LaOCl$	23

3. 4. Manipulations of C–N containing lanthanide compounds	23
4. Results and discussion.....	25
4. 1. Solid state metathesis reaction between LaCl_3 and Li_3N	25
4. 2. Synthesis and structural characterisation of $\text{LnCl}(\text{CN}_2)$ with $\text{Ln} = \text{La, Ce, and Pr}$	26
4. 2. 1. Reaction between LaCl_3 and $\text{Li}_2(\text{CN}_2)$	26
4. 2. 2. Thermal analysis (DTA/TG) of the reaction between LaCl_3 and $\text{Li}_2(\text{CN}_2)$	27
4. 2. 3. Infrared spectra of $\text{LaCl}(\text{CN}_2)$ and $\text{La}_2\text{Cl}(\text{CN}_2)\text{N}$	30
4. 2. 4. Crystal Structure of $\text{LaCl}(\text{CN}_2)$ from X-ray powder diffraction.....	31
4. 2. 5. Crystal structure of $\text{LaCl}(\text{CN}_2)$ from single crystal.....	32
4. 2. 6. Isotypic compounds in this structure type.....	34
4. 3. Synthesis, structure and characterisation of $\text{Ln}_2\text{X}(\text{CN}_2)\text{N}$ with $\text{La} = \text{La, Ce, Pr, Nd, and Gd, X} = \text{Cl, Br, and I}$	39
4. 3. 1. Reaction between LnCl_3 , $\text{Li}_2(\text{CN}_2)$ and Li_3N	39
4. 3. 2. Reaction between LnBr_3 , $\text{Li}_2(\text{CN}_2)$ and Li_3N	39
4. 3. 3. Reaction between LaI_3 , $\text{Li}_2(\text{CN}_2)$ and Li_3N	40
4. 3. 4. Thermal analysis (DTA/TG) of the reaction between LaX_3 with $\text{X} = \text{Cl and Br, Li}_2(\text{CN}_2)$ and Li_3N	41
4. 3. 5. Infrared spectra of $\text{La}_2\text{Cl}(\text{CN}_2)\text{N}$	44
4. 3. 6. Crystal structures of $\text{La}_2\text{X}(\text{CN}_2)\text{N}$ with $\text{X} = \text{Cl, Br, and I}$	44
4. 3. 7. Crystal structure of $\text{Ce}_2\text{Cl}(\text{CN}_2)\text{N}$	53
4. 3. 8. Magnetic properties of $\text{Ce}_2\text{Cl}(\text{CN}_2)\text{N}$	54

4. 3. 9. Isotypic compounds in this structure type.....	54
4. 4. Reaction between LaCl_3, $\text{Li}_2(\text{CN}_2)$ and $\text{C}_3\text{N}_3\text{Cl}_3$.....	56
4. 5. Reaction between LaCl_3 and structure directing agents.....	58
4. 5. 1. Reaction between $\text{La}(\text{NO}_3)_3 \cdot 6\text{H}_2\text{O}$ and $\text{K}[\text{C}(\text{CN})_3]$	59
4. 5. 2. Synthesis of $\text{KLa}[\text{C}(\text{CN})_3]_4 \cdot \text{H}_2\text{O}$	59
4. 5. 3. Crystal structure of $\text{KLa}[\text{C}(\text{CN})_3]_4 \cdot \text{H}_2\text{O}$	60
4. 6. Reaction between LaCl_3 and MCN with $\text{M} = \text{Na}, \text{K}$.....	67
4. 7. Reaction between LaCl_3 and $\text{Li}_2(\text{CN}_2)$ in the presence of metal.....	67
4. 7. 1. Reaction between LaCl_3 , $\text{Li}_2(\text{CN}_2)$ and Li	67
4. 7. 2. Reaction between LaCl_3 , $\text{Li}_2(\text{CN}_2)$ and Ca	68
4. 8. Synthesis and structure of $\text{Pr}_3\text{O}_4\text{Br}$.....	68
4. 8. 1. Synthesis of $\text{Pr}_3\text{O}_4\text{Br}$	68
4. 8. 2. Crystal structure of $\text{Pr}_3\text{O}_4\text{Br}$	68
4. 8. 3. Isotypic compounds in this structure type.....	71
4. 9. Synthesis and structure of $\text{La}_2\text{O}(\text{CN}_2)_2$.....	71
4. 9. 1. Synthesis and structure of known $\text{Ln}_2\text{O}_2(\text{CN}_2)$ $\text{Ln} = \text{La}, \text{Ce}, \text{Pr}, \text{Nd}, \text{Sm}, \text{Eu}, \text{and Gd}$	71
4. 9. 2. Reaction between LaCl_3 , LaOCl and $\text{Li}_2(\text{CN}_2)$	73
4. 9. 3. Crystal structure of $\text{La}_2\text{O}(\text{CN}_2)_2$	74
4. 9. 4. Reaction between LaOCl and $\text{Li}_2(\text{CN}_2)$	80
4. 9. 5. Reaction between CeOCl and $\text{Li}_2(\text{CN}_2)$	80
5. Summary and outlook.....	82

5. 1. Summary	82
5. 2. Outlook	84
6. Appendix	85
7. List of publications	97
8. Literature	98

1. Introduction

The research on lanthanum cyanamides dates back to 1948, when Hartmann et. al. [1] explained the formation of $\text{La}_2(\text{CN}_2)_3$ from a reaction of lanthanum oxide and HCN gas. Later Pavlov et. al. [2] in 1973 described the formation of $\text{La}_2(\text{CN}_2)_3$ by treating lanthanum oxide with urea. However, the presence of cyanamide from these works were characterised only from elemental analyses and the structural details are still not known for lanthanide cyanamide/carbodiimide. Calcium cyanamide [3] is historically famous for its industrial applications and an environment friendly multi-purpose fertilizer to supply nitrogen as well as lime to plants and soil. Later many cyanamide containing compounds with alkali [4], alkaline earth [5], transition metal [6], and main group metals [7] were known from the literature. Zinc cyanamide was found to be useful in non-polluting anticorrosive white pigment [6].

In the system Ln/B/C/N (Ln = lanthanide), boride carbides and nitridoborates of lanthanides were studied extensively of which some compounds are known to have interesting structural features and properties. For lanthanide boride carbides, crystal structures with different anions such as $(\text{BC})^n$, $(\text{BC}_2)^{5-}$, $(\text{BC}_2)^{7-}$, $(\text{B}_2\text{C}_2)^{3-}$, $(\text{B}_2\text{C})^n$ [8] and different anions composed from the combination of these anions with the covalent B-C chains have been reported. $\text{LnN}_{1/2}(\text{B}_2\text{C})$ (Ln = lanthanide) is a well studied system for its coexistence of magnetic properties and superconductivity [9]. $\text{LnN}_{1/2}(\text{B}_2\text{C})$ (Ln = Sc, Y, Lu) compounds containing $(\text{B}_2\text{C})^n$ anions are found to exhibit superconductivity with $T_c = 15\text{-}16\text{ K}$ [10]. $\text{La}_9\text{Br}_5(\text{BC}_2)_3$, containing $(\text{BC}_2)^{7-}$ unit is superconducting with $T_c = 6\text{ K}$ [11]. Lanthanide nitridoborates contain molecular anions such as $(\text{BN})^n$, $(\text{BN}_2)^{3-}$, $(\text{BN}_3)^{6-}$, $(\text{B}_2\text{N}_4)^{8-}$, $(\text{B}_3\text{N}_6)^{9-}$ [12]. In structures, these anions may occur in combinations with each other and with nitride ions. In the crystal structures of lanthanide nitridoborates, these anions are arranged in layers surrounded by the metal atoms in a characteristic fashion. Terminal N atoms are capped by the metal atoms forming a square-pyramid, and B atoms prefer a trigonal-prismatic environment of the metal atoms. $\text{La}_3\text{Ni}_2\text{B}_2\text{N}_3$ exhibit superconductivity at $T_c = 14\text{ K}$. It contains BN units capping the square planar Ni layers with isolated N atoms reside in the La_6 octahedra [13].

In the metal-C-N system, there are different forms such as cyanide, cyanamide or carbodiimide, dicyanamide, tricyanomethanide, tricyanoguanidine, tricyanomelamine known in the literature as CN^- [14], $(\text{CN}_2)^{2-}$ [4], $[\text{C}(\text{CN})_3]^-$ [15] $[\text{N}(\text{CN})_2]^-$ [16], $[\text{C}(\text{NCN})_3]^{2-}$ [17], and $[\text{N}(\text{CN})_2]_3^{3-}$ [18] respectively for alkali metal compounds. The special feature of these anions is that one form can be formed or transformed in to another anionic form. For

example, $\text{Na}(\text{C}_2\text{N}_3)$ can be obtained from $\text{Na}_2(\text{CN}_2)$ and trimerised to $\text{Na}_3(\text{C}_6\text{N}_9)$ [18]. These anions are considered as highly stable because of the alternating carbon-nitrogen connectivity and hence compounds having this anion are supposed to be a good precursor for the synthesis of hard materials. Dicyanamides and tricyanomethanide compounds of the divalent transition metals are isostructural. The rutile related network structures of dicyanamides of Co, Ni, and Cu were shown to behave as ferromagnets [19]. A strong nonlinear optical effect by second harmonic generation was observed for the compound $\text{Na}_2(\text{C}_4\text{N}_6)\cdot\text{H}_2\text{O}$ [17].

The cyanamide or carbodiimide compounds of lanthanides are relatively unexplored and hence an investigation is required. A summary of compounds in the metal/B/N and metal/B/C system were presented as attachment in the dissertation of Olaf Reckeweg [20] and the structural principles with different properties of lanthanide nitridoborates were presented in the dissertation of Björn Blaschkowski [21]. In this work, newly synthesised and structurally characterised C–N containing lanthanide compounds along with different metal–C–N compounds known from the literature are presented. Reactivity in the system $\text{LaC}_3/\text{Li}_2(\text{CN}_2)$ is also studied and discussed. The list of compounds known from the literature along with their space group, unit cell, special features of the structure in the metal/C/N system are tabulated in the appendix.

2. Introduction to carbodiimides and cyanamides

The designation of compounds as cyanamide and carbodiimide has often been misinterpreted in the literature. The main difference is with the C–N bond distances and different nitrogen positions of $(\text{CN}_2)^{2-}$ units in the crystal structure of their respective compounds. The carbodiimide containing compounds have only one distinguishable C=N bond with their C–N bond distances around 1.2 Å and N–C–N bond angle of 180°. In cyanamide molecule ($\text{H}_2\text{N}-\text{C}\equiv\text{N}$), the bond distances of C≡N and C–N are 1.15 and 1.31 Å respectively with the N–C–N bond angle of 178.1(1)° [22]. Some of the known cyanamide/carbodiimide compounds from the literature with their bond distances and bond angle are listed in Table 1. The name cyanamide is historically followed in the literature for some compounds. For example, $\text{Li}_2(\text{CN}_2)$ and $\text{Ca}(\text{CN}_2)$ are to be assigned as carbodiimides according to the symmetry of CN_2^{2-} units instead of cyanamides.

Cyanamide and its salts are well known compounds with a versatile field of applications. Due to the electronic structure and high chemical reactivity, N-substituted carbodiimides play an important role as precursors of new advanced ceramic materials, of synthesis in organic chemistry and in studies of biological membranes [23]. Carbodiimides are used in the formation of heterocycles via cycloaddition reactions, they have broad utility in biochemical process, and they are important in polymer chemistry [24]. Most important reactions of carbodiimides all involve nucleophilic attack across one of the imine bonds and the nucleophilic addition of water to dicyclohexylcarbodiimide is widely used for dehydration [25]. According to Pump and Rochow, polymeric silylcarbodiimide was formed in an exothermic reaction between silver cyanamide and dichloro silane [26]. The polysilyl- and polytitanyl- carbodiimides are presently investigated as single source precursors for the synthesis of novel carbide/nitride-based ceramics [27].

With respect to the complexing ability of molecular cyanamide, H_2NCN can be expected to show similar coordination properties such as ammonia. $\text{Cu}(\text{NCNH}_2)_4\text{Cl}_2$, $\text{Ni}(\text{NCNH}_2)_4\text{Cl}_2$ and $\text{Co}(\text{NCNH}_2)_4\text{Cl}_2$ are the complexes known with cyanamide as a neutral ligand [28].

Over the last decade, synthetic and crystallographic as well as theoretical studies in solid state cyanamide and carbodiimide chemistry have progressed enormously. The relatively simple crystal chemistry of the cyanamides involving alkaline and alkaline-earth metal cations are easily understood in terms of electrostatic interactions, whereas the effects of covalent

bonding in the main-group and transition-metal representatives show greater structural varieties.

Table 1. Bond distances and bond angle in some of the known cyanamide/carbodiimide compounds.

Compound	Bond distances C-N in Å	Bond angle NCN in °	(CN ₂) ²⁻ moiety	Reference
Li ₂ (CN ₂)	1.230	180	carbodiimide	[4]
Na ₂ (CN ₂)	1.236	180	carbodiimide	[4]
Mg(CN ₂)	1.248	180	carbodiimide	[5]
Ca(CN ₂)	1.22	180	carbodiimide	[3]
Ca ₄ (CN ₂)N ₂	1.219, 1.241	179.7	carbodiimide	[29]
Ca ₁₁ (CN ₂) ₂ N ₆	1.216, 1.236	180	carbodiimide	[29]
Si(CN ₂) ₂	1.10	180	carbodiimide	[30]
Ag ₂ (CN ₂)	1.194, 1.266	177.1	cyanamide	[6b]
PbCN ₂	1.17, 1.25	177.5	cyanamide	[7]
HgCN ₂	1.12, 1.35	172.4	cyanamide	[6h]
Hg ₂ (CN ₂)Cl ₂	1.24	177	carbodiimide	[31]
Hg ₃ (CN ₂) ₂ Cl ₂	1.13, 1.28	174	cyanamide	[31]
In _{2.24} (CN ₂) ₃	1.208	178.5	carbodiimide	[7]
Eu(CN ₂)	1.215, 1.229	177.4	carbodiimide	[32]
LiEu ₂ (CN ₂)I ₃	1.211	180	carbodiimide	[33]
LiEu ₄ (CN ₂) ₃ I ₃	1.214	180	carbodiimide	[33]

For example, chain structures are present in the structures of silver cyanamide, mercury carbodiimide and mercury cyanamide. Three-dimensional bonding arrangements can be seen in indium carbodiimides, zinc cyanamides and in silicon carbodiimide, which bears striking resemblance with interpenetrating networks such as of the cristobolite (SiO₂) type. The

polymeric network involving metal cyanamide is also reported for $\text{Hg}_2(\text{CN}_2)\text{Cl}_2$ and $\text{Hg}_3(\text{CN}_2)_2\text{Cl}_2$. In $\text{Hg}_3(\text{CN}_2)_2\text{Cl}_2$, the polymeric network is built up from both carbodiimide and cyanamide units. When it comes to the building up of crystalline porous materials, various organic and inorganic spacer ligands coordinating to metal cations have been explored. For example, N-containing spacers such as pyridine and cyano ligands were typically and successfully used [34]. On the other hand, the probably smallest N, N^\dagger -type ligand- $(\text{CN}_2)^{2-}$ anion, either in carbodiimide or in cyanamide form can also form pore or channel structures [29, 31, 33]. It is also clear that the metal cation plays a decisive role for the total structure since its preferences for coordination number, coordination geometry and chemically matching ligands must be taken into account.

Later two calcium carbodiimide nitrides, $\text{Ca}_4(\text{CN}_2)\text{N}_2$ and $\text{Ca}_{11}(\text{CN}_2)_2\text{N}_6$ [29] were discovered from their respective stoichiometric reaction mixtures of calcium nitride and graphite. The crystal structure of both the compounds contains an open, three-dimensional network consisting of distorted NCa_6 -octahedra connected over joint edges and corners with one-dimensional channels along [010] occupied by $(\text{CN}_2)^{2-}$ guest species.

In the carbodiimide/cyanamide chemistry of lanthanide, Hashimoto et. al. synthesised the first characterised compound containing $(\text{CN}_2)^{2-}$ unit, $\text{Ln}_2\text{O}_2(\text{CN}_2)$ with $\text{Ln} = \text{La}, \text{Ce}, \text{Pr}, \text{Nd}, \text{Sm}, \text{Eu}, \text{Gd}$ [35]. Tetragonal $\text{La}_2\text{O}_2(\text{CN}_2)$ doped with other lanthanide ions like Eu^{2+} , Pr^{3+} , etc. are prominent for their luminescence properties [36]. Even though the presence of $\text{La}_2\text{O}_2^{2+}$ layers in the structure of $\text{La}_2\text{O}_2(\text{CN}_2)$ was accounted for their luminescence properties, there is no single crystal diffraction study known for this system and the reason for their prominence as a luminescent material is still not understood well. After $\text{La}_2\text{O}_2(\text{CN}_2)$ is known for a decade, the research interest in this area has grown only in the past few years.

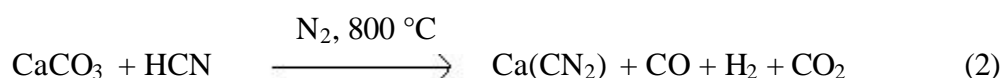
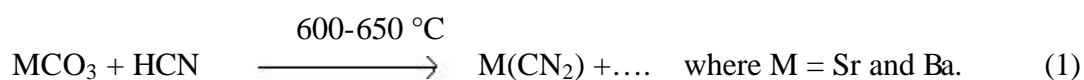
$\text{Eu}(\text{CN}_2)$ isotopic to $\text{Sr}(\text{CN}_2)$ is the first quite expected lanthanide carbodiimide compound, since the chemistry of alkaline earth and divalent lanthanides have more similarities in solid state. $\text{Eu}(\text{CN}_2)$ synthesised from europium nitride, sodium azide and graphite has the structure containing distorted metal centered octahedra interconnected by corner sharing and by bridging $(\text{CN}_2)^{2-}$ units [32]. Recently two novel carbodiimides of europium, $\text{LiEu}_2(\text{CN}_2)\text{I}_3$ and $\text{LiEu}_4(\text{CN}_2)_3\text{I}_3$ were discovered from fluxes of europium iodide, sodium azide, sodium cyanide and lithium iodide [33]. In $\text{LiEu}_2(\text{CN}_2)\text{I}_3$, the bitetrahedral units are connected into one-dimensional linkages which run along [001], and the bridging $(\text{CN}_2)^{2-}$ units generate a framework such that there are one-dimensional channels to accommodate the LiI_6 octahedra. In

$\text{LiEu}_4(\text{CN}_2)_3\text{I}_3$, the europium/carbodiimide/iodide framework exhibits one-dimensional hexagonal channels occupied by lithium ions.

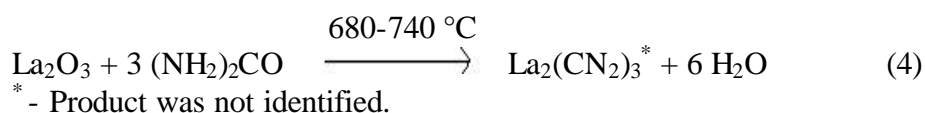
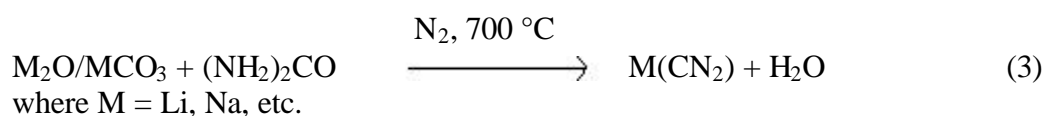
Investigations in the system M-X-N-C (M = lanthanides, X = halide) with nitride (lanthanide Nitrides) and graphite have yielded products that resemble both, typical halide nitride and typical halide carbide structures. The halide carbide structures reported in the literature usually contain discrete or condensed octahedral $[\text{Ln}_6]$ clusters with C or C_2 units as interstitial atoms. Examples of carbide nitrides are $\text{Y}_6\text{I}_9\text{C}_2\text{N}$, $\text{Ln}_4\text{I}_6\text{CN}$ (Ln = La, Gd; X = Br, I) [37] and $\text{Ln}_7\text{I}_{12}\text{C}_2\text{N}$ (Ln = Y, Ho) [38] with C_2 centered $[\text{M}_6\text{X}_{12}]$ type clusters and N atoms in tetrahedral voids of metal atom arrangements. The conditions employed in the synthesis for these compounds did not assist to the formation of stable C-N bonds.

2. 1. Different synthetic methods of carbodiimides/cyanamides

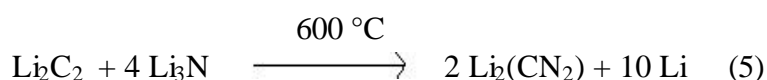
(1) From HCN



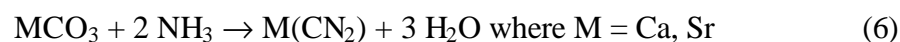
(2) From urea [2]

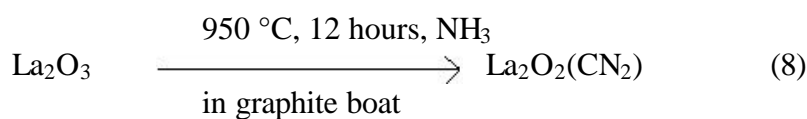
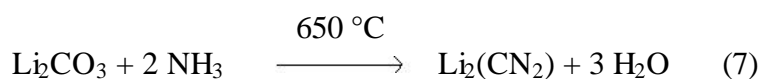


(3) From carbide and nitride [4]

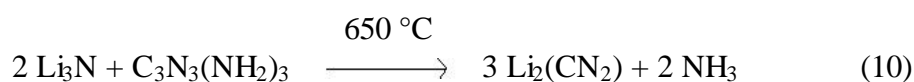
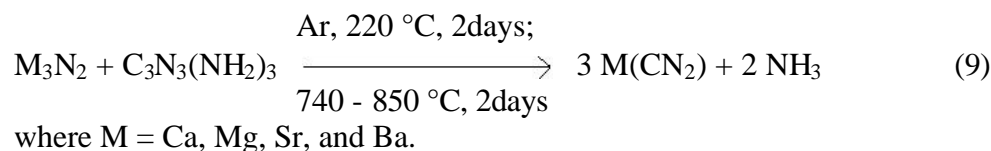


(4) From NH_3 [39]

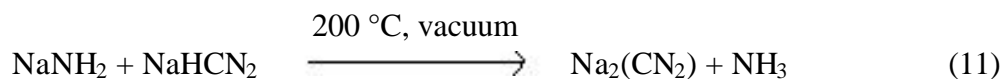




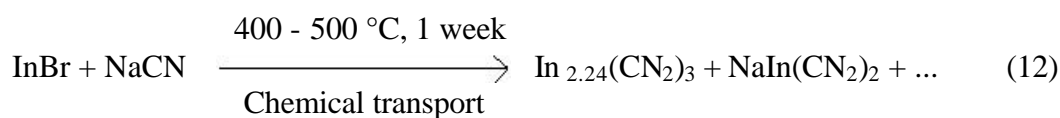
(5) From melamine [5]



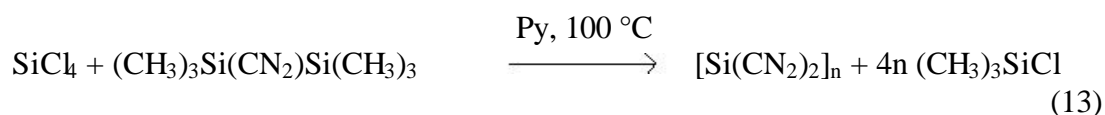
(6) From amide [4]



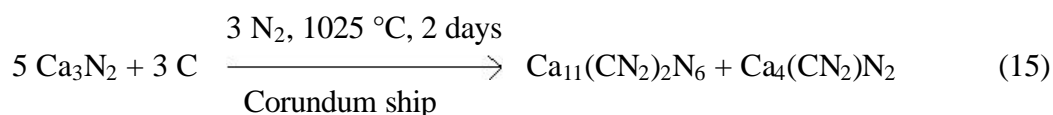
(7) From cyanide [7]



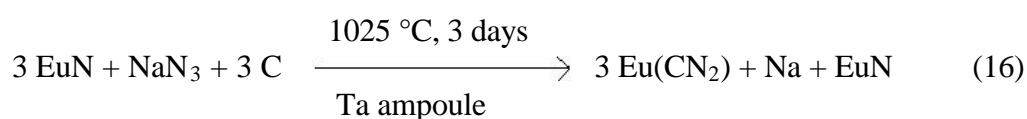
(8) From carbodiimide [30]



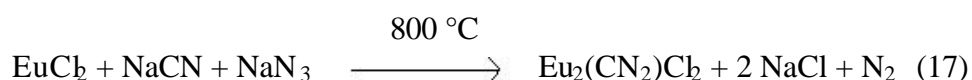
(9) From Ca_3N_2 [29]



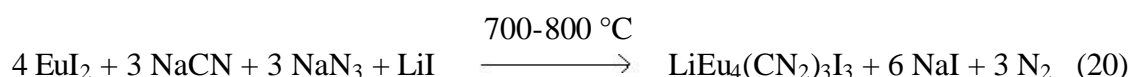
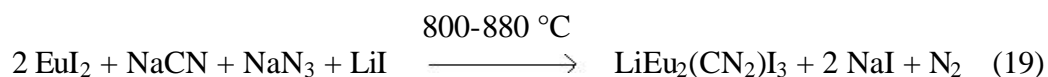
(10a) From nitride and azide [29]



(10b) From cyanide and azide [33]



(11) From LiI flux [33]

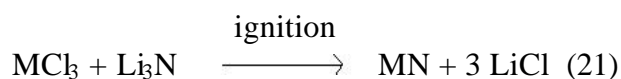


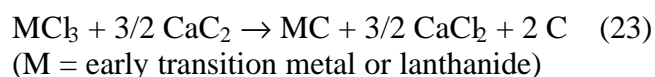
(12) From solution chemistry [6, 16, 19]

Metal cyanamides/carbodiimides of Cu, Zn, Cd, Hg, Ag, Pb, and Tl were precipitated from the aqueous solutions of their respective hydrated nitrates/sulphates and $\text{Na}_2(\text{CN}_2)$ or $\text{Ca}(\text{CN}_2)$ or $\text{H}_2(\text{CN}_2)$. The dicyanamides of alkali, alkaline earth metal, divalent transition metal, and lead were made by the ion exchange of their respective hydrated salts from $\text{Na}(\text{C}_2\text{N}_3)$. Tricyanomethanide compounds of divalent transition metals were also precipitated from the aqueous solutions of their respective hydrated nitrates and $\text{K}[\text{C}(\text{CN})_3]$.

2. 2. Solid state metathesis reaction (SSM)

1. A subclass of self propagating high temperature synthesis. A rapid method for producing ceramic materials by utilising the energy given out in a chemical reaction.
2. SSM reactions involve chemical exchange of the reacting partners and are driven largely by the lattice energy of a coproduced salt.
3. SSM reactions have been used extensively for the formation of transition metal, main group, lanthanide and actinide metal nitrides and carbides using a wide range of starting materials [40].

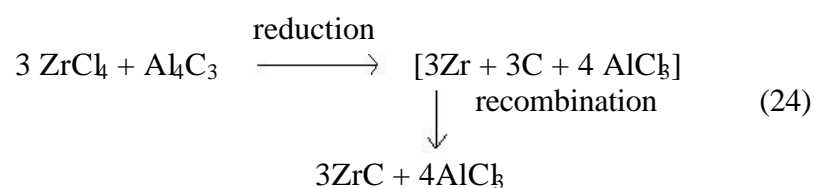




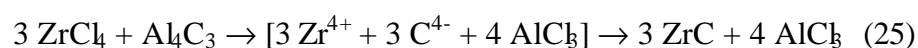
4. SSM reactions are considered to proceed via two pathways either by reductive recombination or ionic metathesis [40].

For example

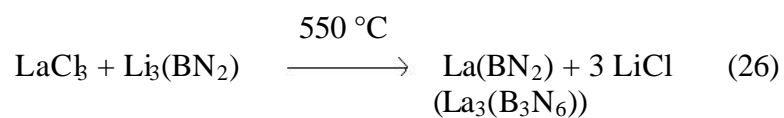
1. Reductive recombination:



2. Ionic metathesis:



5. SSM route was also applied to synthesise lanthanum nitridoborates [41].



Hence the strategy of using solid state metathesis route is followed in this work for studying the reaction pathways in the system LaCl₃/Li₂(CN₂).

3. Experimental techniques

3. 1. Physical measurements and software packages used

3. 1. 1. Phase analysis

The phase analyses of starting materials and reaction products were done by X-ray powder diffraction studies. The powder patterns were recorded on a StadiP diffractometer (Stoe, Darmstadt), using germanium monochromated Cu-K_{α1} radiation ($\lambda = 1.540598 \text{ \AA}$). The samples were mounted between two pieces of mylar foil (double foil technique) for the X-ray powder measurement. First the routine analyses were done between 2θ angles 10 and 60°. When a new structure was evident from the powder pattern, the long measurements were done in the 2θ range 5-130° in step of 0.2° with exposure time of 120 seconds for the period of approx. 22 hours. The reflections from powder pattern were indexed using either by Werner's or Visser's or Louer's algorithm in the software program STOE WinXPOW. The observed powder patterns were compared with the calculated pattern obtained from the program Powder Cell.

3. 1. 2. Crystal structure determination

Air stable single crystals were selected under the microscope and mounted on the tip of a glass fiber for the X-ray measurements. Air sensitive crystals were mounted in a 0.1 mm capillary in the Ar filled glove box and sealed later. Measurements were performed on a IPDS (Stoe, Darmstadt) X-ray Diffractometer in the appropriate 2θ range at 293 K, using graphite monochromated Mo-K_α radiation ($\lambda = 0.71073 \text{ \AA}$). The intensity data were corrected by XRED/XSHAPE for Lorentz, polarization, and absorption effects. The structures were solved by direct methods (SHELXS-97) and refined by full-matrix least-squares calculations on F^2 (SHELXL-97) [42].

3. 1. 3. Structure solution and refinement from powder patterns

The structure solution from the indexed powder pattern was solved using the software program EXPO [43] and the obtained solution was refined by Rietveld refinement using the

program FullProf 2000 [44].

3. 1. 4. Infrared spectra

Infrared spectra were recorded on Perkin Elmer FT-IR spectrometer. The measurements were done in the range 400 - 4000 cm^{-1} using KBr pellets of the compounds.

3. 1. 5. Thermal analysis

Thermal analysis (DTA/TG) were performed using a Netzsch STA 409C thermal analyzer between 25 and 800 $^{\circ}\text{C}$ with the sample fused in a self-made quartz ampoule container. For the DTA/TG of the decomposition reaction, the product was washed well with ethanol or water to remove LiCl and dried for twelve hours before performing the measurements. The measurements were performed in the presence of nitrogen or argon with heating and cooling rates of 5 K.

3. 1. 6. Magnetic susceptibility studies

The magnetic susceptibility data were obtained with a SQUID (Superconducting Quantum Interference Device, MPMS, Quantum Design) magnetometer in the temperature range between 22 and 285 K in a gelatin capsule. The data obtained have been corrected for the diamagnetic moments of the gelatin capsule and all atoms involved. Measurements were performed using a magnetic field of $H = 0.05$ Tesla.

3. 1. 7. Graphics

The crystal structures were drawn using the software program 'DIAMOND'-Visual crystal structure information system, version 2.1. CRYSTAL IMPACT. The IR spectras, DTA/TG plots and magnetic susceptibility graphs were drawn using the program Origin 5.0.

3. 2. List of chemicals used

LaCl₃ (Alfa aesar, sublimed)

CeCl₃ (Alfa aesar, sublimed)

PrCl₃ (Alfa aesar, sublimed)

NdCl₃ (Alfa aesar, sublimed)

GdCl₃ (Alfa aesar, sublimed)

DyCl₃ (Alfa aesar, sublimed)

Li₃N (Strem, 99.5 %)

NaCN (Merck, 95%)

KCN (Merck, 96%)

C₃N₃Cl₃ (ALDRICH, 99%)

C₃N₃(NH₂)₃ (Fluka, 99 %)

Na(N(CN)₂) (ABCR, 96%)

K[C(CN)₃] (Alfa Aesar)

K₄[Fe(CN)₆]

Ca₃N₂ (Strem, 97%)

AlCl₃ (Alfa aesar, 99.9%)

NH₄Cl (Merck, 99.8%)

NH₄Br (Merck, 99.8%)

NH₄I (ChemPUR, 99%)

HCl (Merck, 32%)

HBr (Riedel-de Haen, 47%)

HI (Riedel-de Haen, 57%)

Li (Strem, 99.99%)

Ca (Alfa Aesar, 99.987%)

La₂O₃ (Merck, max.0.0005% Ca)

Pr₂O₃ (Ventron, 99.99%)

La(NO₃)₃ · 6H₂O (Merck, 99%)

LiCl (Merck, 99.5%)

KCl (Merck, 99.5%)

3. 3. Synthesis of starting materials

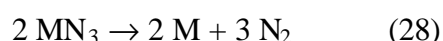
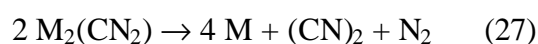
3. 3. 1. Preparation of Li₂(CN₂) and Ca(CN₂)

Li₂(CN₂) was synthesized from a finely ground 2:1 stoichiometric mixture of Li₃N and melamine (slight excess) according to the reaction 10 [5]. A molybdenum boat with the ground mixture was placed in a quartz tube and preheated at 250 °C for two hours under flowing argon. Then the preheated mixture was heated slowly to 650 °C and kept at this temperature for three hours to obtain X-ray pure Li₂(CN₂) which was suitable for further synthesis without any purification. The XRD powder pattern and IR spectra of Li₂(CN₂) are shown in Figure 1 and Figure 2 respectively. The broad strong absorption peak around 2024 cm⁻¹ corresponds to the asymmetric stretching of C=N and a sharp peak at 688 cm⁻¹ corresponds to the bending vibration mode of C=N.

Ca(CN₂) was synthesised from 1:1 molar ratio of Ca₃N₂ and melamine (slight excess) respectively at 800 °C under flowing argon as shown in the reaction 9 [5].

3. 3. 2. Decomposition of Li₂(CN₂)

The cyanamides or carbodiimides form a class of compounds isoelectronic with the azides. The decomposition of a simple metal cyanamide may be represented by the general equation 27 [6c] which is analogue to the decomposition of azides (equation 28).



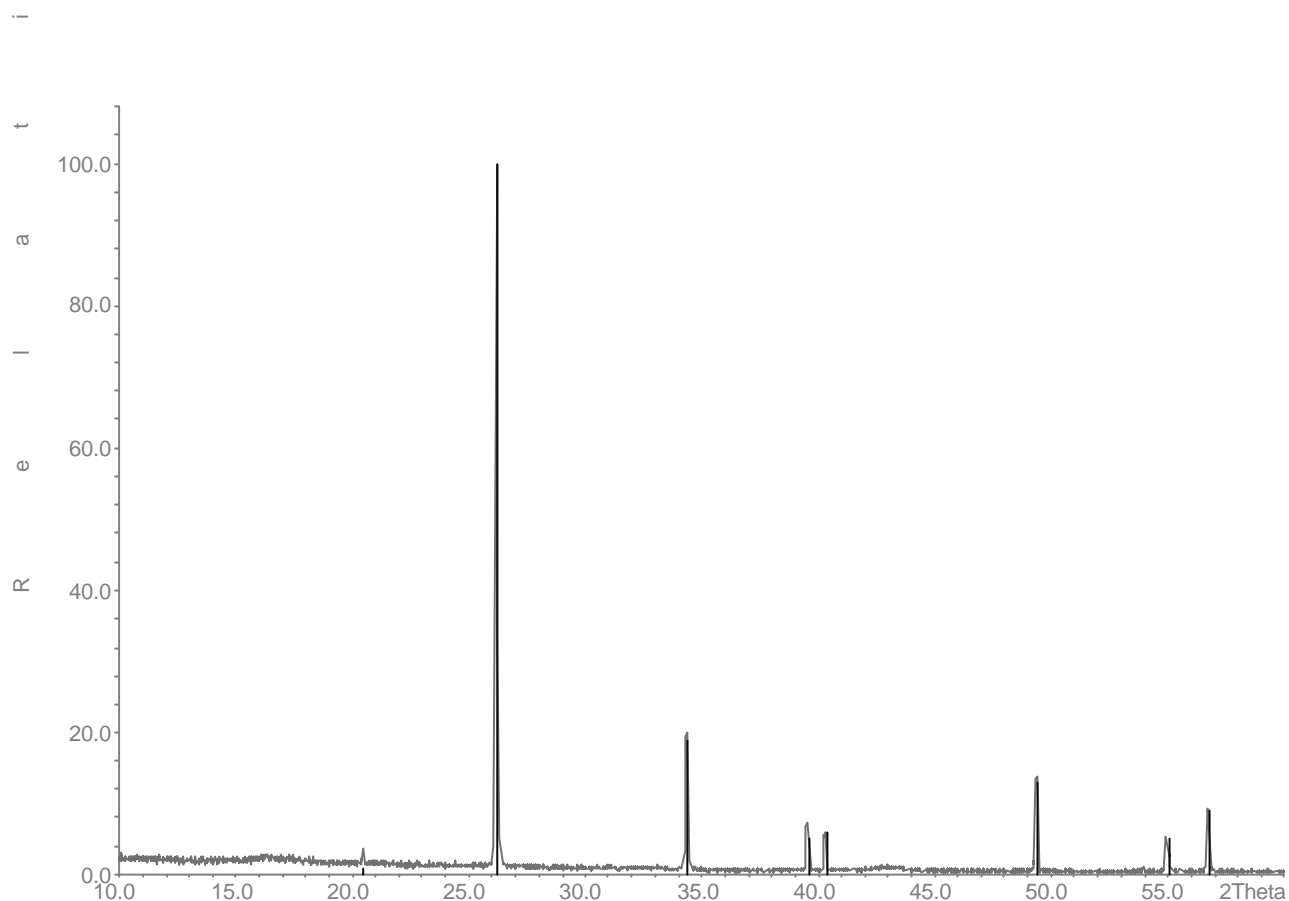


Figure 1. XRD powder pattern from $\text{Li}_2(\text{CN}_2)$ corresponding to ICDD no. 70,648. Lines in black indicate the calculated positions of Bragg reflections for $\text{Li}_2(\text{CN}_2)$.

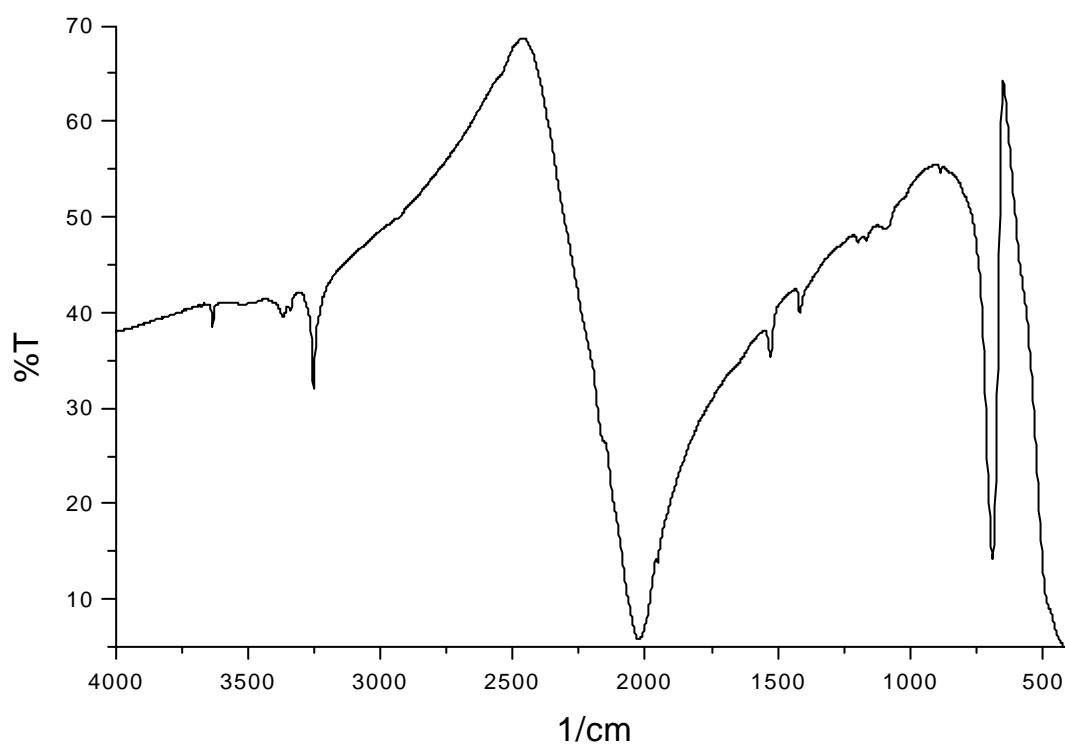


Figure 2. IR spectrum of $\text{Li}_2(\text{CN}_2)$.

From literature, it is known that $\text{Li}_2(\text{CN}_2)$ undergoes decomposition to give lithium cyanide, lithium metal and nitrogen gas [2]. In this decomposition, stainless steel container was reported to act as a catalyst.



The DTA of $\text{Li}_2(\text{CN}_2)$ was performed in an open system under N_2 atmosphere upto $800 \text{ }^\circ\text{C}$. There are two endothermic peaks observed while heating with a sharp exothermic effect while cooling observed at around $700 - 750 \text{ }^\circ\text{C}$ as shown in Figure 3. The observed small endothermic peak near $700 \text{ }^\circ\text{C}$ could be attributed to the fragmentation of nitride from the carbodiimide. When the DTA of $\text{Li}_2(\text{CN}_2)$ was performed in a closed system, the same endothermic effect was observed with the container ampoule exploded at $800 \text{ }^\circ\text{C}$. The explosion for quartz ampoule may be due to the release of $(\text{CN})_2$ gas as shown in the reaction 30.

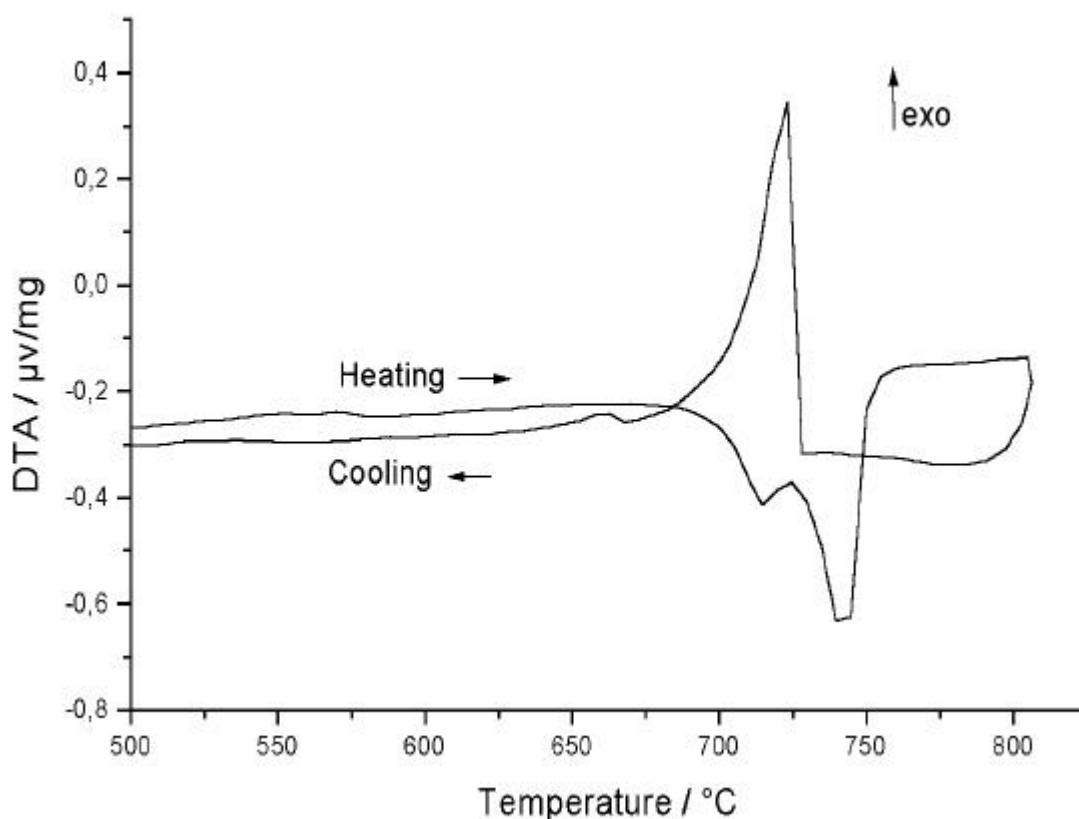
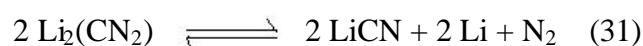


Figure 3. DTA of $\text{Li}_2(\text{CN}_2)$.

3. 3. 3. Reactivity of $\text{Li}_2(\text{CN}_2)$

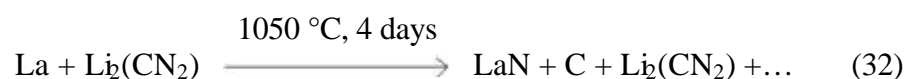
$\text{Li}_2(\text{CN}_2)$ was heated alone in a sealed tantalum ampoule to different temperatures at 750 - 950 °C, but there was no change observed and the X-ray powder pattern showed the reflections of $\text{Li}_2(\text{CN}_2)$. Hence $\text{Li}_2(\text{CN}_2)$ can be considered as a good carbodiimide source at high temperatures.

So in closed system, it is appropriate to written as



Another observation supporting this reaction was that the ampoule getting bulged after the reaction time due to the pressure build up at 750 - 950 °C and the ampoules were very brittle and easy to break at high temperatures of 950 °C.

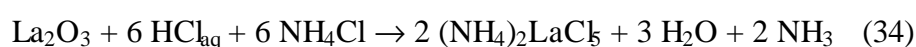
The reactivity of $\text{Li}_2(\text{CN}_2)$ was studied by reacting with metal powders like Ta and La in a tantalum container. With lanthanum, lanthanum nitride was obtained along with the side products of carbon and unreacted lithium cyanamide. And with tantalum, lithium tantalum nitride was formed as the product. The partial decomposition of $\text{Li}_2(\text{CN}_2)$ in the reactions 32 and 33 led to the formation of nitride in the products at high temperatures.



3. 3. 4. Preparation of LaX_3 with $\text{X} = \text{Cl}, \text{Br}, \text{and I}$

LaCl_3

The preparation of LaCl_3 [45] was carried out according to reaction 34 and 35. The reaction mentioned in 34 was carried out in two steps, followed by reaction 35.



In the first step, the weighed lanthanum sesqui oxide (La_2O_3) taken in a 150 ml beaker was dissolved in HCl (32%) slowly to get a clear solution. The addition of HCl should be done slowly as large amount of heat is liberated from the process. Then to the clear solution of lanthanum sesquioxide in HCl, weighed eight equivalents of NH_4Cl was added. The NH_4Cl is added always in excess to ensure all the sesqui oxide get reacted and the excess NH_4Cl can be sublimed at the next step. The clear solution containing HCl and NH_4Cl was heated to $200\text{ }^\circ\text{C}$ with constant stirring in the next step, till all the solution was evaporated to become white solid or gum like semi solid. The white solid should be removed in hot condition from the beaker before it gets cooled down. Otherwise, the removal of white solid from the beaker is difficult as it get more hard and can be removed from the beaker only by breaking. The purity of $(\text{NH}_4)_2\text{LaCl}_5$ without sesqui oxide was assured from XRD powder pattern. The white solid collected from the second step should be better as coarse material or as big chunks rather than as a fine powder. In the following step, the obtained white solid was transferred to a small quartz tube covered by an another long quartz tube equipped with stop cock. The vacuum was introduced slowly in to the system before heating it to $400\text{ }^\circ\text{C}$. The heating rate is controlled for $1^\circ/\text{min}$ and allowed to remain at this temperature for an overnight before cooled down to room temperature. Then NH_4Cl was separated fully and sublimed on the walls of the big quartz tube by leaving the anhydrous LaCl_3 in the small quartz tube. Anhydrous LaCl_3 obtained from this step was X-ray pure without any LaOCl impurity. But the obtained anhydrous LaCl_3 cannot be used for reactions without further purification. For the purification of LaCl_3 from $\text{NH}_4\text{Cl}/\text{HCl}$ route, there are two ways.

One way is to sublime the obtained LaCl_3 under vacuum (0.001 mbar) at $800\text{ }^\circ\text{C}$ in a platinum crucible covered with a big quartz tube. Another way to purify the obtained LaCl_3 is by using AlCl_3 through the process of chemical vapour transport. As LaCl_3 is forming a gas phase complex with AlCl_3 [46] at comparatively low temperature of $300\text{ }^\circ\text{C}$ and decomposes at around $450\text{ }^\circ\text{C}$, pure LaCl_3 can be obtained at the hot end by subliming the AlOCl and AlCl_3 to the cool end of the quartz tube. For example, the XRD powder pattern of LaCl_3 after sublimation and after purification with AlCl_3 are shown in Figure 4 and Figure 5 respectively.

LaBr_3

LaBr_3 and PrBr_3 were prepared by the usual $\text{NH}_4\text{Br}/\text{HBr}$ route from their sesqui oxides and HBr (47%) according to the literature [47].

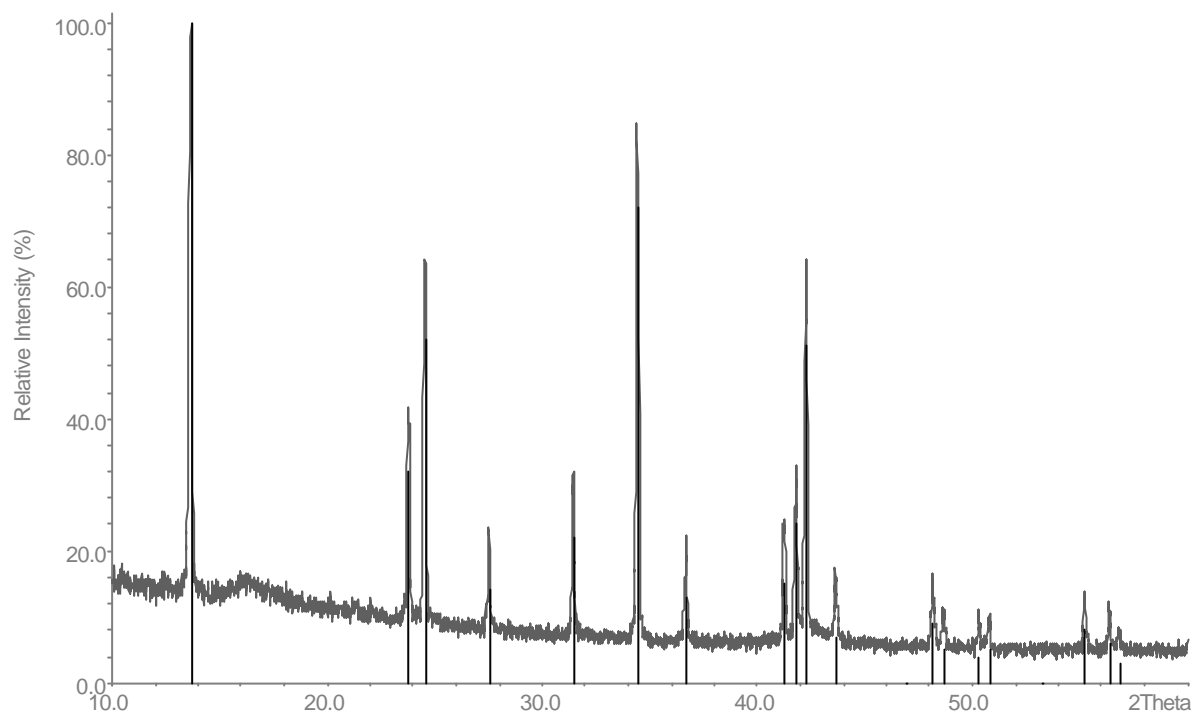


Figure 4. XRD powder pattern of LaCl_3 after sublimation at $800\text{ }^\circ\text{C}$ compared with ICDD no 73,725. Lines in black indicate the calculated positions of Bragg reflections for LaCl_3 .

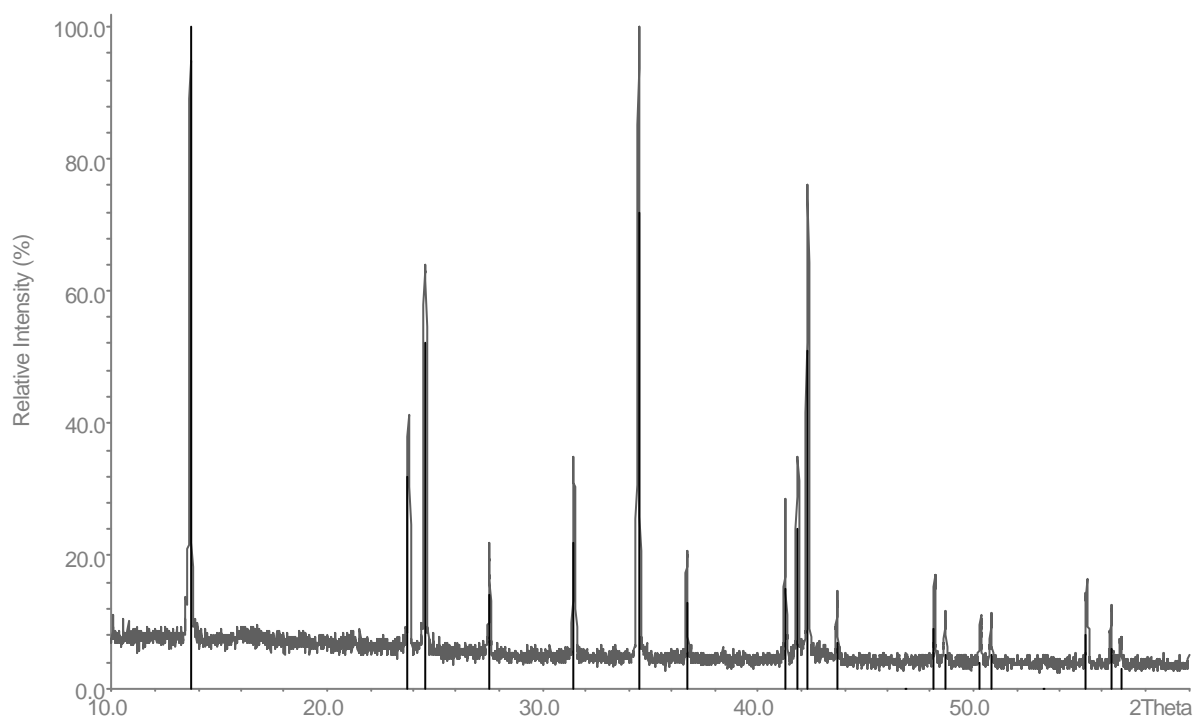


Figure 5. XRD powder pattern of LaCl_3 after purification by AlCl_3 compared with ICDD no 73,725. Lines in black indicate the calculated positions of Bragg reflections for LaCl_3 .

LaI₃

LaI₃ was prepared by the NH₄I/HI route from lanthanum sesquioxide and HI (57%) according to literature [48].

3. 3. 5. Preparation of LaOCl

LaOCl was prepared from La₂O₃ and NH₄Cl according to the reaction 36 [49]. The reaction mixture was heated in a corundum container at 300 °C for six hours and then heated at 650 °C for ten hours to obtain phase pure LaOCl. The obtained powder pattern of LaOCl is shown in Figure 6.

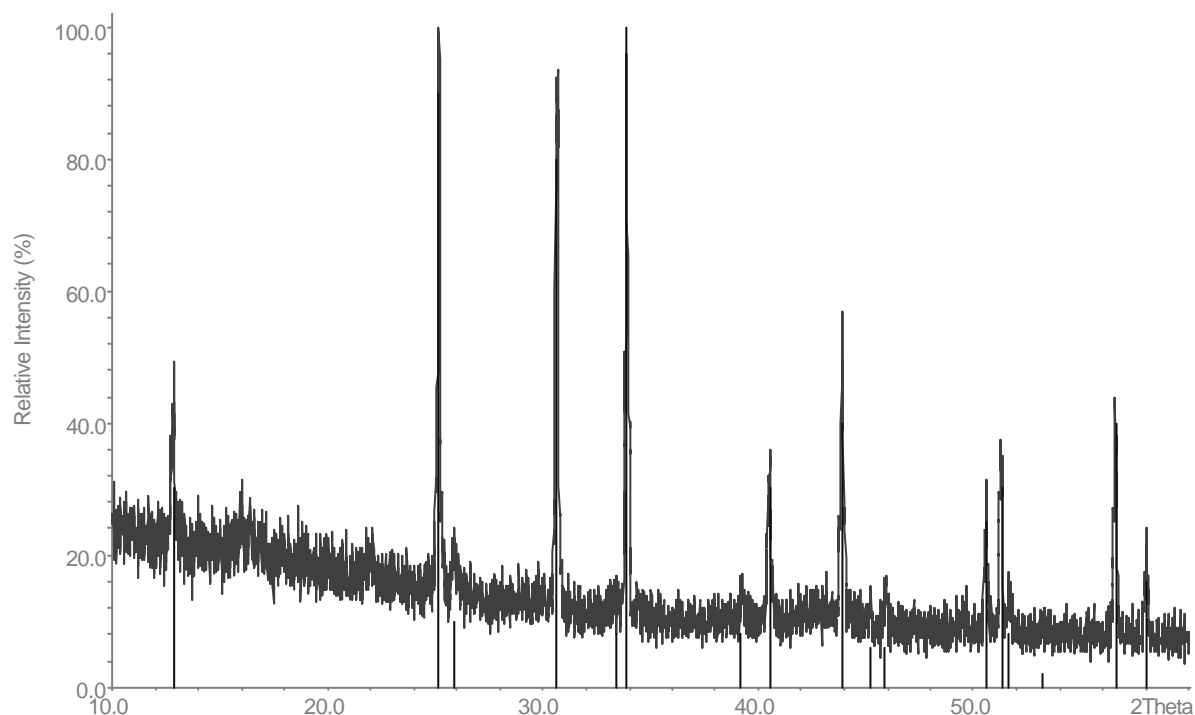
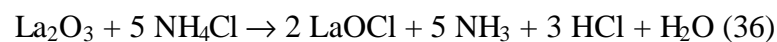


Figure 6 XRD powder pattern of LaOCl compared with ICDD no 8,477. Lines in black indicate the calculated positions of Bragg reflections for LaOCl.

3. 4. Manipulations of C–N containing lanthanide compounds

The reactions at temperatures above 750 °C were carried out in sealed tantalum ampoules

made from tantalum tube (Plansee, 99.99%). Prior to reactions, the tantalum tube was cut in to pieces of 3 cm length, cleaned with a mixture of H_2SO_4 (97%), HNO_3 (65%), and HF (38%), and dried in air at 100 °C. The reactions can be performed in tantalum as well as the copper ampoules, but the copper ampoule was preferred for the reactions carried out at ≤ 800 °C due to the availability at cheaper prices. Prior to reactions, the Cu tube was cut in to pieces of length 5-6 cm and washed thoroughly with HCl acid before air dried at 100 °C in an oven. The reactions were also carried out in quartz ampoules at temperatures below 750 °C.

The cleaned tantalum pieces were sealed under 600 mbar argon pressure with an arc welder, first at one side and after loading with starting materials on the other side. All manipulations of compounds before and after the reactions were performed in a glove box under dry argon with oxygen and moisture levels below 1 ppm. The sealed tantalum ampoules containing starting materials were covered with silica ampoules under vacuum. The quartz ampoules were filled with reaction mixture and then sealed under vacuum.

The reaction duration ranges from one day to several weeks. For reactions containing reactive Li compounds (i.e. $\text{Li}_2(\text{CN}_2)$) as starting materials, it was observed sometimes that the quartz get reacted during the reaction time at temperatures in the range 650-750 °C. The reactions up to 700° C were performed over several weeks in self made quartz furnaces equipped with Eurotherm temperature controllers and reactions at 750 °C were carried out in a commercial furnace (Carbolite). The reaction temperature were usually reached over the period of one day. After the reaction duration, the ampoules were allowed to cool down to room temperature within one or two days.

4. Results and discussion

4. 1. Solid state metathesis reaction between LaCl_3 and Li_3N

LaN and La_2NCl_3 [50] were synthesised from the stoichiometric metathesis reaction between 1:1 and 2:1 LaCl_3 and Li_3N respectively at 500 - 600 °C in a quartz ampoule.



DTA studies were performed to understand the reaction pathway between LaN and La_2NCl_3 [51]. An ignition of the 1:1 molar reaction with two strong exothermic peaks corresponds to the formation of LaN as obtained near 495 °C, followed by an endothermic peak near 600 °C due to the melting of LiCl . The formation of LaN and LiCl was confirmed by X-ray powder pattern. If the molar ratio of the reaction partners is changed to halide rich 2:1, La_2NCl_3 and LiCl were obtained under similar conditions as for LaN . DTA measurements revealed one weak shoulder peak (495 °C) followed by strong exothermic peak (505 °C) for the 2:1 molar mixture of LaCl_3 and Li_3N as shown in Figure 7.

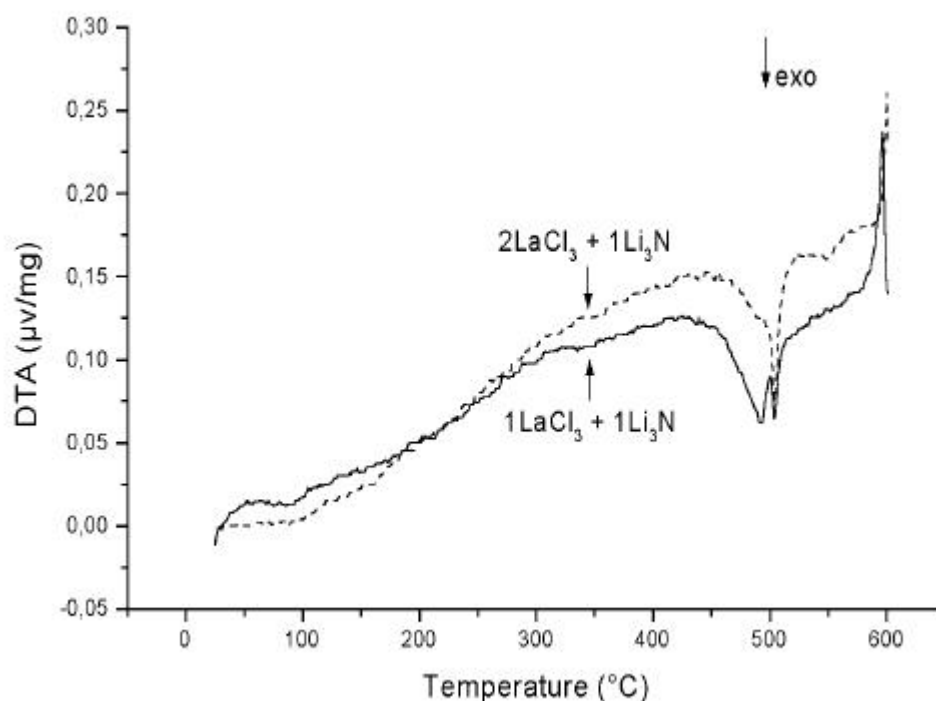


Figure 7. DTA of the reaction between LaCl_3 and Li_3N in the 1:1 (solid line) and 2:1 (dotted line) molar ratios. The exothermic signal at 495 °C corresponds to LaN formation and the one

at 505 °C corresponds to La_2NCl_3 .

The DTA peak obtained at 495 °C was stronger in the reaction designed for LaN and that of at 505 °C was stronger in the reaction designed for La_2NCl_3 .

La_2NCl_3 has been considered as an intermediate compound for the synthesis of LaN [52]. The results obtained in this experiments would rather allow an opposite interpretation, because the exothermic effect assigned to the LaN formation is at comparatively lower temperature [51]. This observation was confirmed through a quartz ampoule reaction of a 2:1 molar mixture at 480 °C over one day. The dark grey product contained mainly LaN, some LiCl and only little La_2NCl_3 . In an attempt to suppress the La_2NCl_3 formation in the synthesis of LaN by stoichiometric means, a halide deficient ($0.9\text{LaCl}_3:1\text{Li}_3\text{N}$) reaction was carried out in the DTA. The exothermic effect at higher temperature assigned to the formation of La_2NCl_3 was significantly suppressed.

4. 2. Synthesis and structural characterisation of $\text{LnCl}(\text{CN}_2)$ with Ln = La, Ce, and Pr.

4. 2. 1. Reaction between LaCl_3 and $\text{Li}_2(\text{CN}_2)$

$\text{LaCl}(\text{CN}_2)$ [53] was synthesised according to reaction 39 from the metathesis reaction between LaCl_3 and $\text{Li}_2(\text{CN}_2)$ in a quartz ampoule at 600 °C over two days.



A powder with better crystallinity was obtained, when the equimolar reaction mixture was heated to 600 °C in one day and allowed to remain at this temperature for four weeks before cooling down to room temperature within two days. Ampoules were opened inside the glove box using a glass cutter and the obtained greyish white powder was further analysed by X-ray powder diffraction studies and IR measurements. Reactions can be successfully performed in the temperature range between 500 - 700 °C over the period of two to three days. $\text{LaCl}(\text{CN}_2)$ is air and water stable and so the side product LiCl can be washed off with water or other solvents to obtain a pure material. Later on transparent colourless single crystals of $\text{LaCl}(\text{CN}_2)$ were obtained by flux route, when 2:3 reaction mixture of LaCl_3 and $\text{Li}_2(\text{CN}_2)$ (163 mg) respectively was treated in the presence of LiCl-KCl (29 mg) at 650 °C for one

week in a quartz sealed tantalum ampoule. The reaction mixture was heated at the rate of 0.4 °/min to 650 °C and allowed to dwell for one week at this temperature before being cooled down slowly to 400 °C first and then to room temperature. In the thermal analysis of LiCl-KCl system, there is an observed eutectic point of 58.7 mol% of LiCl at 354.4 °C [54]. The eutectic melt aided the crystallisation of $\text{LaCl}(\text{CN}_2)$, which otherwise was difficult to crystallise in this temperature range even after reacting the mixture for several weeks.

After the reaction, the added LiCl-KCl flux can be washed off with water to get pure $\text{LaCl}(\text{CN}_2)$. The indexed powder pattern is in agreement with the calculated pattern from a single crystal data. The presence of pure LaCl_3 was important to obtain single crystals as the presence of oxide impurity affects the yield of $\text{LaCl}(\text{CN}_2)$, resulting along with the mixture of oxide chloride and oxide cyanamide.

4. 2. 2. Thermal analysis (DTA/TG) of the reaction between LaCl_3 and $\text{Li}_2(\text{CN}_2)$

To understand the formation and decomposition of $\text{LaCl}(\text{CN}_2)$, DTA/TG studies were performed. The DTA for the formation of the product is shown in Figure 8.

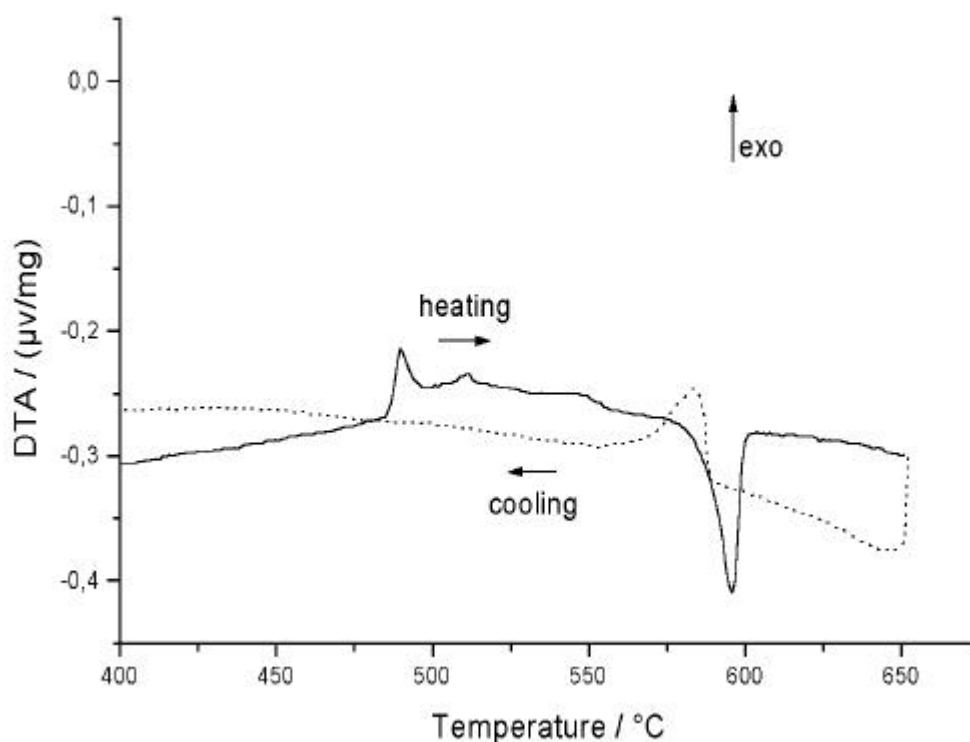


Figure 8. DTA of an equimolar reaction between LaCl_3 and $\text{Li}_2(\text{CN}_2)$ measured upto 650 °C.

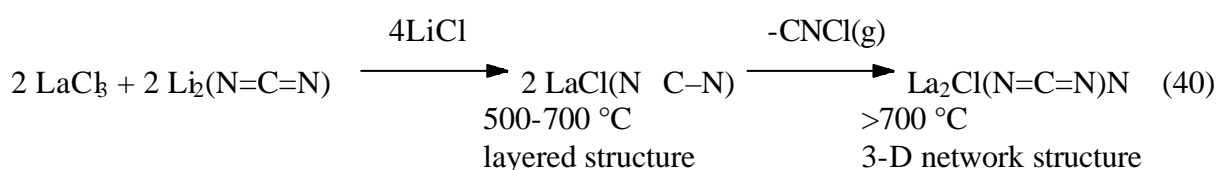
In the DTA of an equimolar reaction between LaCl_3 and $\text{Li}_2(\text{CN}_2)$, an exothermic peak is obtained around 480 °C for the formation of $\text{LaCl}(\text{CN}_2)$. The X-ray powder pattern of the obtained greyish powder after DTA was indexed to the corresponding cell parameters of $\text{LaCl}(\text{CN}_2)$.

The decomposition reaction of $\text{LaCl}(\text{CN}_2)$ and its transformation to $\text{La}_2\text{Cl}(\text{CN}_2)\text{N}$ [55] around 700 - 750 °C was found out later, when heating temperatures up to 800 °C were employed. The DTA/TG of the decomposition reaction of $\text{LaCl}(\text{CN}_2)$ is shown in Figure 9. The X-ray powder pattern was measured for the obtained greyish black powder and indexed with the cell parameters of $\text{La}_2\text{Cl}(\text{CN}_2)\text{N}$ [55] (orthorhombic $a = 13.367(3) \text{ \AA}$, $b = 9.618(3) \text{ \AA}$, $c = 3.966(1) \text{ \AA}$, $V = 509.9(3) \text{ \AA}^3$) along with LaOCl . When two equivalents of $\text{LaCl}(\text{CN}_2)$ are considered for the decomposition, the calculated mass loss of 14.3% corresponds to CNCl would have been obvious from the equation: $2 \text{LaCl}(\text{CN}_2) \rightarrow \text{La}_2\text{Cl}(\text{CN}_2)\text{N} + \text{CNCl}$. Since the observed mass loss of approx.16% is close to the calculated mass loss of 14.3%, the evolution of gaseous CNCl is likely to occur in this reaction.

The stoichiometric equimolar reaction carried out between LaCl_3 and $\text{Li}_2(\text{CN}_2)$ in a quartz sealed tantalum ampoule also resulted the same product of $\text{La}_2\text{Cl}(\text{CN}_2)\text{N}$ at 750 °C over the period of four days. There were some difference observed between results from DTA/TG and the ampoule reactions regarding the transformation temperature. Even though the transformation temperature of $\text{LaCl}(\text{CN}_2)$ into $\text{La}_2\text{Cl}(\text{CN}_2)\text{N}$ has started around 650 °C in the DTA/TG as shown in Figure 9, $\text{LaCl}(\text{CN}_2)$ was stable in the ampoule reactions at this temperature and showed decomposition only after being heated at 700 °C.

Hence the transformation of layered $\text{LaCl}(\text{CN}_2)$ into the 3-D network structured $\text{La}_2\text{Cl}(\text{CN}_2)\text{N}$ is not only dependent on the temperature but also on the reaction conditions.

An interesting interplay of different types of CN_2^{2-} ions is observed here in the reaction (40) as the starting material $\text{Li}_2(\text{CN}_2)$ has a carbodiimide unit $(\text{N}=\text{C}=\text{N})^{2-}$ that converts to a cyanamide unit $(\text{N}-\text{C}=\text{N})^{2-}$ in the layered structure of $\text{LaCl}(\text{CN}_2)$, which is transformed back to a carbodiimide unit $(\text{N}=\text{C}=\text{N})^{2-}$ in the 3-D network structure of $\text{La}_2\text{Cl}(\text{CN}_2)\text{N}$.



Thermodynamically, the carbodiimide form is more stable than the cyanamide form and that could be the reason for the structural changes shown in reaction 40.

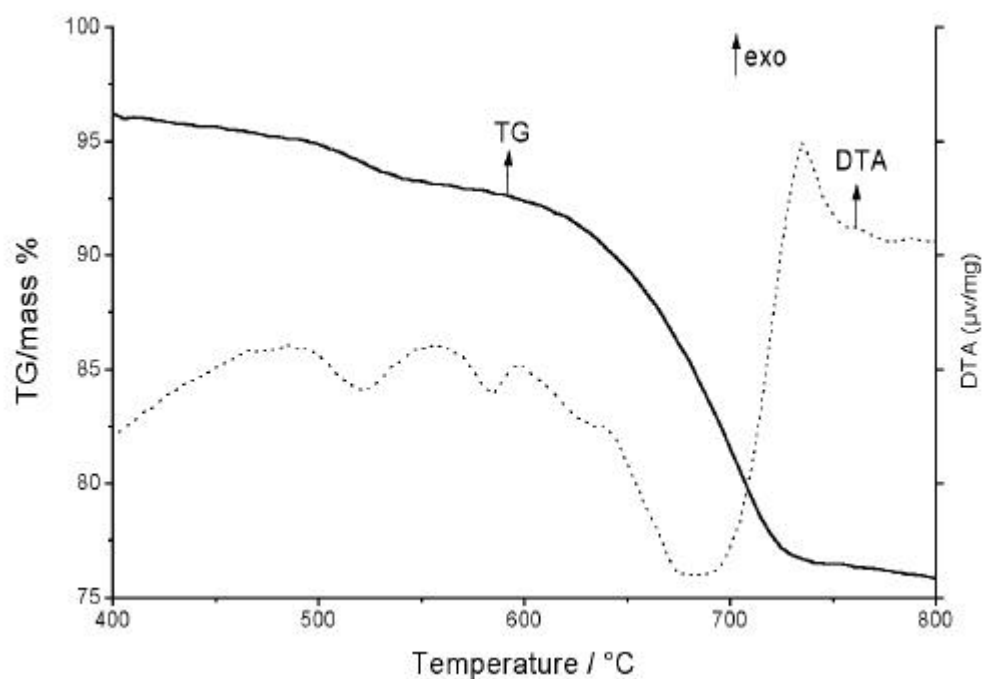


Figure 9. DTA/TG of the transformation of $\text{LaCl}(\text{CN}_2)$ into $\text{La}_2\text{Cl}(\text{CN}_2)\text{N}$.

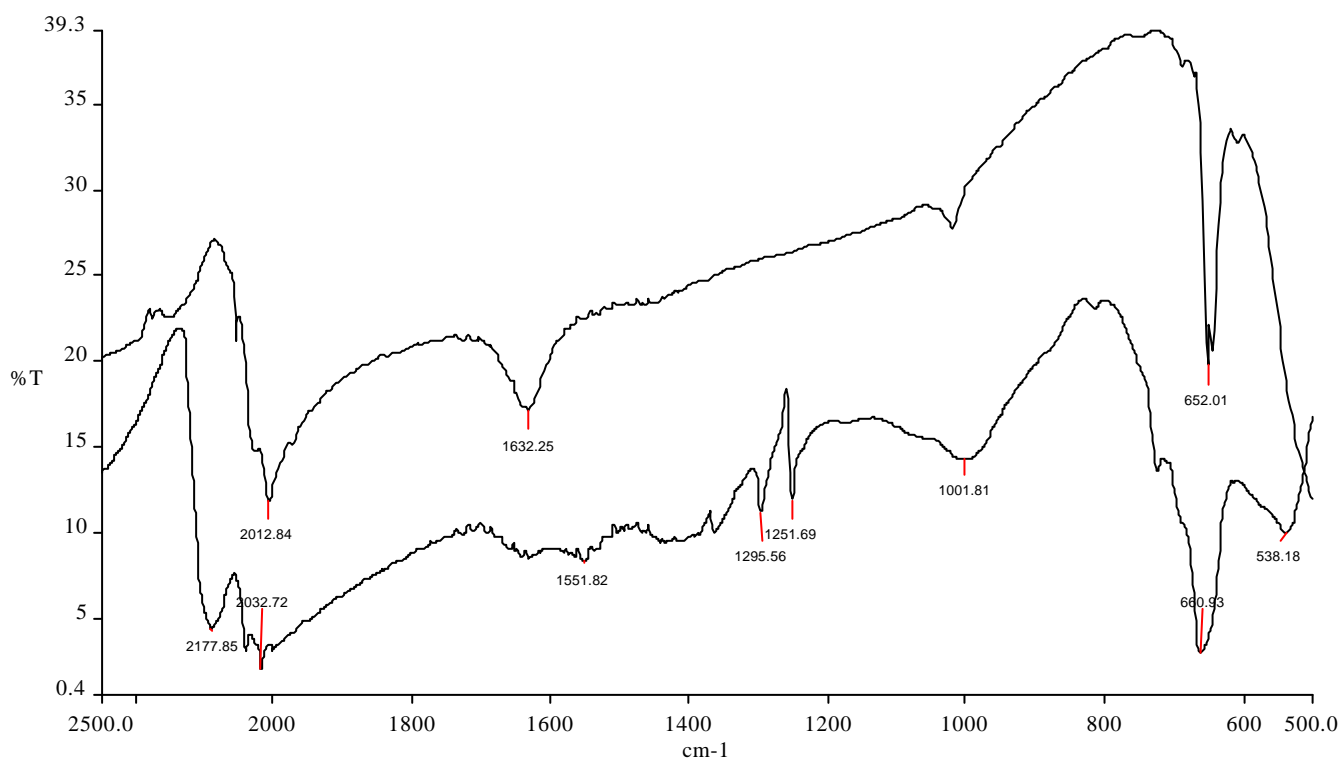


Figure 10. IR spectra of $\text{LaCl}(\text{CN}_2)$ (below) and $\text{La}_2\text{Cl}(\text{CN}_2)\text{N}$ (above).

4. 2. 3. Infrared spectra of LaCl(CN₂) and La₂Cl(CN₂)N

The presence of the (CN₂)²⁻ unit was confirmed also by infrared spectra of LaCl(CN₂). The characteristic $\hat{\nu}_{\text{sym}}$ (1252; 1296 cm⁻¹), $\hat{\nu}_{\text{asym}}$ (2033; 2178 cm⁻¹), and δ (660 cm⁻¹) peaks for (CN₂)²⁻ were observed as shown in Figure 10 and are similar to the some of the other known cyanamide compounds from the literature [56] as shown in Table 2. According to the literature, absorption bands at frequencies around 2000 cm⁻¹ are due to a stretching vibration of the triple bond in the cyanamide ion whereas that at near 650 cm⁻¹ is attributed to the vibration of a single bond (C–N). Berger et al. [5] have observed the $\hat{\nu}_{\text{as}}$ splitting for $\acute{\alpha}$ -Sr(CN₂). According to their explanation, this splitting is the result of two crystallographically independent nitrogen atoms in the cyanamide ion. The splitting of the band at about 2000 cm⁻¹ is also observed for lead cyanamide which has two significantly different C–N bond lengths [7].

Table 2. Vibrational frequencies (in cm⁻¹) from some of the known cyanamides/ carbodiimides in the literature along with LaCl(CN₂) (* = carbodiimide).

Compound	$\hat{\nu}_{\text{as}}$ (CN ₂) ²⁻	$\hat{\nu}_{\text{s}}$ (CN ₂) ²⁻	$\ddot{\alpha}$ (CN ₂) ²⁻	Reference
H ₂ CN ₂	2218/2270	1152	604	[21]
$\acute{\alpha}$ -Sr(CN ₂)	1989/2023	1251	663/677	[5]
Ba(CN ₂)	1947	1238	662/673	[5]
Ag ₂ (CN ₂)	1980	1191	633	[6b]
Hg(CN ₂)	1942/2036	1214	653/666	[6h]
Zn(CN ₂)	2048	1293	677/694	[6e]
Pb(CN ₂)	1950/1995	1216/1306	628/641	[7]
Eu(CN ₂)	1969/2087	1244	655/666	[31]
LiEu ₂ (CN ₂)I ₃ [*]	1959	-	662	[32]
LaCl(CN ₂)	2033/2178	1252/1296	660	[52]
La ₂ Cl(CN ₂)N [*]	2010	-	625	[54]
Li ₂ (CN ₂) [*]	2024	-	688	[4]

4. 2. 4. Crystal Structure of LaCl(CN₂) from X-ray powder diffraction

The crystal data, experimental conditions, data collection, and structure refinement of LaCl(CN₂) from X-ray powder diffraction studies are given in Table 3. The final Rietveld refinement plot is shown in Figure 11. The crystalline powder sample obtained from reaction 8 at 550 °C (treated for 4 weeks) was washed with ethanol and dried overnight to perform long measurements. All the reflections were indexed using Louer's algorithm (DICVOL) to the monoclinic cell with $a = 5.3271(6)$ Å, $b = 4.0286(3)$ Å, $c = 7.5403(9)$ Å, $\hat{a} = 100.728(7)^\circ$, $V = 158.99(4)$ Å³ for LaCl(CN₂) except a few unidentified low intensity reflections. The number of single indexed lines obtained was 47 with the figure of merit of 120 for the selected 50 reflections. The structure solution was obtained straight forward, although the refinements of light atoms were not precise. Therefore to some degree of uncertainty, the composition turned out to be LaCl(CN₂). Later Rietveld refinements were done using the atomic coordinates of atoms obtained from the powder pattern. The final R_{Bragg} factor was 12% after all the 35 parameters were refined.

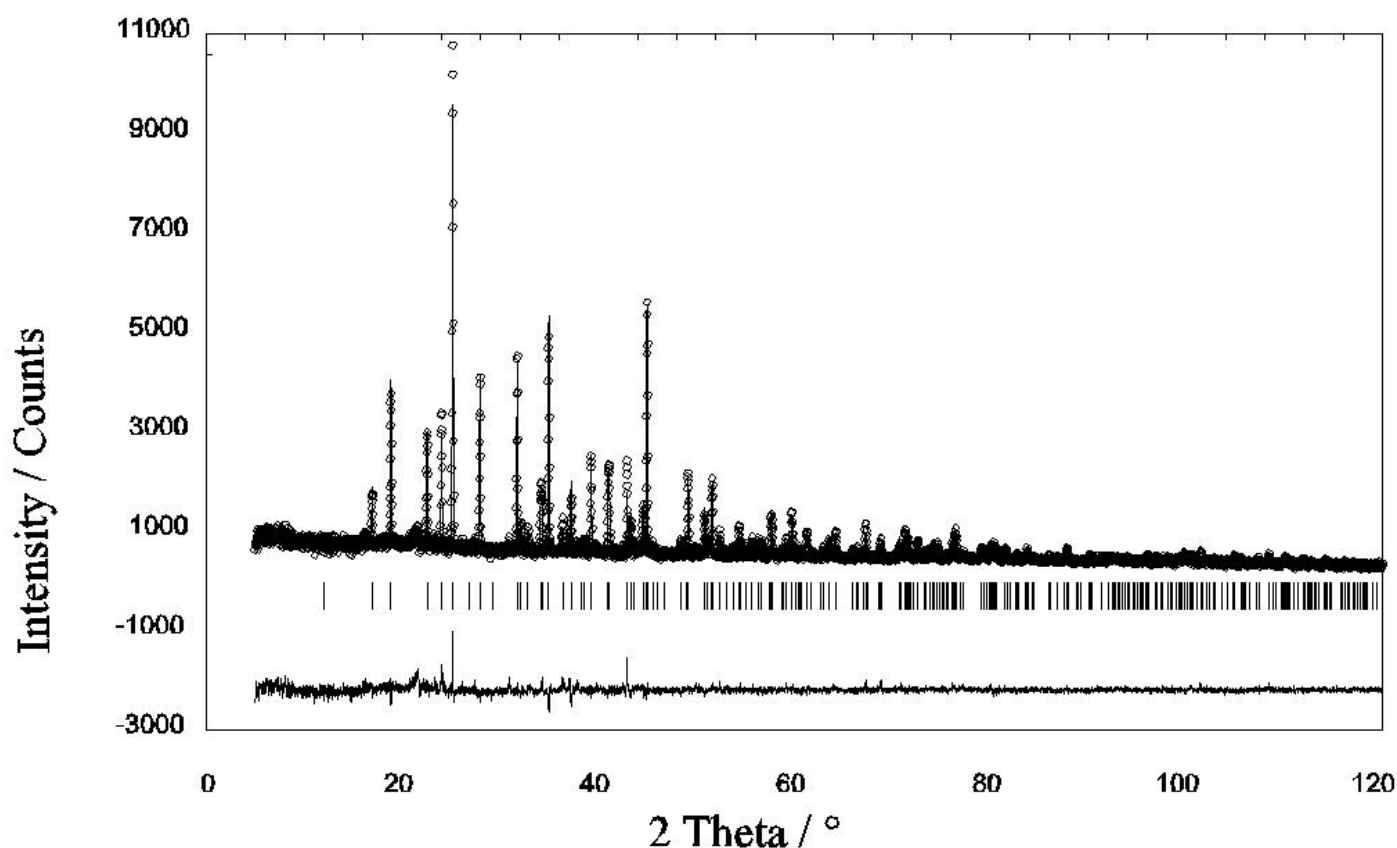


Figure 11. Final Rietveld plot for LaCl(CN₂) with measured pattern (solid line), calculated pattern (dotted line), calculated Bragg positions and difference curve.

Further refinement with better results were unsuccessful as the reflections from the impurity phase and the main phase coincides at the same 2θ values of the powder pattern. The need to grow single crystals of $\text{LaCl}(\text{CN}_2)$ became inevitable to get a more reliable solution on the structure of $\text{LaCl}(\text{CN}_2)$. Well developed colourless transparent plate like single crystals were grown later by flux route as mentioned in the synthesis.

Table 3. Crystal data, experimental conditions, data collection, structure refinement of $\text{LaCl}(\text{CN}_2)$ from the powder diffraction studies.

Crystal data	
Empirical formula	$\text{LaCl}(\text{CN}_2)$
Formula weight	214.38
Crystal system	Monoclinic
Space group(no.), Z	$P2_1/m$ (11), 2
Lattice parameters (Å)	$a = 5.3274(2), b = 4.0293(1), c = 7.5419(3), \hat{a} = 100.716(2)$
Volume (Å ³)	159.06(1)
Density calculated (g/cm ³)	2.235
Data collection	
Temperature (K)	298
Wavelength (Cu K α_1) in Å	1.5406
2θ Scan range (°)	5-120
Increment in step 2θ (°)	0.02
Exposure time (Sec)	120
No. of indexed lines	79
No. of refined parameters	35
Refinement	
Program used	Fullprof
R_p / R_{wp}	0.0657/ 0.0858
R_{Bragg} / R_F	0.1202/ 0.1013
χ^2	3.72

4. 2. 5. Crystal structure of $\text{LaCl}(\text{CN}_2)$ from a single crystal

Suitable colourless transparent single crystals of $\text{LaCl}(\text{CN}_2)$ were selected for single crystal X-ray diffraction studies under the microscope and mounted on the tip of glass fibres. Some of the crystallographic details are given in Table 4. The atomic positions and isotropic-equivalent displacement parameters are given in Table 5. A summary of selected bond lengths and the N-C-N bond angle are given in Table 6.

The crystal structure of lanthanum chloride cyanamide was found to be related to LaOCl (PbFCl type) [53]. The structures of lanthanide oxide halides such as LnOX [57] (Ln = lanthanide and X = Cl, Br, I), lanthanide fluoride sulfides [58], dysprosium oxide fluoride sulphide [59], and lanthanum oxide nitrate [60] are some of the examples with a related PbFCl structure. The majority of the LnOX (X = Cl, Br, I) compounds exist in the tetragonal PbFCl structure type (Ln = La – Ho) while their heavier ones (Ln = Er – Lu) exist in the rhombohedral SmSI type. The structural features of all these compounds are their $[M_2X_2]$ or $[M_2O_2]$ block layers arranged in an alternating sequence with anionic layers in different ways. A more general concept for the description of such structures has been provided by *Sillén* [61] for oxide halides. The concept of *Sillén* is worthwhile when different numbers of individual layers and layer sequences are involved. *Sillén* adopted the notation X_n ($n = 1, 2, 3$) to indicate the number of (n) halide layers separating the $[M_2O_2]$ block layers, e.g. for the X_2 -type BiOI [62]. The oxygen atoms can be replaced by fluoride, as is the case of the X_2 -type PbFX (X = Cl, Br). The structures of PbFCl and PbFBr [63] were the first to be characterized by X-ray diffraction techniques within this structure family. The tetragonal $La_2O_2(CN_2)$ [35] structure is also containing a block layer of $[La_2O_2]^{2+}$ ions and one layer of disordered $(CN_2)^{2-}$ ions arranged in an alternating sequence, thus can be assigned to the *Sillén* X_1 -type. The employment of a LiCl-KCl flux [64] adopted from the syntheses of LnOCl compounds with Ln = Y, Ho, Er, Tm, Yb was considered as being favorable for the crystal growth of $LaCl(CN_2)$. The unit cells of $LaCl(CN_2)$ and LaOCl are shown in Figure 12.

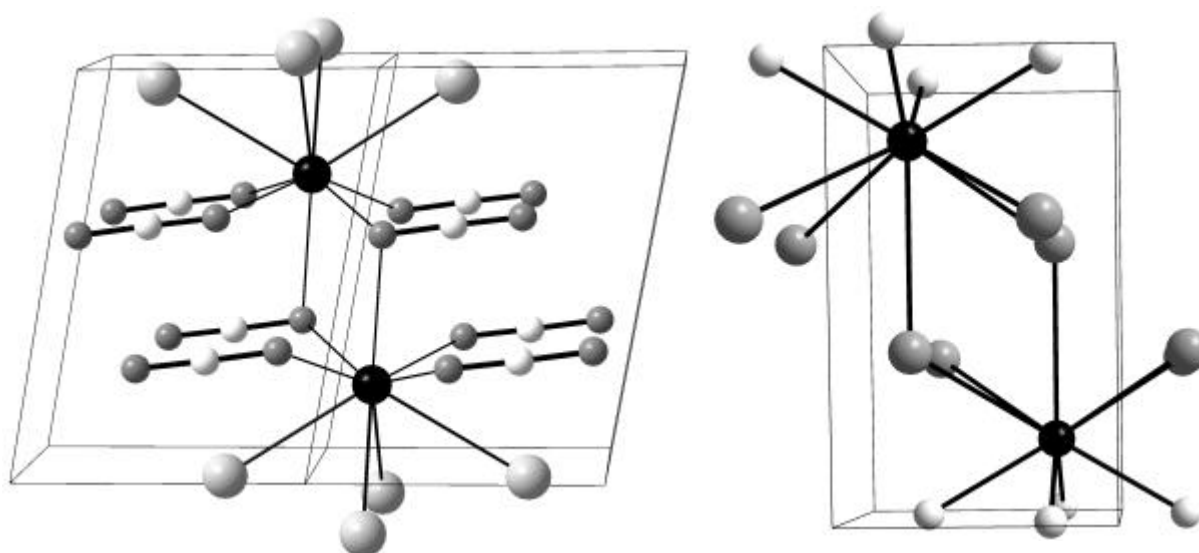


Figure 12. The unit cells of $LaCl(CN_2)$ (left) and LaOCl (right). Lanthanum atoms are shown black, nitrogen and chlorine atoms dark grey, carbon atoms white and oxygen atoms light grey.

The LaOCl structure corresponds to a *Sillén* X₂-type structure where two layers of Cl ions are arranged in an alternating sequence with one [La₂O₂]²⁺ block layer. Similarly, the structure of LaCl(CN₂) contains two layers of cyanamide ions arranged in an alternating sequence with one [La₂Cl₂]⁴⁺ block layer as shown in Figure 13 [53].

In the structure of LaCl(CN₂), the La³⁺ ion in LaCl(CN₂) is situated in a polyhedron composed of four chloride ions on one side and five cyanamide ions on the other side. The coordination number of La³⁺ ion in LaCl(CN₂) and LaOCl is nine, having the typical coordination pattern that is well known for Pb in the PbFCl structure type are compared in Figure 14. The asymmetrical coordination environment around the (CN₂)²⁻ unit with three lanthanum neighbors from one side and two lanthanum neighbors from the other side is shown in Figure 15. In LaCl(CN₂), the (CN₂)²⁻ unit is a cyanamide ion in contrast to the carbodiimide ion in La₂Cl(CN₂)N, possessing two equal C–N bond lengths of 1.234 Å. The variations within the C–N bond lengths and the NCN angle of the (CN₂)²⁻ ion in LaCl(CN₂) are slightly outside the 3σ limit (1.251(6) Å and 1.202(6) Å, and 178.8(5)°), and thus represents a cyanamide rather than a carbodiimide ion. In spite of the similar C–N bond lengths, the presence of the ν_s vibration indicates a cyanamide for LaCl(CN₂) which is not observed in the carbodiimide containing compound La₂Cl(CN₂)N (Table 2). However, we note that the borderline between both forms of these ions can be fluent. The average La–N bond distance of 2.607 Å in LaCl(CN₂) is slightly longer than that of 2.502 Å in La₂Cl(CN₂)N. The corresponding average La–Cl distance of 3.096 Å in LaCl(CN₂) is shorter than that of 3.239 Å in La₂Cl(CN₂)N.

4. 2. 6. Isotypic compounds within this structure type

Synthesis of LnCl(CN₂) type compounds were also performed by adding AlCl₃ to a 1:2 molar reaction mixture of (unsublimed) LnCl₃ (Ln = La, Ce, Pr) and Li₂(CN₂) in a silica ampoule at 600 °C over two days. The silica ampoules used for the reactions were positioned in such a way that the cooler end resided outside the Simon-Müller furnace to induce a temperature gradient. The lanthanide chloride cyanamides remained at the hot end while AlOCl and AlCl₃ sublimed to the cold end of the silica tube. LnCl(CN₂) phases were obtained as main products in these reactions, as determined by X-ray powder patterns. The indexed cell parameters of LnCl(CN₂) with Ln = La, Ce, and Pr are presented in Table 7 [53].

Table 4. Crystallographic data of LaCl(CN₂).

Space group (no.), Z	P2 ₁ /m (11), 2
Lattice constants /Å, angle /°	$a = 5.330(1)$, $b = 4.0305(8)$, $c = 7.545(1)$, $\hat{a} = 100.75(2)$
Cell volume /Å ³	159.24(5)
Density calc. /g·cm ⁻³	4.471
Molecular weight /g·mol ⁻¹	214.38
Crystal appearance	transparent colourless plates
Crystal size /mm ³	0.12 x 0.12 x 0.04
Diffractometer	STOE, IPDS
Radiation, temperature	Mo-K _α ($\lambda = 0.71073$ Å ³), graphite monochromator, 293(2) K
Range: θ /°	3.89 to 30.44
Index range	$-7 \leq h \leq 7$, $-5 \leq k \leq 5$, $-10 \leq l \leq 10$
Data correction	Lorentz, polarisation and absorption
μ /mm ⁻¹	13.98
Collected reflections ($F_0 > 2\sigma(F_0)$)	3021
Unique reflections	513
Parameters refined	31 (all atoms refined anisotropically)
R indices (all data)	$R1^a = 0.0215$, $wR2^b = 0.0506$
Final R indices [$I > 2\sigma(I)$]	$R1^a = 0.0195$, $wR2^b = 0.0496$
Goof (all reflections)	0.961
Res. peak: max.; min. /e/Å ³	1.265, -1.235

$$^a R1 = \sum ||F_o| - |F_c|| / \sum |F_o|; ^b wR2 = [\sum w(F_o^2 - F_c^2)^2 / [\sum w(F_o^2)^2]]^{1/2}$$

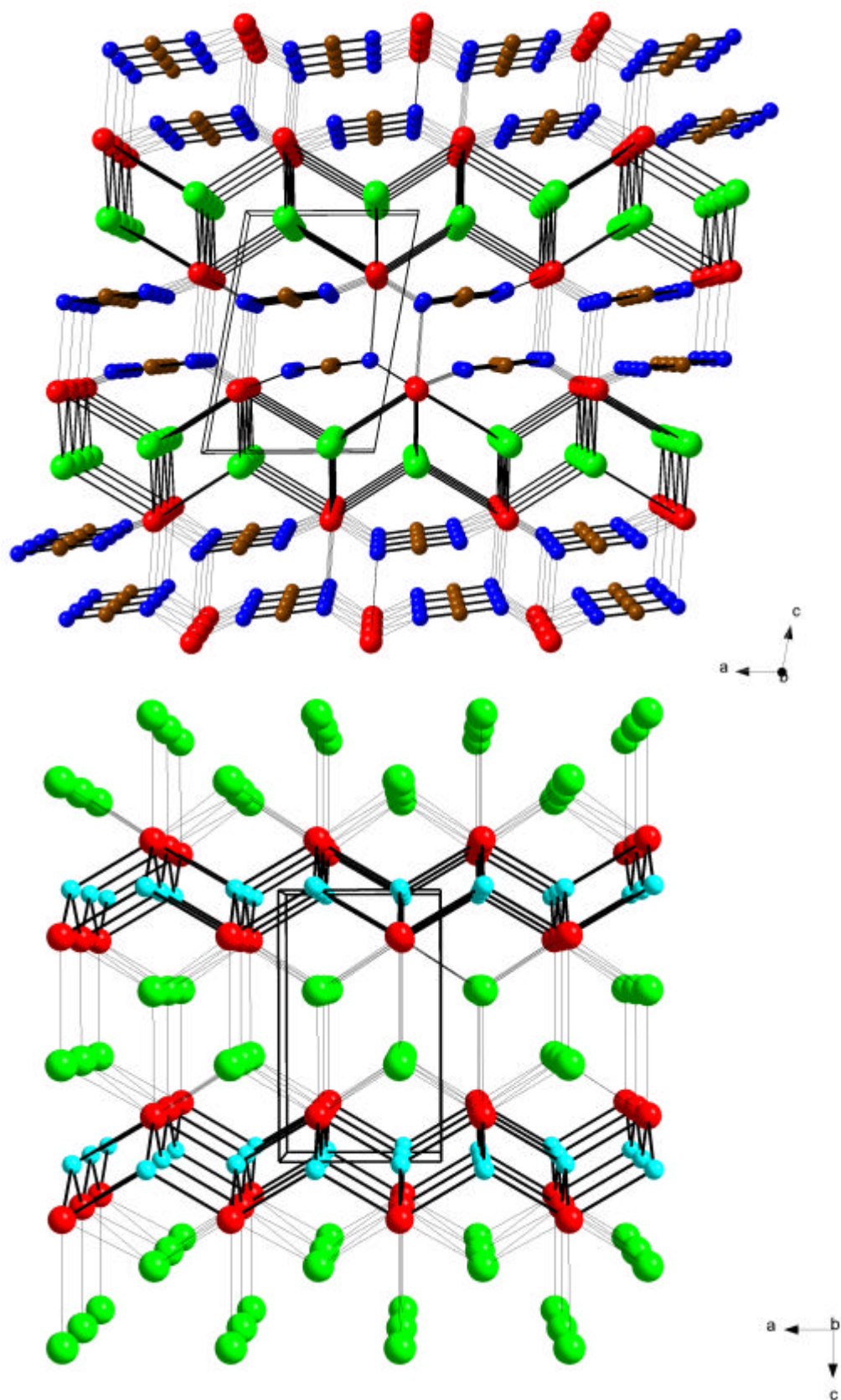


Figure 13. Perspective view of the structures of LaCl(CN₂) and LaOCl. Lanthanum atoms are shown red, nitrogen atoms blue, carbon atoms brown and oxygen atoms cyan.

Table 5. Atomic coordinates and isotropic-equivalent displacement parameters (\AA^2) for $\text{LaCl}(\text{CN}_2)$.

Atom	Multiplicity, symmetry	x	y	z	U_{eq}^a
La	2 m	0.82426(4)	0.25	0.26333(3)	0.0095(1)
Cl	2 m	0.7442(2)	-0.25	-0.0435(2)	0.0136(2)
N1	2 m	1.1213(7)	-0.25	0.3814(6)	0.0124(7)
N2	2 m	0.5671(7)	-0.25	0.3405(6)	0.0130(7)
C	2 m	0.6521(8)	-0.75	-0.3588(6)	0.0111(7)

^a U_{eq} is defined as one-third of the trace of the orthogonalized U_{ij} tensor.

Table 6. Bond lengths (\AA) and bond angle ($^\circ$) in $\text{LaCl}(\text{CN}_2)$.

La–N1	2.614(3)	x2
La–N1	2.642(4)	x1
La–N2	2.565(2)	x2
La–Cl	3.0385(9)	x2
La–Cl	3.077(1)	x1
La–Cl	3.172(1)	x1
C–N1	1.251(6)	x1
C–N2	1.202(6)	x1
N2–C–N1	178.8(5)	

Table 7. Cell parameters (in \AA) and volumes (in \AA^3) from the indexed powder patterns of $\text{LnCl}(\text{CN}_2)$ system for Ln = La, Ce, and Pr.

Ln	<i>a</i>	<i>b</i>	<i>c</i>	<i>b</i> ($^\circ$)	<i>V</i>	No. of indexed lines
La	5.3297(6)	4.0299(5)	7.545(1)	100.711(9)	159.23(5)	56
Ce	5.322(3)	4.022(2)	7.530(5)	100.75(4)	158.3(2)	35
Pr	5.296(2)	3.934(1)	7.460(2)	100.43(1)	152.8(1)	21

The lanthanide contraction obtained in the trend of cell parameters suggests that the compounds are isostructural. Hence in these reactions, the LnCl_3 $\text{Ln} = \text{La, Ce, Pr}$ can be either purified with AlCl_3 before starting the reaction or can be used in-situ to obtain their respective cyanamide halides as explained above.

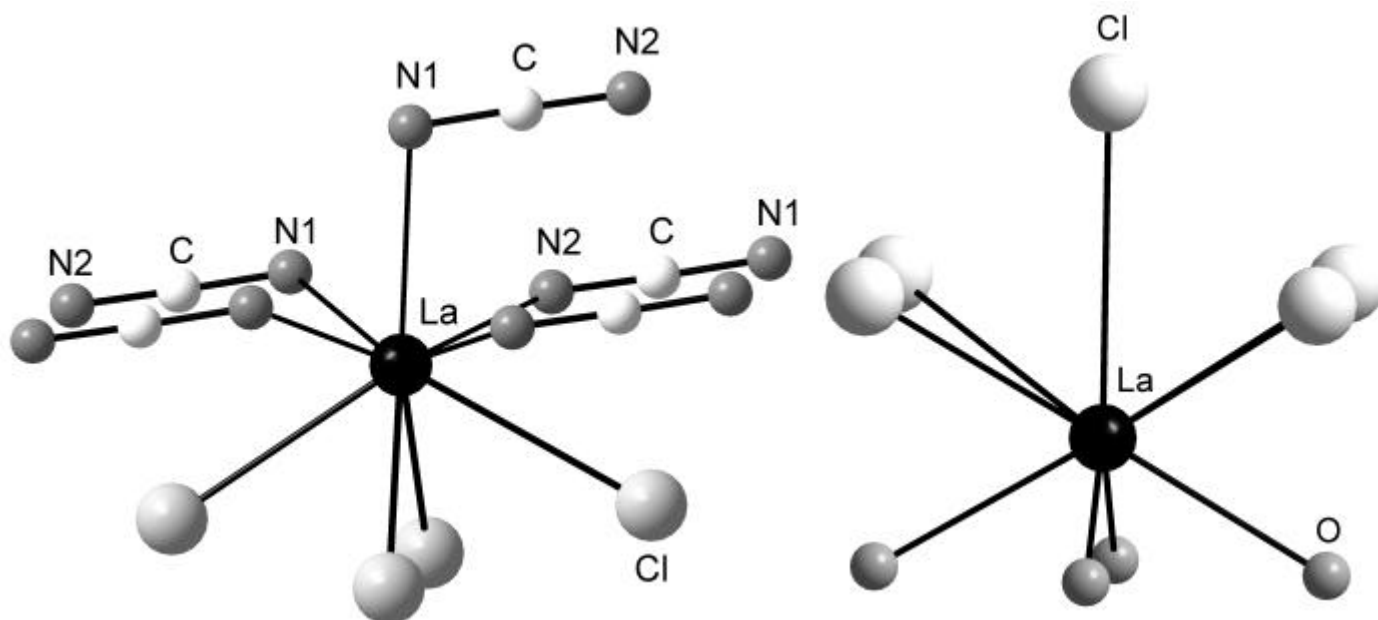


Figure 14. Coordination arrangement of the La atom in $\text{LaCl}(\text{CN}_2)$ and LaOCl .

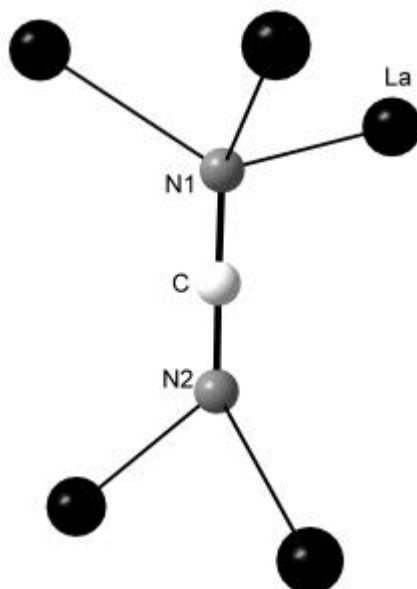
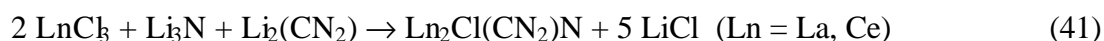


Figure 15. Coordination environment around the cyanamide ion.

4. 3. Synthesis, structure and characterisation of $\text{Ln}_2\text{X}(\text{CN}_2)\text{N}$ with $\text{La} = \text{La, Ce, Pr, Nd,}$ and Gd , $\text{X} = \text{Cl, Br, and I}$

4. 3. 1. Reaction between LnCl_3 , $\text{Li}_2(\text{CN}_2)$, and Li_3N

The tantalum capsule containing starting material LnCl_3 with $\text{Ln} = \text{La, Ce}$ and $\text{Li}_2(\text{CN}_2)$ in the ratio 2:3 was jacketed with quartz under vacuum. The quartz fused tantalum ampoule was heated with a rate of 2 °C per minute to 950 °C. After four days, the temperature was slowly (with in six hours) reduced to room temperature. Single crystals were obtained as yellow needles for $\text{Ln} = \text{La}$ and as black needles for $\text{Ln} = \text{Ce}$ along with LiCl as a side product, that can be washed off with water. After the compositions of the new products were established from single crystal diffraction, high purity phases were obtained from stoichiometric 2:1:1 molar reactions of LnCl_3 , Li_3N , and $\text{Li}_2(\text{CN}_2)$ respectively at 800 °C over one day according to the reaction 41.



The synthesis can be well performed in the temperature range of 750–800 °C for one or two days to obtain good crystalline powders. The powder patterns were successfully indexed with an orthorhombic unit cell that could not be addressed to any known compound in a related system. Consequently the crystal structures of $\text{La}_2\text{Cl}(\text{CN}_2)\text{N}$ and $\text{Ce}_2\text{Cl}(\text{CN}_2)\text{N}$ [55] were determined from single crystal X-ray diffraction data. The X-ray diffraction patterns of the products were consistent with the calculated pattern from the single crystal structure refinements and contained a few weak unidentified reflections besides those of LiCl as shown in Figure 16.

4. 3. 2. Reaction between LnBr_3 , $\text{Li}_2(\text{CN}_2)$, and Li_3N

Greenish yellow crystalline powder of $\text{Ln}_2\text{Br}(\text{CN}_2)\text{N}$ with $\text{Ln} = \text{La, Pr}$ were obtained from 2:1:1 stoichiometric ratio of LnBr_3 , $\text{Li}_2(\text{CN}_2)$ and Li_3N respectively at 750 °C over one or two days using sealed copper ampoules as a container jacketed with quartz ampoule according to the reaction 42.



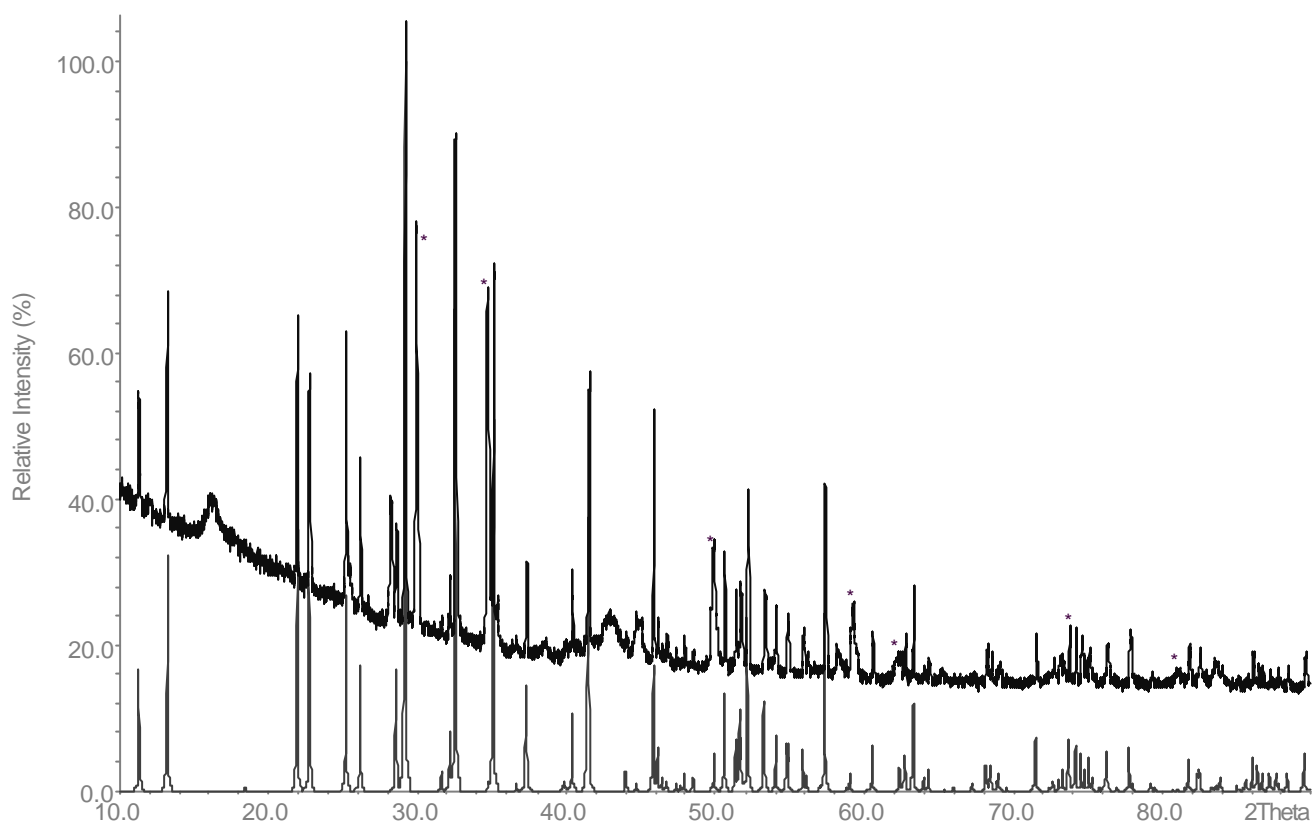


Figure 16. The calculated powder pattern from single crystal data (below) is compared with the measured X-ray powder pattern (above) of $\text{La}_2\text{Cl}(\text{CN}_2)\text{N}$ containing LiCl (*).

Single crystals of $\text{La}_2\text{Br}(\text{CN}_2)\text{N}$ suitable for measurement were obtained, when one equivalent of lithium metal was used in the 1:1 reaction mixture of LaBr_3 and $\text{Li}_2(\text{CN}_2)$. The reaction mixture was slowly heated to $850\text{ }^\circ\text{C}$ and kept at this temperature for four days before cool down to room temperature over the period of six hours. The major product, lanthanum bromide carbodiimide nitride was found along with some LaOBr and LiBr . Single crystals of $\text{Pr}_2\text{Br}(\text{CN}_2)\text{N}$ suitable for measurements were obtained, when 2:3 molar ratio of PrBr_3 and $\text{Ca}(\text{CN}_2)$ respectively were reacted at $850\text{ }^\circ\text{C}$ in a sealed tantalum ampoule jacketed with an quartz ampoule for four days and cool down slowly to room temperature.

The powder patterns of $\text{Ln}_2\text{Br}(\text{CN}_2)\text{N}$ $\text{Ln} = \text{La}$, and Pr were indexed to the analogues cell parameters of $\text{La}_2\text{Cl}(\text{CN}_2)\text{N}$. The crystals of bromide phases without the deficiency of bromide ion in the crystal structure refinements were difficult to obtain. Only by adding one equivalent of lithium metal, well developed crystals of $\text{La}_2\text{Br}(\text{CN}_2)\text{N}$ having full occupancy of bromide ion in the channels of the structure were obtained.

4. 3. 3. Reaction between LaI_3 , $\text{Li}_2(\text{CN}_2)$, and Li_3N

A greenish yellow powder of $\text{La}_2\text{I}(\text{CN}_2)\text{N}$ was obtained by treating 2:1:1 stoichiometric ratio of LaI_3 , $\text{Li}_2(\text{CN}_2)$, and Li_3N at $700\text{ }^\circ\text{C}$ for one or two days. The reactions were performed in a quartz sealed copper ampoule. The single crystals were selected from the batch, when 1:2 molar ratio of LaI_3 and $\text{Li}_2(\text{CN}_2)$ respectively along with one equivalent of lithium were reacted at $750\text{ }^\circ\text{C}$ for seven days in a quartz sealed copper ampoule and cool down within seven hours to attain room temperature.

The powder pattern contained $\text{La}_2\text{I}(\text{CN}_2)\text{N}$ as a major phase with some LaOI besides LiI . The powder patterns of $\text{La}_2\text{I}(\text{CN}_2)\text{N}$ were indexed to the analogues cell parameters of $\text{La}_2\text{Cl}(\text{CN}_2)\text{N}$. Here also the crystals of iodide phases with out the deficiency of iodide ion in the crystal structure refinements were difficult to obtain. Only by adding one equivalent of lithium metal, well developed crystals suitable for single crystal X-ray measurements were obtained with maximum occupancy of 92% iodide in the channels of the structure.

All the lanthanide halide carbodiimide nitride explained above were air as well as water stable and hence the side product LiX can be washed off easily by water or other polar solvents to obtain pure materials. The purity of LaX_3 and $\text{Li}_2(\text{CN}_2)$ was vital to obtain the compounds in all these above mentioned synthesis as a major phase, whereas oxide impurities drove reactions more towards lanthanide oxide halide and oxide cyanamide with low yields of desired products.

4. 3. 4. Thermal analysis (DTA/TG) of the reaction between LaX_3 with $\text{X} = \text{Cl}$ and Br , $\text{Li}_2(\text{CN}_2)$, and Li_3N

To understand the mechanism of the reaction, the thermal analysis followed by X-ray powder diffraction studies were performed for reactions with LaC_3 . The DTA/TG of the 2:1:1 stoichiometric reaction of LaC_3 , $\text{Li}_2(\text{CN}_2)$, and Li_3N respectively exhibits an exothermic effect near $475\text{ }^\circ\text{C}$, as shown in Figure 17A [55], that is consistent with the results on the formation of LaN or La_2NC_3 as shown in Figure 7. An endothermic effect near $600\text{ }^\circ\text{C}$ in this DTA corresponds to the melting of LiCl . Consequently the X-ray powder pattern of the reaction mixture heated at $600\text{ }^\circ\text{C}$ indicated the presence of LiCl and La_2NC_3 besides (nearly) X-ray amorphous material.

The supposed intermediate La_2NC_3 [51], prepared from a 2:1 molar mixture of LaC_3 and

Li₃N at 600 °C (reaction 43), was successfully reacted with Li₂(CN₂) to form La₂Cl(CN₂)N plus LiCl (reaction 44) at 800 °C over one day. Due to the presence of LaCl₃ in the reaction, part of the Li₂(CN₂) decomposes to form La₂NCl₃ as concluded from the above combined thermal and X-ray diffraction studies and further reacts to yield the product as shown in the reaction 44.



The metathesis reaction between LaCl₃ and Li₂(CN₂) in 2:3 molar ratio at ≥750 °C leads to La₂Cl(CN₂)N instead of the hypothetical ‘La₂(CN₂)₃’.

The DTA/TG for the 2:1:1 stoichiometric reaction of LaBr₃, Li₂(CN₂), and Li₃N respectively exhibits an exothermic effect near 450 °C, as shown in Figure 16B. This is consistent with the exothermic peak obtained from stoichiometric ratio of 2:1 LaBr₃ and Li₃N respectively. Hence this peak is assumed for the formation of La₂NBr₃ similar to La₂NCl₃. According to the literature, La₂NBr₃ is isotopic to Ce₂NBr₃ [65]. The obtained yellow powder after DTA was indexed to the analogues tetragonal cell. An endothermic effect near 550 °C in these DTA corresponds to the melting of LiBr.

However the presence of an exothermic peak at around 480 °C in the DTA/TG of the reaction between 1:1 LaCl₃ and Li₂(CN₂) shown in Figure 8, suggests that the formed lanthanum chloride cyanamide may be an intermediate of La₂Cl(CN₂)N. As expected, the DTA/TG decomposition reaction of LaCl(CN₂) (Figure 9) clearly indicated the transformation of LaCl(CN₂) into La₂Cl(CN₂)N at the temperature around 650-700° C. Consequently the X-ray powder pattern was measured for the obtained greyish black powder and the reflections were successfully indexed to the cell parameters of La₂Cl(CN₂)N. Further the equimolar reaction between LaCl₃ and Li₂(CN₂) carried out separately in a tantalum container also resulted the same product of La₂Cl(CN₂)N at temperatures 750-800 °C over the period of four days.

Therefore, the mechanism of the reaction proceeds via intermediate LaCl(CN₂) in the absence of Li₃N at comparatively low temperatures (500 - 650 °C), which undergoes transformation to La₂Cl(CN₂)N at higher temperatures (≥750 °C).

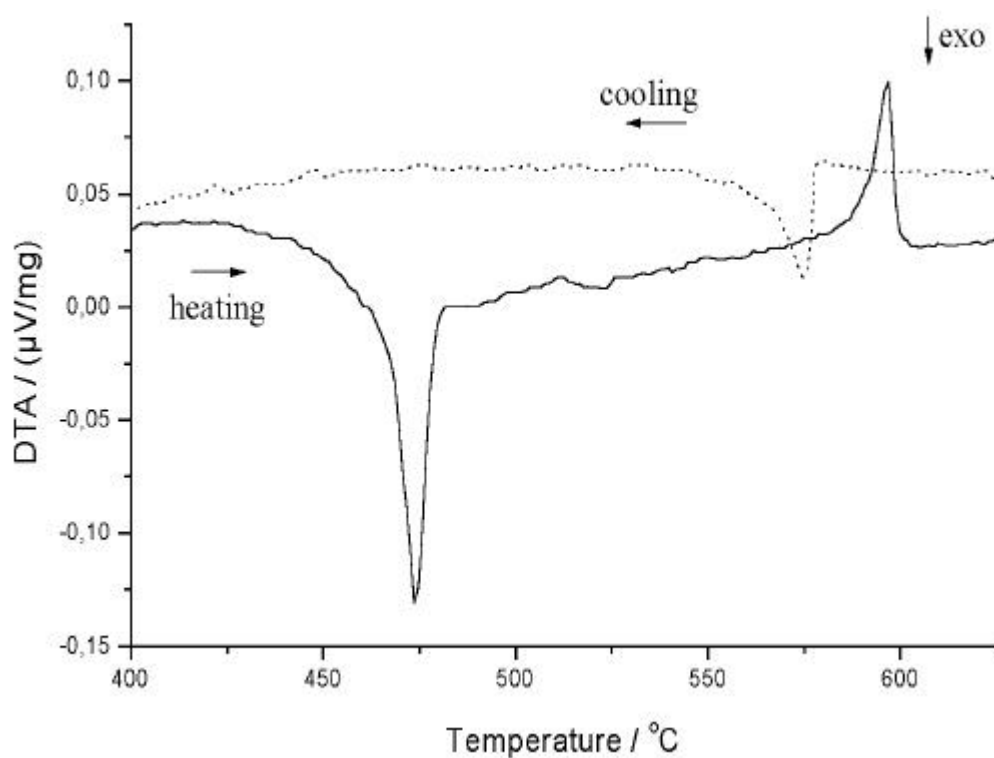
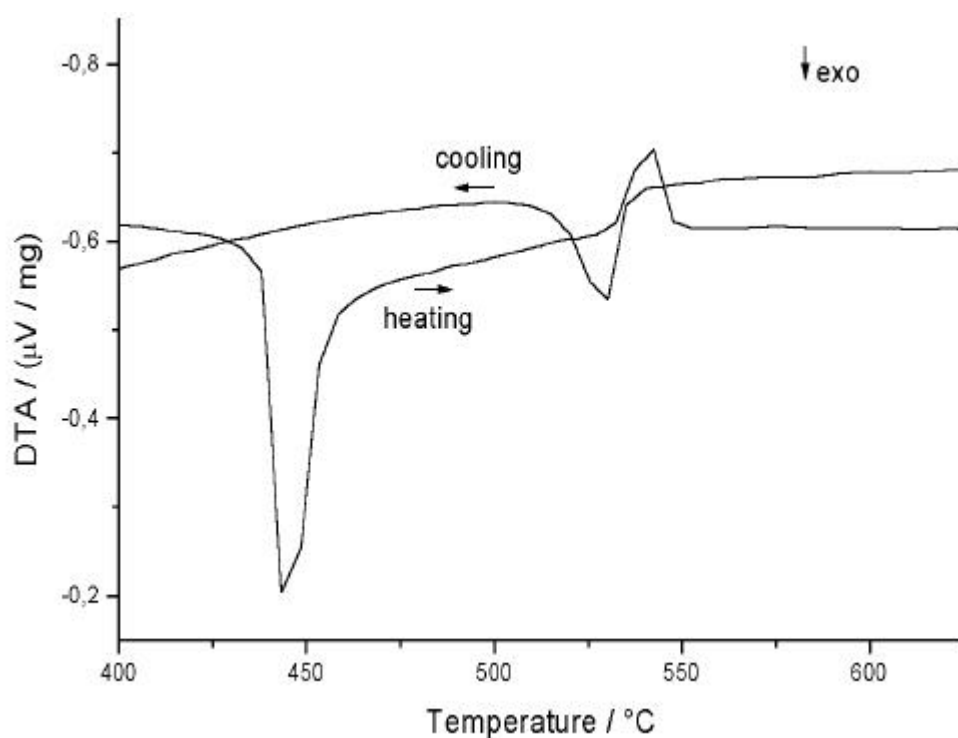
A**B**

Figure 17(A). DTA of the 2:1:1 stoichiometric reaction between LaC_3 , $\text{Li}_2(\text{CN}_2)$, and Li_3N heated upto $800\text{ }^{\circ}\text{C}$. **(B).** DTA of the 2:1:1 stoichiometric reaction between LaBr_3 , $\text{Li}_2(\text{CN}_2)$, and Li_3N heated upto $800\text{ }^{\circ}\text{C}$. (Shown is only the temperature interval of $400 - 625\text{ }^{\circ}\text{C}$).

Eventually in the presence of Li_3N , the formation of La_2NCl_3 as an intermediate is more probable as mentioned earlier in the reaction 43 and 44. When stoichiometric 3:3:1 reaction mixture of LaCl_3 , $\text{Li}_2(\text{CN}_2)$ and Li_3N respectively was reacted at $650\text{ }^\circ\text{C}$ for two weeks in a quartz sealed tantalum ampoule, $\text{La}_2\text{Cl}(\text{CN}_2)\text{N}$ crystals were obtained [53] without the formation of $\text{LaCl}(\text{CN}_2)$.

Hence the reactivity of LaCl_3 and $\text{Li}_2(\text{CN}_2)$ in these reactions are controlled by different mechanistic pathways with the presence and absence of Li_3N .

The DTA/TG for the decomposition of $\text{La}_2\text{Cl}(\text{CN}_2)\text{N}$ was studied in an open system upto $1000\text{ }^\circ\text{C}$. Decomposition was observed only at $>800\text{ }^\circ\text{C}$ and the subsequent X-ray powder pattern of the mixture shows the presence of La_2O_3 . When the reaction between 2 LaCl_3 and 3 $\text{Li}_2(\text{CN}_2)$ was performed in a quartz sealed tantalum ampoule, $\text{La}_2\text{Cl}(\text{CN}_2)\text{N}$ crystals were stable up to $1050\text{ }^\circ\text{C}$.

4. 3. 5. Infrared spectra of $\text{La}_2\text{Cl}(\text{CN}_2)\text{N}$

The characteristic vibrational frequencies of carbodiimide ions (strong peak around 2000 cm^{-1} for asymmetric stretching of NCN and peak around 625 cm^{-1} for bending mode) were detected from the infrared spectra of the lanthanide chloride carbodiimide nitride compounds and thereby confirmed the presence of the $(\text{CN}_2)^{2-}$ ions (Figure 10). The infrared spectra obtained from lanthanum chloride carbodiimide nitride is tabulated with the other carbodiimide compounds in Table 2.

4. 3. 6. Crystal structures of $\text{La}_2\text{X}(\text{CN}_2)\text{N}$ with $\text{X} = \text{Cl, Br, and I}$

Suitable single crystals of $\text{La}_2\text{X}(\text{CN}_2)\text{N}$ $\text{X} = \text{Cl, Br, I}$ for single crystal X-ray diffraction studies were selected under the microscope and mounted on the tip of glass fibers. The crystallographic data for $\text{La}_2\text{X}(\text{CN}_2)\text{N}$ $\text{X} = \text{Cl, Br, I}$ are given in Table 8. The atomic positions and isotropic-equivalent displacement parameters are given in Table 9. A summary of selected bond lengths is provided in Table 10. The unit cell of $\text{La}_2\text{X}(\text{CN}_2)\text{N}$ with $\text{X} = \text{Cl, Br, I}$ is shown in Figure 18. In the crystal structure of $\text{La}_2\text{I}(\text{CN}_2)\text{N}$, the iodide position was refined at 75% only.

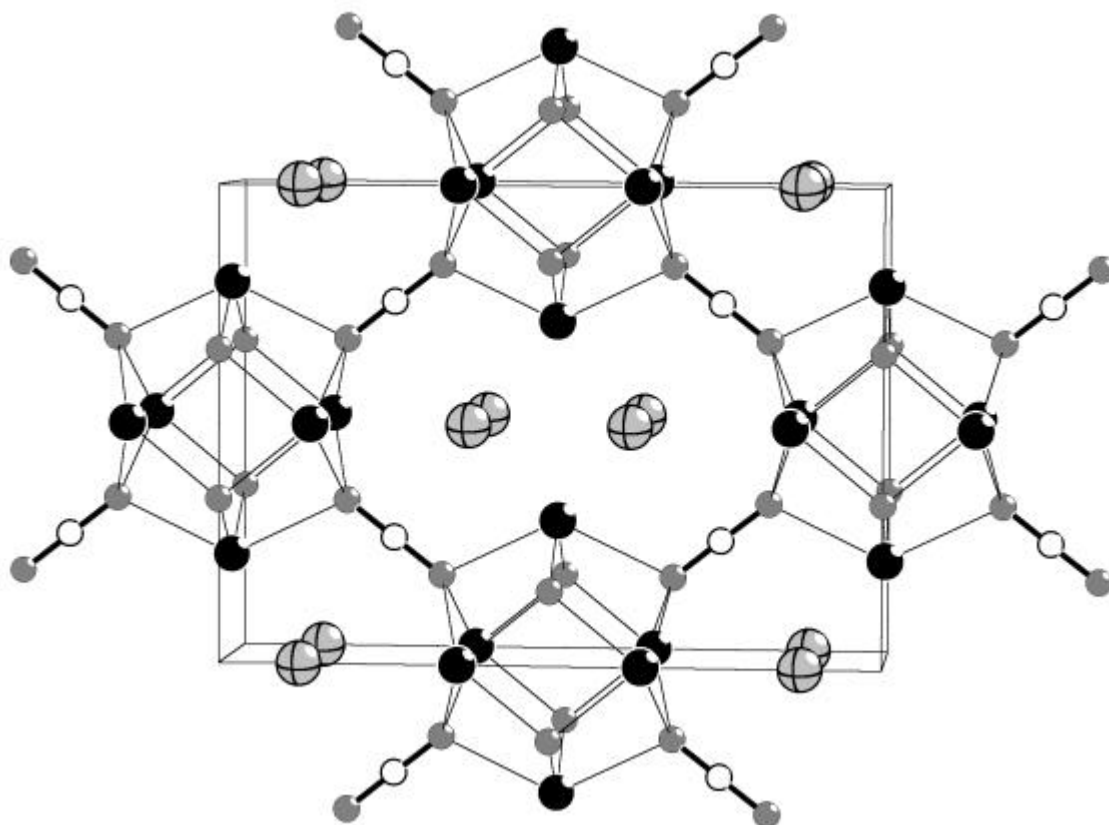


Figure 18. Unit cell of $\text{La}_2\text{X}(\text{CN}_2)\text{N}$ $\text{X} = \text{Cl, Br, I}$. Lanthanum atoms are shown black, halide atoms dark grey with cross, nitrogen dark grey and carbon atoms white.

The crystal structures of lanthanum halide carbodiimide nitride contain linear chains of edge-sharing octahedra built from lanthanum atoms. The basic building unit of $[\text{La}_6]$ octahedra is surrounded by ligands similar to the well-known $[\text{M}_6\text{X}_8]$ cluster type moiety, with face-capping atoms as shown in Figure 19 [55]. The building $[\text{La}_6(\text{CN}_2)_4\text{N}_4]$ units are connected with each other to form one-dimensional chains as shown in Figure 20. The individual chains are closely related to those in the lanthanide sesquihalide structures. All the octahedral faces are capped by eight nitrogen atoms from four N^{3-} , and four $(\text{NCN})^{2-}$ ions. The octahedra are linked via trans-edges to form chains, similar to those in Y_2Cl_3 [66], or rather $(\beta\text{-})\text{Y}_2\text{Cl}_3\text{N}$ [67].

Table 8. Crystallographic data of La₂X(CN₂)N.

	X = Cl	X = Br	X = I _{0.75}
Space group (no.), Z	Cmmm (no. 65), 4		
Unit cell dimension (in Å)	a = 13.3914(8) b = 9.6345(7) c = 3.9568(2)	a = 13.6177(15) b = 9.6868(12) c = 3.9697(4)	a = 13.935(1) b = 9.832(1) c = 4.0348(4)
Cell volume (in Å ³)	510.50(5)	523.65(10)	552.8(1)
Density calc. (g/cm ³)	4.779	5.223	5.323
Molecular weight (g/mol)	367.31	411.77	458.71
Crystal appearance	Transparent yellow needles	Greenish yellow needles	Greenish yellow needles
Crystal size (in mm ³)	0.02 x 0.02 x 0.15	0.02 x 0.02 x 0.1	0.02 x 0.02 x 0.2
Diffractometer	STOE, IPDS		
Radiation, Temperature	Mo-K _α (λ = 71.073 pm), Graphite Monochromator, 293(2) K		
Range: θ	4.23 → 32.86 ⁰	4.21 → 30.18 ⁰	4.15 → 32.69 ⁰
Range: h, k, l	-20 ≤ h ≤ 20 -14 ≤ k ≤ 14 -5 ≤ l ≤ 5	-19 ≤ h ≤ 19 -13 ≤ k ≤ 13 -5 ≤ l ≤ 5	-21 ≤ h ≤ 20 -14 ≤ k ≤ 14 -6 ≤ l ≤ 5
Data correction	Lorentz, polarisation and absorption		
μ (mm ⁻¹)	16.884	23.581	19.321
Reflections collected, Unique	5224, 552	3658, 475	4261, 617
Observed reflections (F ₀ > 4σ(F ₀))	491	432	598
Parameters refined(all atoms refined anisotropically)	27	27	29
R1, wR2 (all reflections)	0.0232, 0.0467	0.0200, 0.0485	0.0220, 0.0484
GooF (all reflections)	1.132	1.129	1.174
Res. peak: max., min. (e/Å ³)	1.124, -1.78	1.110, -1.129	1.813, -2.010
Structure solution	SHELXS-97 (direct method),		
Strucutre refinement	SHELXL-97 (full matrix least squares calculations on F ²)		

$$^a R1 = \sum ||F_o| - |F_c|| / \sum |F_o|; ^b wR2 = [\sum w(F_o^2 - F_c^2)^2 / [\sum w(F_o^2)^2]]^{1/2}$$

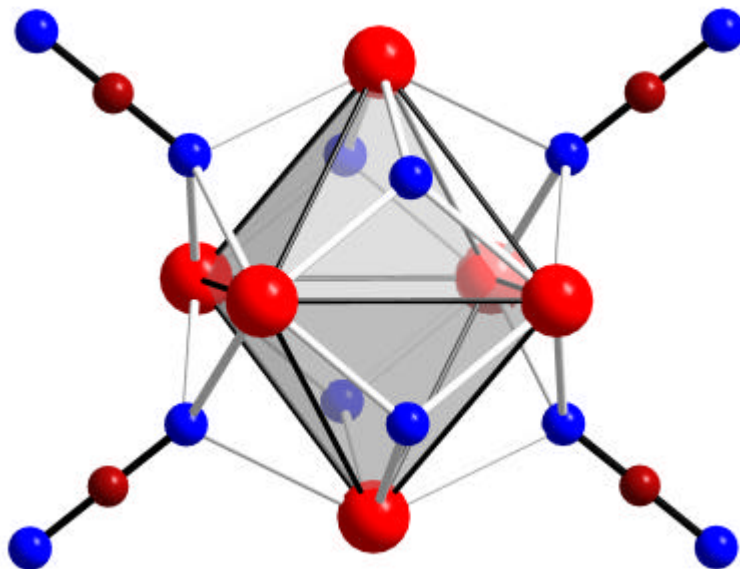


Figure 18. Basic building unit $[\text{La}_6(\text{CN}_2)_4\text{N}_4]$. Lanthanum atoms are shown red, nitrogen atoms blue and carbon atoms brown.

In the structures of $(\beta\text{-})\text{Y}_2\text{Cl}_3\text{N}$, as well as in the lanthanum halide carbodiimide nitride, the nitride ions occupy tetrahedral interstices above and below the shared edge along the chain of (La_6) octahedra as shown in Figure 20. In a different view, the structure can be considered to contain double chains of (NLa_4) tetrahedra as shown in Figure 21. The one-dimensional chain of $[\text{La}_6]$ octahedra shown in Figure 20 are interconnected by bridging CN_2^{2-} ions to form a beautiful three dimensional network structure with linear channels occupied by halide ions, as shown in Figure 22. Due to the increase of the ionic radii from Cl to I, the corresponding cell parameters and atomic distances in bromide and iodide phases are increased.

The C–N distances (in Å) and N–C–N angle are of consistent values with 1.234(3) for chloride phase, 1.236(5) for the bromide phase and 1.244(3) for the iodide phase and 180° ($D_{\infty h}$ symmetry) respectively. The average C–N distance (in Å) and NCN angle in $\text{LaCl}(\text{CN}_2)$ are 1.227 and 178.8° respectively.

In $\text{LaCl}(\text{CN}_2)\text{N}$, the presence of relatively long La–Cl [68] distances of the chloride phase (1 x 3.2026(2) Å, 4 x 3.2754(8) Å) in the channels gave rise to the possibility for occupation of bromide and iodide ions instead of chloride ion. As expected, the channels were occupied by bromide and iodide ions and their distances from La atoms are slightly longer in comparison to La–Cl distances. A section of channels from Figure 22 is rotated by 90° and the occupation of halide ion in the channels are shown in Figure 23. The distance between La2 and La2 in

Figure 23 are varying from 4.1 - 4.3 Å and that between La1 and La1 from 9.7 - 10.2 Å respectively when the halide ion changes from Cl to I in La₂X(CN₂)N crystal structures.

Table 9. Atomic coordinates with equivalent displacement parameters (Å²) for La₂X(CN₂)N with X = Cl, Br, and I.

Atom	Multiplicity, symmetry	x	y	z	U _{eq} ^a
La1	4, 2mm	(Cl) 0.3612(2)	0	0	0.00866(9)
		(Br) 0.36311(3)	0	0	0.0104(1)
		(I) 0.3653(1)	0	0	0.0128(1)
La2	4, m2m	½	0.71113(3)	½	0.0095(1)
		½	0.71519(4)	½	0.0112(1)
		½	0.7209(1)	½	0.0114(1)
C	4, 2/m	¼	¼	½	0.0108(9)
		¼	¼	½	0.011(1)
		¼	¼	½	0.013(1)
N1	4, m2m	½	0.8434(5)	0	0.0093(8)
		½	0.8454(6)	0	0.012(1)
		½	0.8471(4)	0	0.0131(6)
N2	8, m	0.3226(3)	0.1713(3)	½	0.0128(6)
		0.3221(3)	0.1725(4)	½	0.0145(8)
		0.3212(2)	0.1737(3)	½	0.0153(5)
X	4, 2mm	0.1222(1)	0	0	0.0229(3)
		0.1257(1)	0	0	0.0182(2)
		0.1287(1)	0	0	0.0157(1)

^a U_{eq} is defined as one-third of the trace of the orthogonalized U_{ij} tensor.

Table 10. Selected bond distances (Å) in La₂X(CN₂)N with X = Cl, Br, and I.

Atoms	X = Cl	X = Br	X = I
La1–La1	3.7142(6)	3.7281(9)	3.8888(4)
La1–La2	3.8870(3)	3.8763(4)	4.0348(4)
La1–N1	2.393(3)	2.391(4)	2.369(2)
La1–N2	2.628(2)	2.654(3)	2.699(3)
La2–N1	2.353(2)	2.352(3)	2.405(3)
La2–N2	2.632(3)	2.655(5)	2.714(2)
La1–X	3.203(2)	3.2335(9)	3.2964(6)
La2–X	3.2754(8)	3.3486(5)	3.4648(4)
C–N2	1.234(3)	1.236(5)	1.244(3)
X–X	3.272(3)	3.425(3)	3.5878(8)

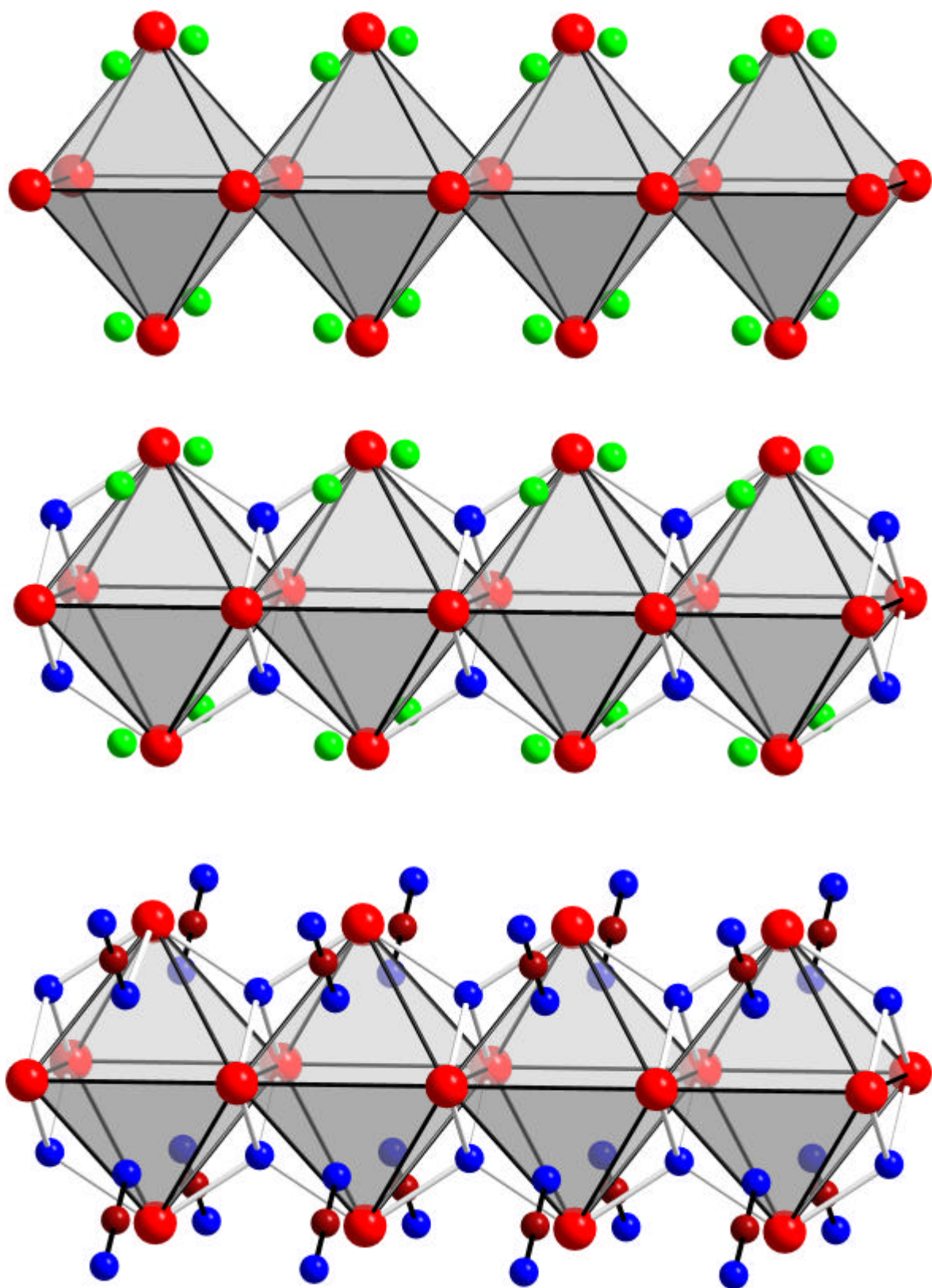


Figure 19. Sections of individual chains in the structures of Y_2Cl_3 (top), β - Y_2Cl_3N (center), and $La_2X(CN_2)N$ with $X = Cl, Br, I$ (below). Terminal chloride atoms over the corners of metal octahedra are always suppressed in the drawings. Metal atoms are shown red, chlorides green, nitrogen atoms blue, and carbon atoms brown.

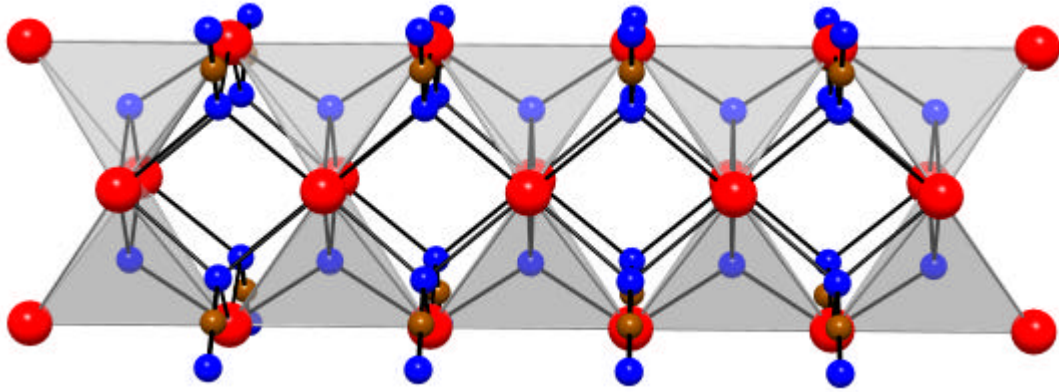


Figure 20. A section of double chains of tetrahedra in an alternative view.

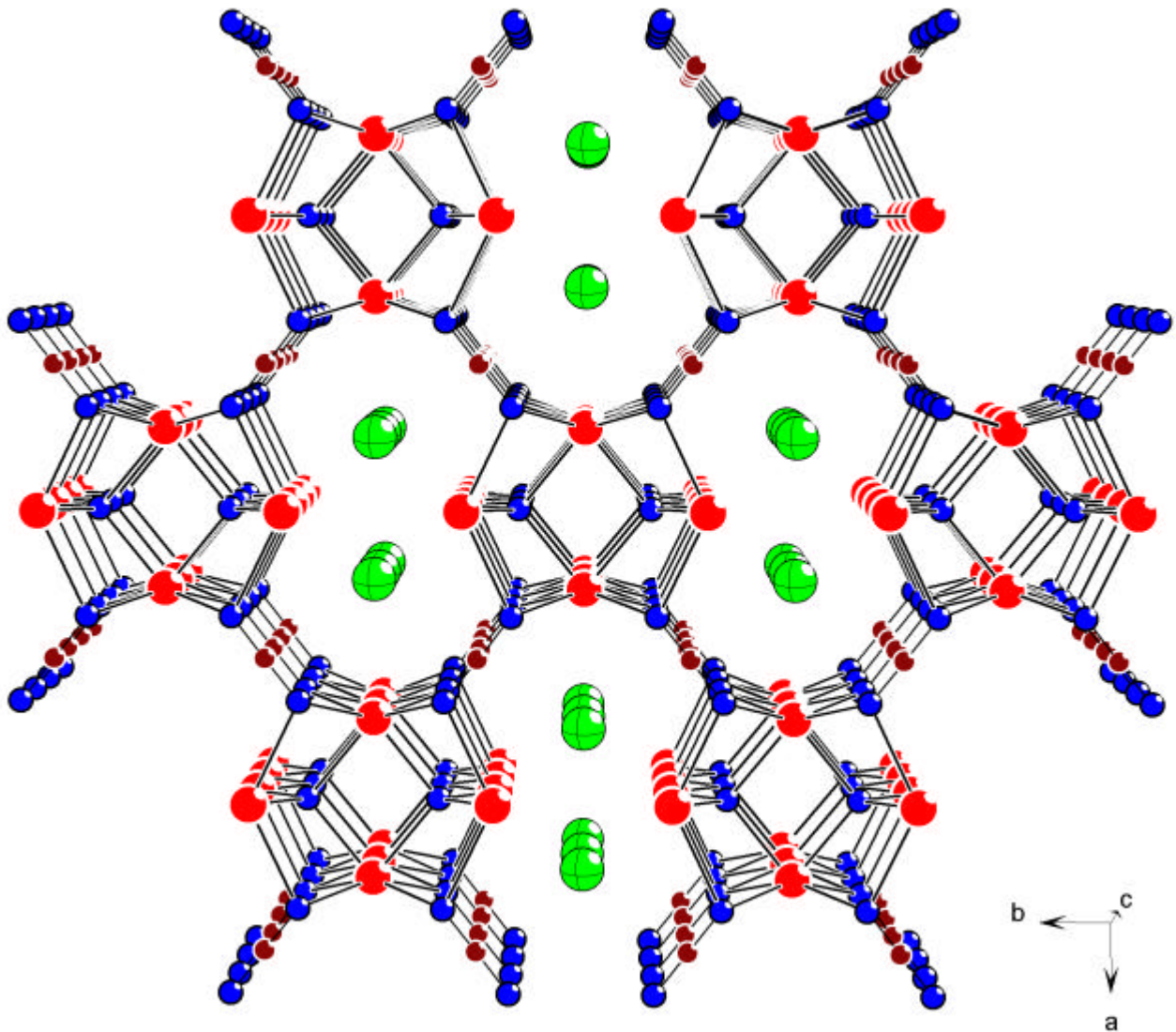


Figure 21. View of the $\text{La}_2\text{X}(\text{CN}_2)\text{N}$ ($\text{X} = \text{Cl}, \text{Br}, \text{I}$) structure parallel to the short c repeat of the chain direction showing the isolated halide ions in tunnels of the framework structure.

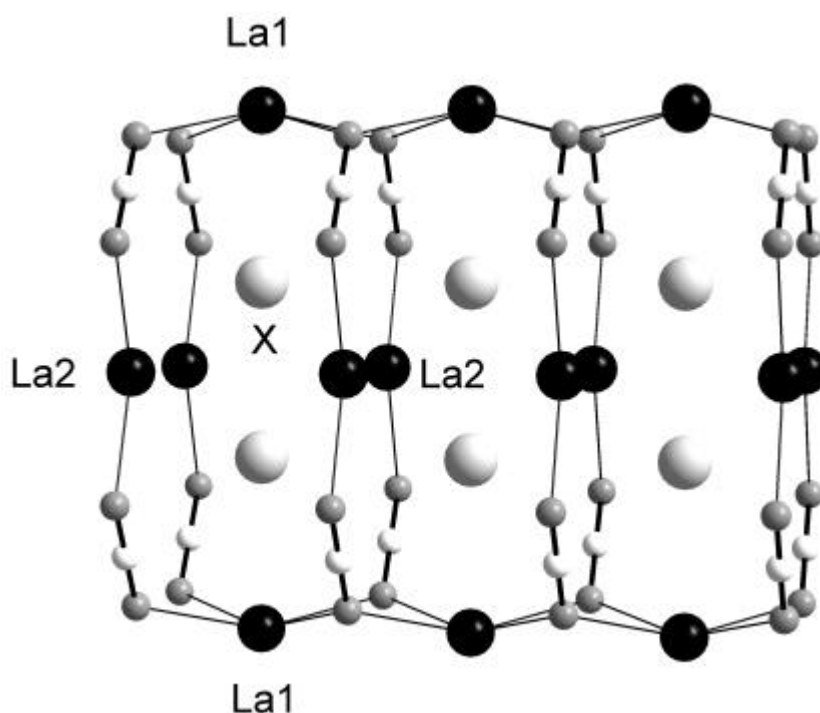


Figure 23. View of the positions of halide ions (X) in the structure of $\text{La}_2\text{X}(\text{CN}_2)\text{N}$ with $\text{X} = \text{Cl}, \text{Br}, \text{and I}$.

The halide-halide ion distances in $\text{La}_2\text{X}(\text{CN}_2)\text{N}$ ($\text{X} = \text{Cl}, \text{Br}, \text{I}$) crystal structures are similar to the van der Waals distances between adjacent X_2 units in solid halogens [69]. When the average La–X distances in $\text{La}_2\text{X}(\text{CN}_2)\text{N}$ ($\text{X} = \text{Cl}, \text{Br}, \text{I}$) crystal structures are compared with those of LaX_3 ($\text{X} = \text{Cl}, \text{Br}, \text{and I}$), the La–X distances are elongated by 0.2 Å in $\text{La}_2\text{Cl}(\text{CN}_2)\text{N}$ and in $\text{La}_2\text{Br}(\text{CN}_2)\text{N}$, but no difference noticed in $\text{La}_2\text{I}(\text{CN}_2)\text{N}$.

The La–La interatomic distance in the chloride and bromide phase along the shared edges are slightly shorter than in lanthanum metal (3.7142(6) Å and 3.7281(9) Å compared to 3.754 Å respectively). But in the case of iodide phase, a slightly longer distance of 3.8888(4) Å is observed due to the anion size. The octahedra are elongated along the chain direction and the distance between basal and apex atoms is 3.8870(3) Å for chloride phase, 3.8763(4) Å for bromide phase and 4.0348(4) Å for iodide phase as shown in Table 10. The average La–Cl distance (in Å) of 3.239 in $\text{La}_2\text{Cl}(\text{CN}_2)\text{N}$ is slightly longer than 3.096 in $\text{LaCl}(\text{CN}_2)$. The average La–N distance (in Å) of 2.502 in the chloride phase, 2.513 in the bromide phase, 2.547 in the iodide phase is in agreement with $\text{LaCl}(\text{CN}_2)$ (2.607 Å) and slightly lesser than in $\text{La}_2\text{O}_2(\text{CN}_2)$ (2.881 Å).

Coordination arrangement of lanthanum atoms

The La1 and La2 are having coordination numbers 7 and 8 respectively in $\text{La}_2\text{X}(\text{CN}_2)\text{N}$, when the adjacent La atoms are neglected. As shown in Figure 24, the La1 atom is having a distorted trigonal prismatic by N monocapped with Cl coordination environment. The La2 atom is coordinated in a square anti-prismatic fashion with four chloride ions and four nitrogen atoms (two from nitrides, N1 and the two from carbodiimides, N2). The symmetrical coordination environment on both sides of the carbodiimide unit by two different lanthanum atoms is also shown in Figure 24.

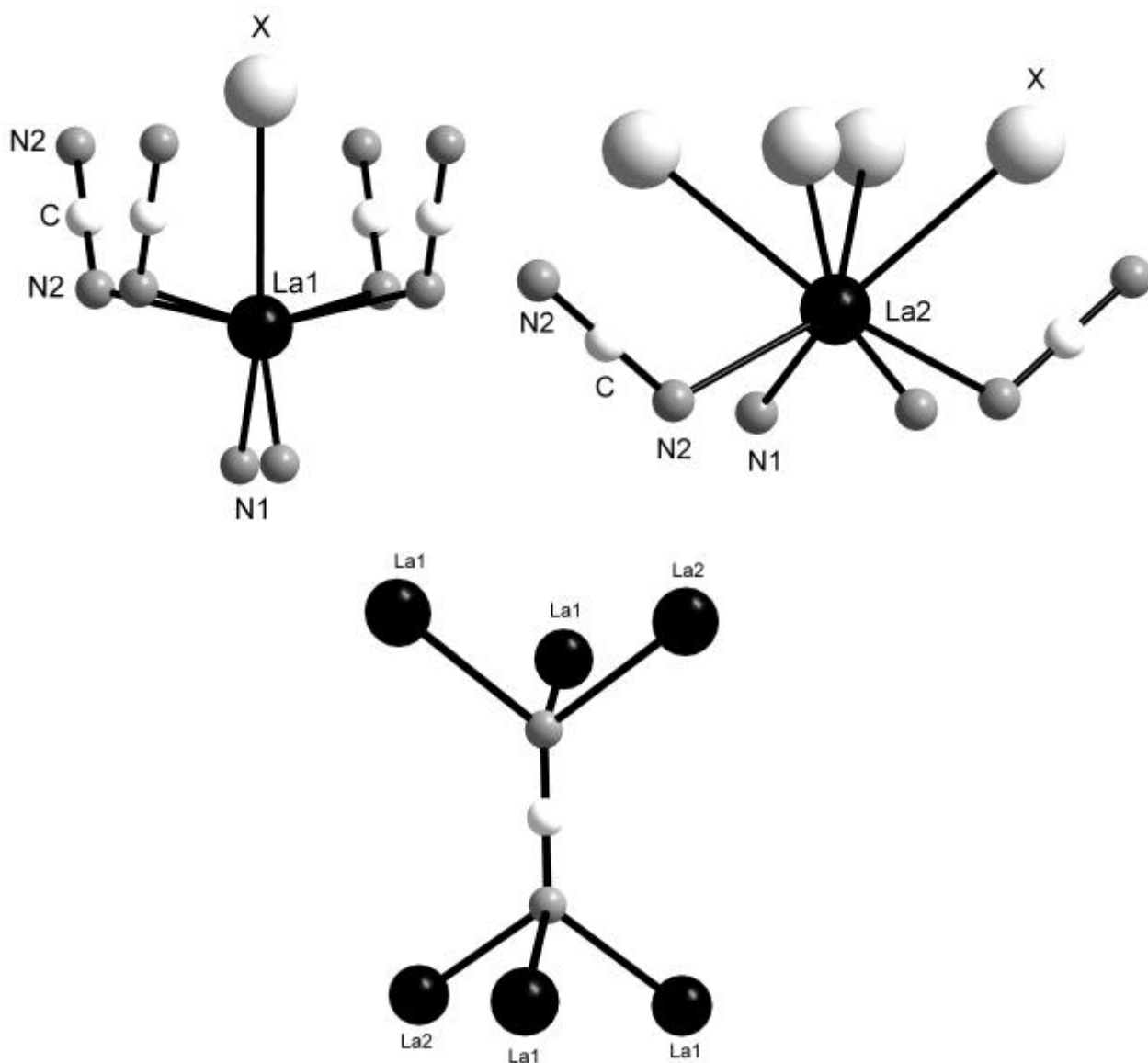


Figure 24. The coordination environment of La1, La2, and NCN unit in the crystal structures of $\text{La}_2\text{X}(\text{CN}_2)\text{N}$ with X = Cl, Br, and I.

4. 3. 7. Crystal structure of Ce₂Cl(CN₂)N

Suitable black needle like single crystals of Ce₂Cl(CN₂)N for single crystal X-ray diffraction studies were selected under the microscope and mounted on the tip of glass fibers. Out of the total 4387 reflections that were collected, 422 reflections were merged as unique reflections. The structure was solved by direct methods (SHELXS-97) and refined by full-matrix least-squares calculations on F² (SHELXL-97). Anisotropic refinements of all atoms with fixed full occupancies yielded R1 = 0.0276, wR2 = 0.0505 with all reflections. The largest residual peak and deepest hole in the \ddot{A} F map were 1.37 and -1.62 e/ \ddot{A}^3 . Some crystal and refinement data are given in Table 11. The atomic positions and isotropic-equivalent displacement parameters are given in Table 12. A summary of selected bond lengths is given in Table 13. The air and water stable black coloured Ce₂Cl(CN₂)N exhibits an isotypic structure to La₂Cl(CN₂)N. As a result of the lanthanide contraction the corresponding distances in Ce₂Cl(CN₂)N are shortened by typically 1-2 %. The C–N distance and N–C–N bond angle are 1.238(6) \ddot{A} and 180° respectively [55].

Table 11. Some crystal and refinement data of Ce₂Cl(CN₂)N.

f_w	368.68
system, space group, Z	Orthorhombic, Cmmm (no.65), 4
unit cell dimensions (\ddot{A} , \ddot{A}^3)	
a	13.340(1)
b	9.5267(8)
c	3.9402(5)
V	500.73(9)
d_{calcd} (g/cm ³)	4.904
μ (mm ⁻¹)	18.33
R1, wR2 [$F_o > 4\sigma(F_o)$]	0.0276, 0.0505

Table 12. Atomic coordinates and equivalent displacement parameters (\ddot{A}^2) for Ce₂Cl(CN₂)N.

Atom	multiplicity, symmetry	x	y	z	U_{eq}^a
Ce1	4 2mm	0.3613(2)	0	0	0.0111(5)
Ce2	4 m2m	0	0.2106(4)	1/2	0.0119(5)
C	4 2/m	1/4	1/4	1/2	0.0138(5)
N1	4 m2m	0	0.3428(7)	0	0.0127(3)
N2	8 m	0.3237(7)	0.1710(4)	1/2	0.0154(7)
Cl	4 2mm	0.1224(3)	0	0	0.0299(7)

^a U_{eq} is defined as one-third of the trace of the orthogonalized U_{ij} tensor.

Table 13. Bond lengths (in Å) in Ce₂Cl(CN₂)N.

Ce1–Ce2	3.85(4)	x4
Ce1–Ce1	3.67(1)	x1
Ce1–N1	2.37(2)	x2
Ce1–N2	2.61(4)	x4
Ce2–N1	2.34(6)	x2
Ce2–N2	2.61(2)	x2
Ce1–Cl	3.20(1)	x1
Ce2–Cl	3.25(6)	x4
C–N2	1.24(8)	x2

4. 3. 8. Magnetic properties of Ce₂Cl(CN₂)N

It is already noted that La₂Cl(CN₂)N occurs as yellow and Ce₂Cl(CN₂)N as black crystalline materials. For La³⁺, salt-like conditions are considered and for the cerium compound, the configuration may be addressed analogous to that of binary CeN, with a salt-like 4f¹5d⁰ or with a metallic 4f⁰5d¹ configuration. CeN adopts the NaCl type structure and would be likely described with the salt-like notation as Ce³⁺N³⁻. However, CeN is a conductor showing Pauli paramagnetism, and is therefore better described as Ce⁴⁺N³⁻̅e⁻ with one delocalized electron in the 5d conduction band. Band structure calculations on CeN [70] have revealed Ce–Ce bonding interactions (at a bond distance of 3.57 Å) with the remaining electron Ce⁴⁺̅e⁻ in a hybrid 5d-4f energy band. The shortest Ce–Ce interatomic distance along the shared edge in Ce₂Cl(CN₂)N is slightly longer (3.67 Å) than that in CeN. The obtained magnetic moment of $\mu = 1.8$ B.M. for Ce₂Cl(CN₂)N is smaller than that would be expected for a free Ce³⁺ ion with the 5d¹ configuration ($\mu_{\text{exp.}} = 2.5$ B.M.). In addition, a small temperature independent portion was assigned to the total susceptibility when a fit according to the formula $\chi = C/(T-\Theta) + \chi_{\text{TIP}}$ is used. This temperature independent contribution in the order of 10⁻³ emu/mol leads to the nonlinear temperature dependency of 1/ χ as shown in Figure 25 [55].

4. 3. 9. Isotypic compounds in this structure type

The other Ln₂Cl(CN₂)N with Ln = Pr, Nd and Gd were synthesised similarly by reacting the 2:1:1 molar ratios of respective halides, L₂CN₂ and L₃N respectively in sealed copper ampoules fused with an quartz ampoule at 700-800 °C in two days. The chloride carbodiimide nitrides of Pr, Nd and Gd are green, blue and black coloured respectively with their cell

parameters indexed from the powder patterns given in Table 14.

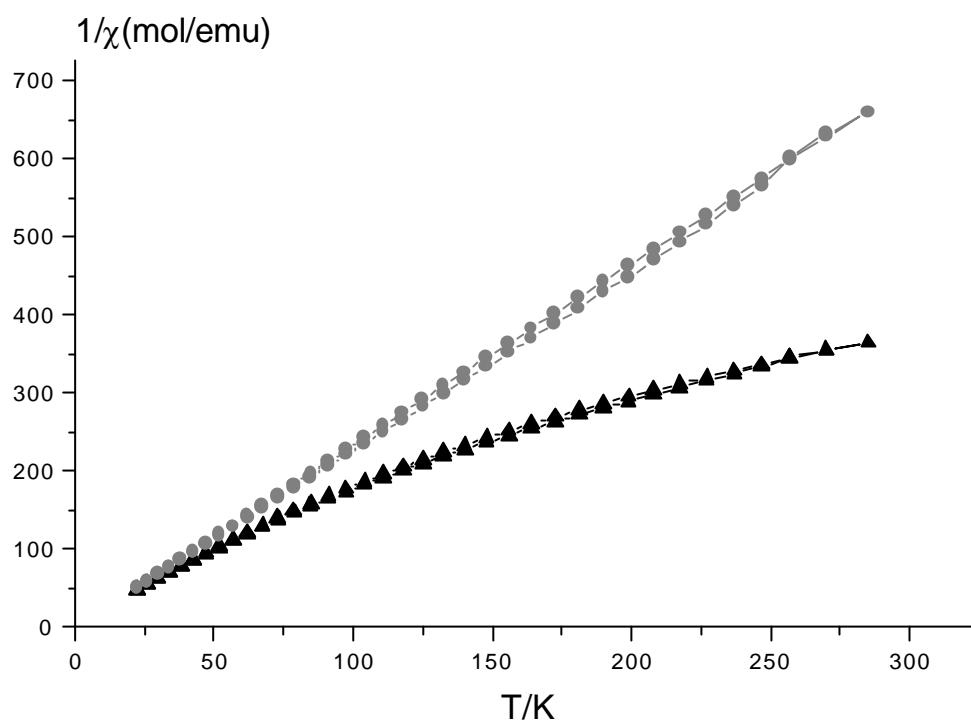


Figure 25. Temperature dependency of the magnetic susceptibility of $\text{Ce}_2\text{Cl}(\text{CN}_2)\text{N}$ shown as $1/\chi$ vs. T plot measured in a cyclic procedure. The total susceptibility (including TIP) is shown by black triangles, and the temperature dependent contribution is indicated by grey dots.

Table 14. Cell parameters (in Å) from powder patterns of $\text{Ln}_2\text{X}(\text{CN}_2)\text{N}$ system with $\text{Ln} = \text{La}, \text{Ce}, \text{Pr}, \text{Nd}, \text{and Gd}$; $\text{X} = \text{Cl}, \text{Br}, \text{and I}$ (* = from single crystal).

Ln	X	a	b	c	V(Å³)	No. of indexed lines
La	Cl	13.3750(3)	9.6203(1)	3.9507(1)	508.40(3)	38
Ce	Cl	13.2829(7)	9.4836(3)	3.9200(6)	493.82(5)	36
Pr	Cl	13.2490(3)	9.4362(1)	3.8747(1)	484.40(3)	24
Nd	Cl	13.1920(7)	9.40(4)	3.84(3)	476.20(7)	20
Gd	Cl	13.2081(7)	9.4288(2)	3.8959(4)	485.18(2)	41
La	Br	13.6177(5)	9.6868(2)	3.9697(4)	523.65(1)	*
Pr	Br	13.2090(3)	9.4209(2)	3.8833(7)	483.24(2)	23
La	I	13.892(3)	9.768(1)	4.0244(5)	546.1(2)	31

4. 4. Reaction between LaCl_3 , $\text{Li}_2(\text{CN}_2)$ and $\text{C}_3\text{N}_3\text{Cl}_3$

The reactions between LaCl_3 and $\text{Li}_2(\text{CN}_2)$ were carried out in the presence of $\text{C}_3\text{N}_3\text{Cl}_3$ at different stoichiometries and reaction conditions.

In the temperature range of 450-700 °C, the reactions were performed for several days. The DTA/TG studies were performed for the salt balanced reaction (45) as shown in Figure 26.

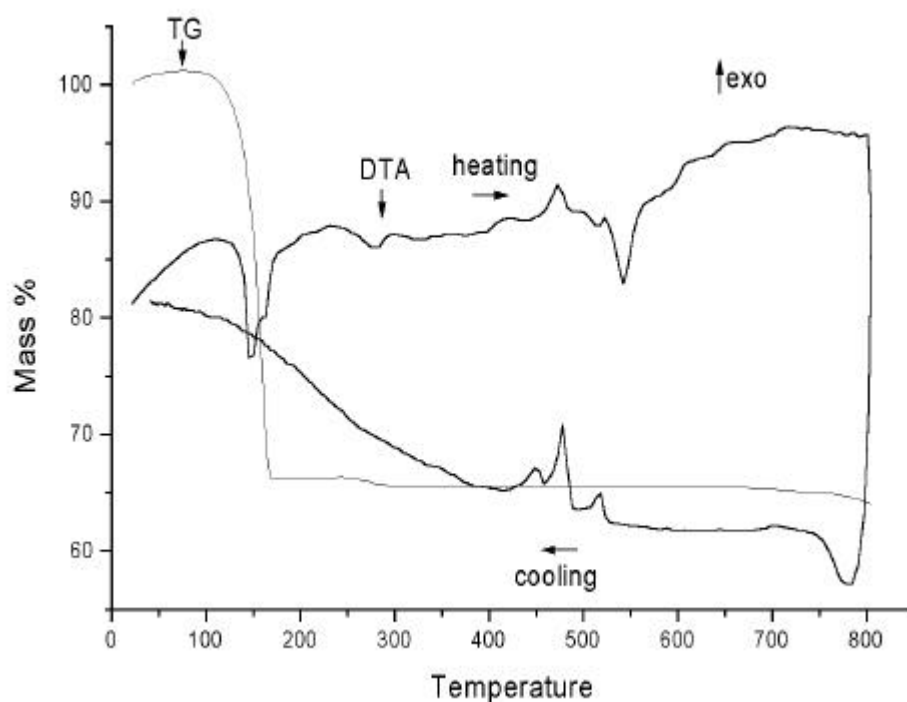


Figure 26. DTA/TG of the reaction between LaCl_3 , $\text{C}_3\text{N}_3\text{Cl}_3$, and $\text{Li}_2(\text{CN}_2)$.

In the DTA/TG, the mass loss at around 150 °C corresponds to the sublimation of $\text{C}_3\text{N}_3\text{Cl}_3$. The small exothermic peak obtained at around 450 °C followed by an endothermic effect which corresponds to the melting of LiCl .

Even after heating the reaction mixture in quartz ampoules for one week at 450 °C, LaCl_3 remains unreacted with side products of LiCl and some broad reflections from amorphous phase that is considered as a carbon nitride. The products obtained from this reaction mixtures were brown in colour upto 650 °C and turned black above 700 °C.

After knowing the existence of $\text{LaCl}(\text{CN}_2)$ in the temperature range of 500 - 700 °C and $\text{La}_2\text{Cl}(\text{CN}_2)\text{N}$ in the temperature range of 750 - 950 °C, it was shown that the same products were obtained from these above mentioned reactions also at the same temperature range. The reactions were also performed in the presence of LiCl/KCl flux. When the reaction mixture in the presence of flux was reacted at 500 °C for ten days, $\text{LaCl}(\text{CN}_2)$ as a major phase along with the unknown amorphous phase was obtained as shown in Figure 27.

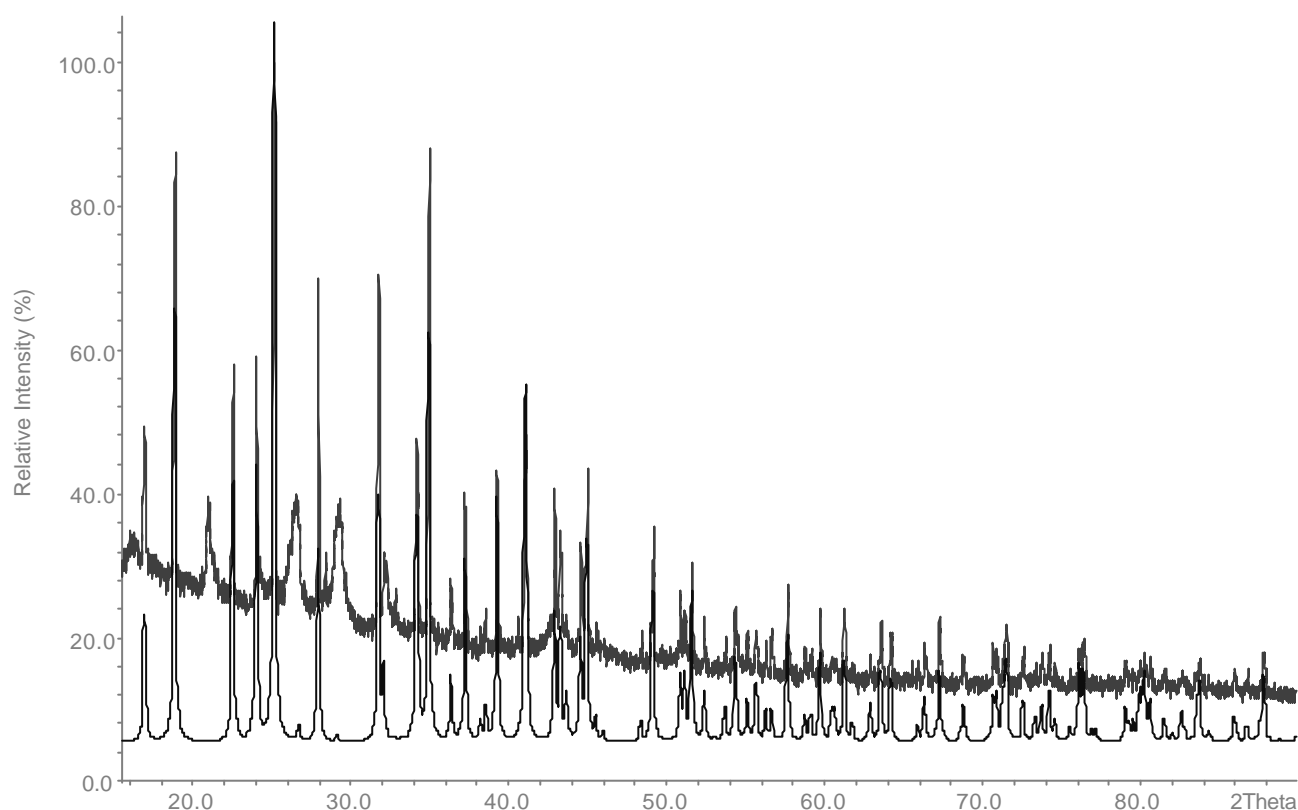


Figure 27. XRD-powder pattern of the brown powder obtained from LaCl_3 , $\text{C}_3\text{N}_3\text{Cl}_3$ and $\text{Li}_2(\text{CN}_2)$ (above) in comparison to the theoretical pattern of $\text{LaCl}(\text{CN}_2)$ (below).

At higher temperatures of 750 °C, the obtained black coloured product showed a XRD powder pattern similar to $\text{La}_2\text{Cl}(\text{CN}_2)\text{N}$. The black colour may be due to the formation of graphite. The DTA/TG studies were performed for the obtained brown product to understand the decomposition as shown in Figure 28. The mass loss in the region of 600 - 700 °C corresponds to the decomposition of $\text{LaCl}(\text{CN}_2)$ along with the decomposition of amorphous phase. Since the region of decomposition of $\text{LaCl}(\text{CN}_2)$ and the amorphous phase are in the same temperature region, the mass loss percentage is more here in comparison to the previously described decomposition studies on $\text{LaCl}(\text{CN}_2)$ (Figure 9).

According to the decomposition region, it may be suspected that the obtained amorphous phase is carbon nitride, which is reported to be decomposing in the temperature range of 550-700 °C [71].

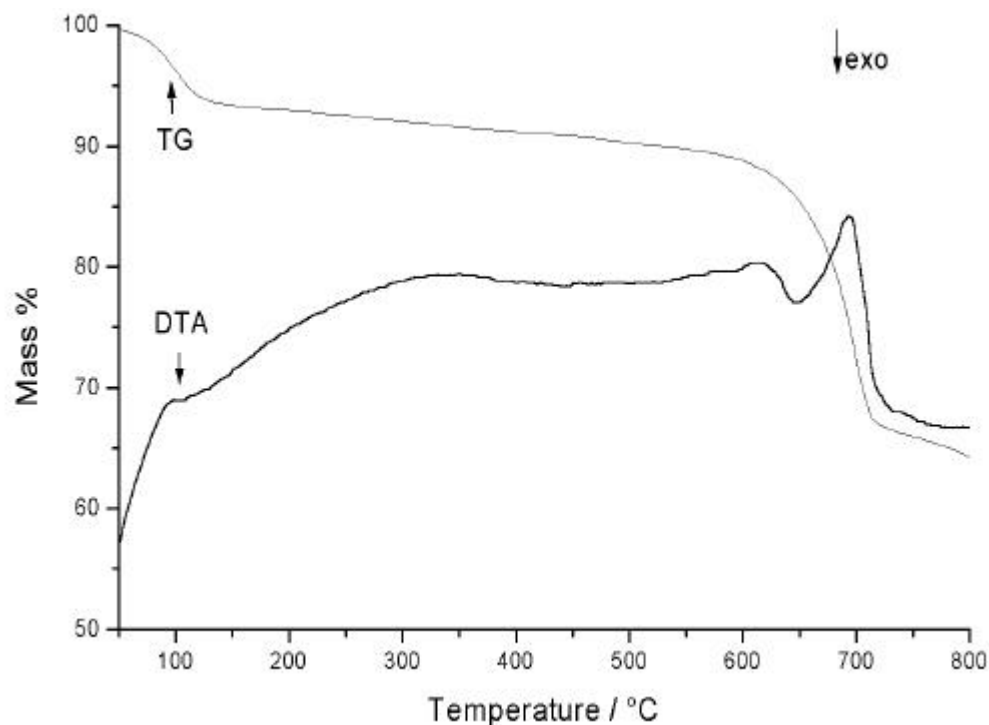
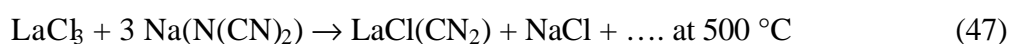


Figure 28. Decomposition of the obtained brown powder from the reaction 45.

4. 5. Reaction between LaCl_3 and Structure directing agents (SDA)

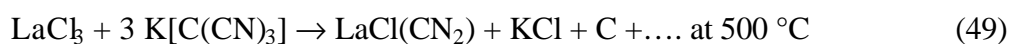
The reaction between LaCl_3 and structure directing agents like $\text{Na}[\text{N}(\text{CN})_2]$, $\text{K}[\text{C}(\text{CN})_3]$ and $\text{K}_4[\text{Fe}(\text{CN})_6]$ were performed.

The stoichiometric 1:3 reaction mixture of LaCl_3 and $\text{Na}[\text{N}(\text{CN})_2]$ was treated in the presence of LiCl/KCl flux at 500 °C for one week. The brown coloured product obtained was identified as $\text{LaCl}(\text{CN}_2)$ from the XRD powder pattern instead of expected lanthanum dicyanamides.



The stoichiometric 1:3 reaction mixture of LaCl_3 and $\text{K}[\text{C}(\text{CN})_3]$ was treated in the presence of LiCl/KCl flux at 500 °C for one week. The black coloured product obtained was identified

as $\text{LaCl}(\text{CN}_2)$ from the XRD powder pattern instead of expected lanthanum tricyanomethanides. The black colour of the product may be due to the formation of graphite as a side product. The XRD powder pattern of black powder at $750\text{ }^\circ\text{C}$ was similar to $\text{La}_2\text{Cl}(\text{CN}_2)\text{N}$.



The reactions carried out between LaCl_3 and $\text{K}_4[\text{Fe}(\text{CN})_6]$ to get the desired lanthanum cyanometallates have also yielded the same $\text{La}_2\text{Cl}(\text{CN}_2)\text{N}$ at temperature around $750\text{-}800\text{ }^\circ\text{C}$ in two days. At comparatively low temperatures like $350\text{ }^\circ\text{C}$, the formation of KCl was indicated from XRD pattern and the other side phases of FeCl_2 appeared at higher temperature near $500\text{ }^\circ\text{C}$.

Hence the reactions between LaCl_3 and structure directing agents resulted in either $\text{LaCl}(\text{CN}_2)$ or $\text{La}_2\text{Cl}(\text{CN}_2)\text{N}$ depending on the temperature range.

4. 5. 1. Reaction between $\text{La}(\text{NO}_3)_3 \cdot 6\text{H}_2\text{O}$ and $\text{K}[\text{C}(\text{CN})_3]$

The reaction between lanthanum nitrate hexahydrate and potassium tricyanomethanide was carried out in aqueous medium to obtain $\text{KLa}[\text{C}(\text{CN})_3]_4 \cdot \text{H}_2\text{O}$ as a crystalline material.

Synthesis of $\text{KLa}[\text{C}(\text{CN})_3]_4 \cdot \text{H}_2\text{O}$

To a 25 ml of clear aqueous solution containing 433 mg of $\text{La}(\text{NO}_3)_3 \cdot 6\text{H}_2\text{O}$, 15ml of yellow aqueous solution containing 388 mg (three equivalents) of $\text{K}[\text{C}(\text{CN})_3]$ was added under constant stirring. The resulting mixture of solution was light yellow in colour without any precipitation or cloudiness [72].

A light yellow powder along with KNO_3 was obtained by boiling the solution mixture to remove water. The presence of KNO_3 and the absence of $\text{La}(\text{NO}_3)_3 \cdot 6\text{H}_2\text{O}$ was indicated by X-ray powder diffraction pattern. The measured powder pattern was indexed with similar cell parameters ($a = b = 12.388(3)\text{ \AA}$, $c = 6.569(3)\text{ \AA}$ $V = 1008.1(6)\text{ \AA}^3$) as obtained from a single

crystal. In addition, there were some unidentified lines in the powder pattern. For the selected 37 peaks, the number of single indexed lines were 27. Well developed light yellow rod-like $\text{KLa}[\text{C}(\text{CN})_3]_4 \cdot \text{H}_2\text{O}$ crystals were obtained by recrystallisation from water. The reaction equation can be written as follows:



Crystal structure of $\text{KLa}[\text{C}(\text{CN})_3]_4 \cdot \text{H}_2\text{O}$

Tricyanomethanide anion $(\text{tcm})^-$ and dicyanamide anion are forming isostructural compounds. They show promise in the field of molecular magnetism [73].

The $(\text{tcm})^-$ ion is an efficient complexing agent that forms co-ordinate bonds with preservation of its planarity. It shows a tendency to act as a bridging ligand and hence to form co-ordination polymers. Because of the high degree of delocalization of the ionic charge, three cyano-N-atoms are equally capable of establishing co-ordinate bonds. This enables the $(\text{tcm})^-$ ion to act not only as a monodentate ligand, but preferably as a bi- and tridentate ligand in bridge function [74].

In $\text{Na}(\text{tcm})$ and $\text{K}(\text{tcm})$, the metal ion is coordinated by seven N atoms [15]. But in $\text{Ag}(\text{tcm})$, the Ag atoms are surrounded by three N atoms forming a sheet, and two such sheets are interconnected to form a double sheet structure [75].

The structures of $\text{M}(\text{tcm})_2$ with divalent $\text{M} = \text{V}, \text{Cr}, \text{Mn}, \text{Fe}, \text{Co}, \text{Ni}, \text{Cu}, \text{Zn}, \text{Cd}, \text{Hg}$ [76] are all isostructural and contain two independent and equivalent 3-D networks having a connectivity similar to the rutile type structure. In $\text{M}(\text{tcm})_2$ where $\text{M} = \text{V}$ and Cr , each $(\text{tcm})^-$ bonds to three different metal ions in a triangular array, affording a geometrical topology similar to a Kagome net leading to competing spin exchange interactions and spin frustrations. Magnetic susceptibility measurements reveal strong antiferromagnetic interactions for both $\text{V}(\text{tcm})_2$ and $\text{Cr}(\text{tcm})_2$ with $\theta = -67 \text{ K}$ and -46 K respectively.

To date, no detailed investigation has been carried out for $(\text{tcm})^-$ containing lanthanide compounds. Hexamethylphosphorotriamide complexes of rare earth element tricyanomethanides is the only work reported long back in the literature [77].

Now our efforts to synthesise lanthanide tricyanomethanides by solution chemistry led to a new structure type, that is different from the known transition metal compounds.

Suitable light yellow rod-like single crystals of $\text{KLa}[\text{C}(\text{CN})_3]_4 \cdot \text{H}_2\text{O}$ were selected for single crystal X-ray diffraction studies under the microscope and mounted on the tip of glass fibres. Some of the crystallographic details are given in Table 15. The atomic positions and isotropic-equivalent displacement parameters are given in Table 16. A summary of selected bond lengths and bond angle are given in Table 17.

The tetragonal crystal structure of $\text{KLa}[\text{C}(\text{CN})_3]_4 \cdot \text{H}_2\text{O}$ shows a beautiful flower-like structure pattern with tcm ions bridging both types of cations, La^{3+} and K^+ (Figures 29 and 30). All the cations are arranged in layers near $z = 0$, with La^{3+} being situated on a fourfold rotation axis, and K^+ on a fourfold inversion axis. The lanthanum ions are situated in the a,b-plane, similar to a 4^4 network arrangement. In this array, each lanthanum ion is bridged with four adjacent La^{3+} neighbours by four pairs of tcm ions (Figure 29). The bridging tcm ions act as bidentate ligands with respect to La^{3+} through their N atoms (N1 and N2), and thereby generate a two-dimensional structure. The third nitrogen atom (N3) of each tcm interpenetrates into an adjacent layer, pointing towards a potassium ion, and thereby connecting adjacent layers through La–tcm–K bridges. The bridging functionality of tcm is shown in Figure 31 [72].

The lanthanum ion is nine coordinated, situated in a square antiprism of nitrogen atoms, which is monocapped by one water molecule. The coordination environment of La^{3+} with two crystallographically distinct nitrogen atoms (N1 and N2) from the eight surrounding tcm ions, and with one oxygen atom from the water molecule is shown in Figure 32.

The potassium ion is surrounded by four nearest nitrogen atoms belonging to four tcm ions, generating an approximate tetrahedral environment (D_{2d} -symmetry) with four equally short K–N distances of 2.74 Å. Both, the low coordination number and the four short K–N distances are anomalous for a potassium ion. For example, the average K–N distances in $\text{K}[\text{C}(\text{CN})_3]$ [15] amount to 2.89 Å, and to approximately 2.90 Å in potassium ferrocyanides [78] with coordination numbers of seven and more.

In the structure of $\text{KLa}[\text{C}(\text{CN})_3]_4 \cdot \text{H}_2\text{O}$, the potassium ion is in fact surrounded by eight tcm ions. In addition to the four tcm ions already mentioned, there are four other tcm ions that shield the potassium ion in an umbrella-like fashion at K–C distances of 3.76 Å with the central tcm carbon atoms (C4), as shown in Figure 33. If the arrangement of the central tcm

carbon atoms (C4) is considered, both groups of tcm ions follow the motive of distorted tetrahedra [72].

The C-C-C angles of the tcm ion deviate only little from 120° (Table 17). Considering a 4σ precision for the estimated standard deviation of the calculated bond angles (in Table 17), the ideal D_{3h} symmetry of $[C(CN)_3]^-$ is retained. This is consistent with the observation of one, although broad, C-N vibration at 2199 cm^{-1} in the recorded infrared spectrum of $KLa[C(CN)_3]_4 \cdot H_2O$ [72].

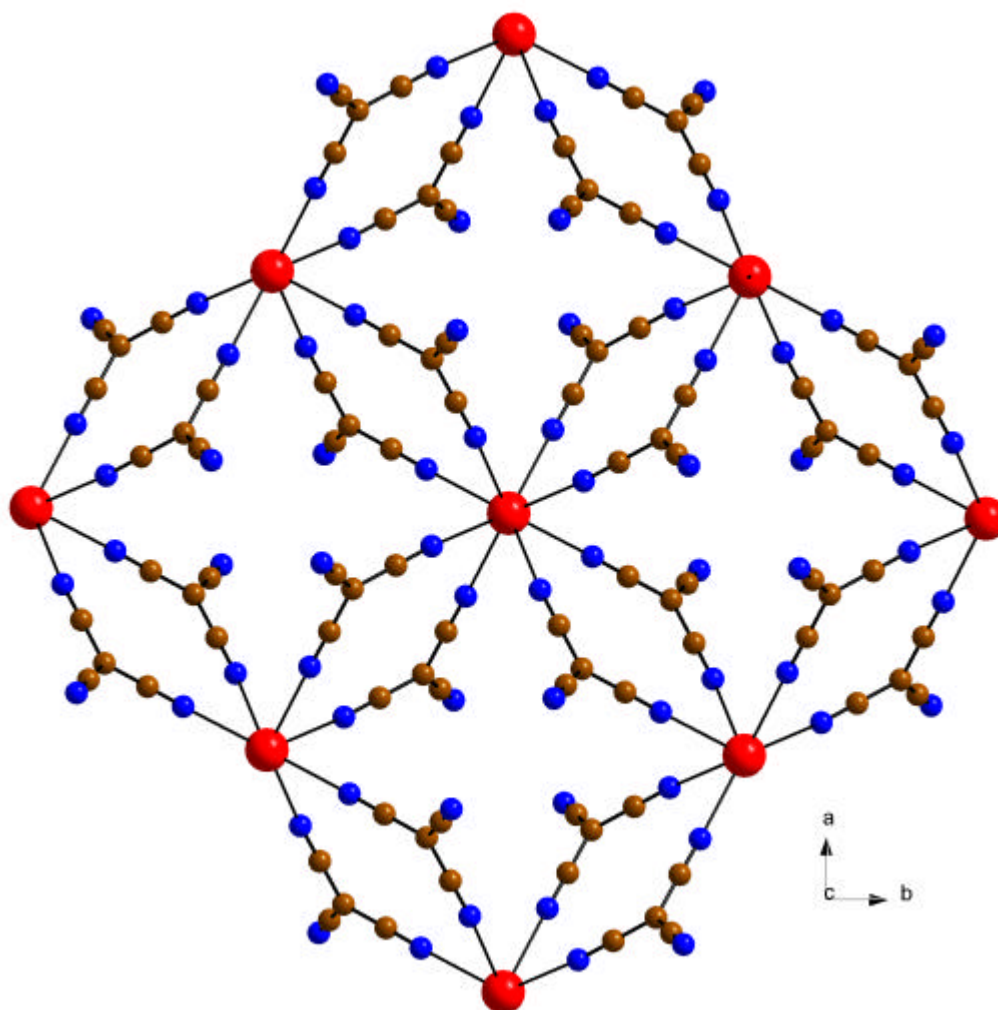


Figure 29. Partial structure with the layer like arrangement of $[La(C(CN)_3)_4]^-$. Lanthanum atoms are shown red, nitrogen atoms blue, and carbon atoms brown.

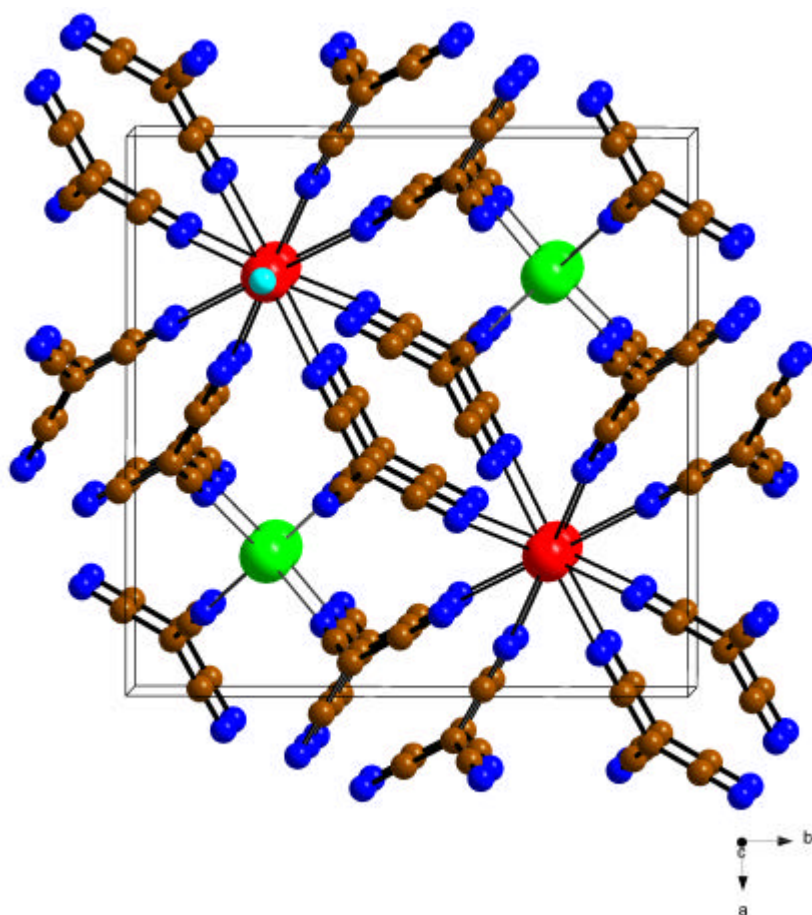


Figure 30. Unit cell of $\text{KLa}[\text{C}(\text{CN})_3]_4 \cdot \text{H}_2\text{O}$. Lanthanum atoms are shown red, potassium atoms green, nitrogen atoms blue, carbon atoms brown and oxygen atoms cyan.

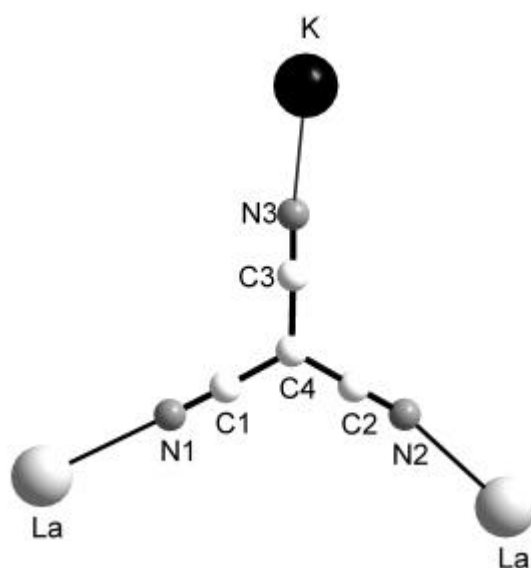


Figure 31. Bridging mode of the $[\text{C}(\text{CN})_3]^-$ ion. Lanthanum atoms are shown light grey, potassium black, nitrogen medium grey and carbon atoms white.

Table 15. Selected crystal data and measuring conditions.

Space group (no.), Z	P4/n (85), 2
Lattice constants /Å	$a = b = 12.3790(13), c = 6.5695(8)$
Cell volume /Å ³	1006.71(19)
Density calc. /g·cm ⁻³	1.832
Molecular weight /g·mol ⁻¹	1108.52
Crystal appearance	light yellow rod-like
Crystal size /mm ³	0.22 x 0.05 x 0.06
Diffractometer	STOE, IPDS
Radiation, temperature	Mo-K _α ($\lambda = 0.71073 \text{ \AA}^3$), graphite monochromator, 293(2) K
Range: $\theta /^\circ$	3.10 to 30.52
Index range	$-17 \leq h \leq 17, -17 \leq k \leq 17, -9 \leq l \leq 9$
μ / mm^{-1}	2.365
Collected reflections ($F_0 > 2\sigma(F_0)$)	17574
Unique reflections	1535
Parameters refined	72
R indices (all data)	$R1^a = 0.0383, wR2^b = 0.0755$
Final R indices [$I > 2\sigma(I)$]	$R1^a = 0.0325, wR2^b = 0.0740$
Goof (all reflections)	1.118
Res. peak: max.; min. /e/Å ³	1.63, -0.5

$$^a R1 = \sum ||F_o| - |F_c|| / \sum |F_o|; ^b wR2 = [\sum w(F_o^2 - F_c^2)^2 / [\sum w(F_o^2)^2]]^{1/2}$$

Table 16. Atomic coordinates and isotropic-equivalent displacement parameters (\AA^2) for $\text{KLa}[\text{C}(\text{CN})_3]_4 \cdot \text{H}_2\text{O}$.

Atom	multiplicity, Wyckoff position	x	y	z	U_{eq}^{a}
La	2 c	0.25	0.25	0.04365(5)	0.0164(1)
K	2 a	0.75	0.25	0	0.0374(3)
O	2 c	0.25	0.25	0.4349(7)	0.038(1)
N1	8 g	0.9250(2)	0.8392(3)	0.8084(5)	0.0391(7)
N2	8 g	0.1803(2)	0.0917(2)	0.8071(5)	0.0375(6)
N3	8 g	0.1439(3)	0.8669(3)	0.2926(6)	0.0513(9)
C1	8 g	0.9995(2)	0.8803(3)	0.7391(5)	0.0291(6)
C2	8 g	0.1394(2)	0.0178(3)	0.7371(5)	0.0271(5)
C3	8 g	0.1207(3)	0.8942(3)	0.4526(5)	0.0330(6)
C4	8 g	0.0896(2)	0.9281(2)	0.6491(5)	0.0277(6)

^a U_{eq} is defined as one-third of the trace of the orthogonalized U_{ij} tensor.

Table 17. Bond distances (in \AA) and bond angle (in $^\circ$) in $\text{KLa}[\text{C}(\text{CN})_3]_4 \cdot \text{H}_2\text{O}$.

La–O	2.570(4) x 1
La–N1	2.619(3) x 4
La–N2	2.646(3) x 4
K–N3	2.741(3) x 4
C1–N1	1.147(4) x 1
C1–C4	1.394(4) x 1
C2–N2	1.141(4) x 1
C2–C4	1.396(4) x 1
C3–N3	1.141(5) x 1
C3–C4	1.411(5) x 1
C1–C4–C2	121.0(3)
C1–C4–C3	118.7(3)
C2–C4–C3	119.7(3)

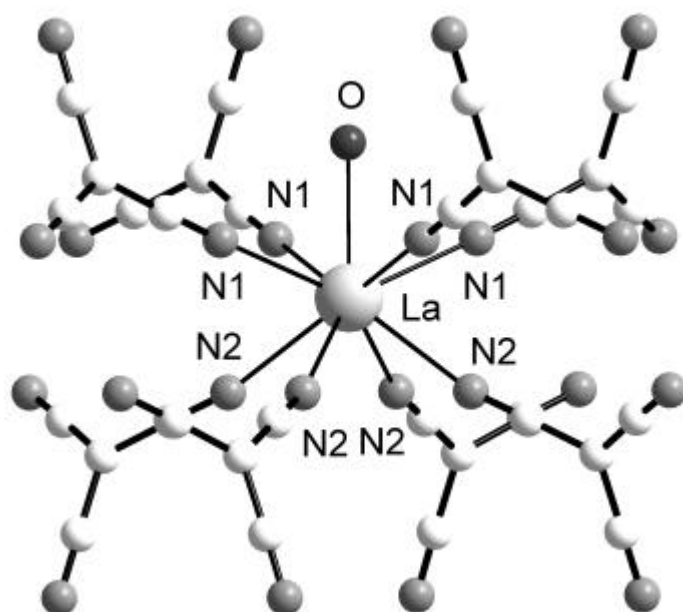


Figure 32. Coordination environment around the La^{3+} ion. Lanthanum atom is shown in light grey, oxygen atom dark grey, nitrogen atoms medium grey and carbon atoms white.

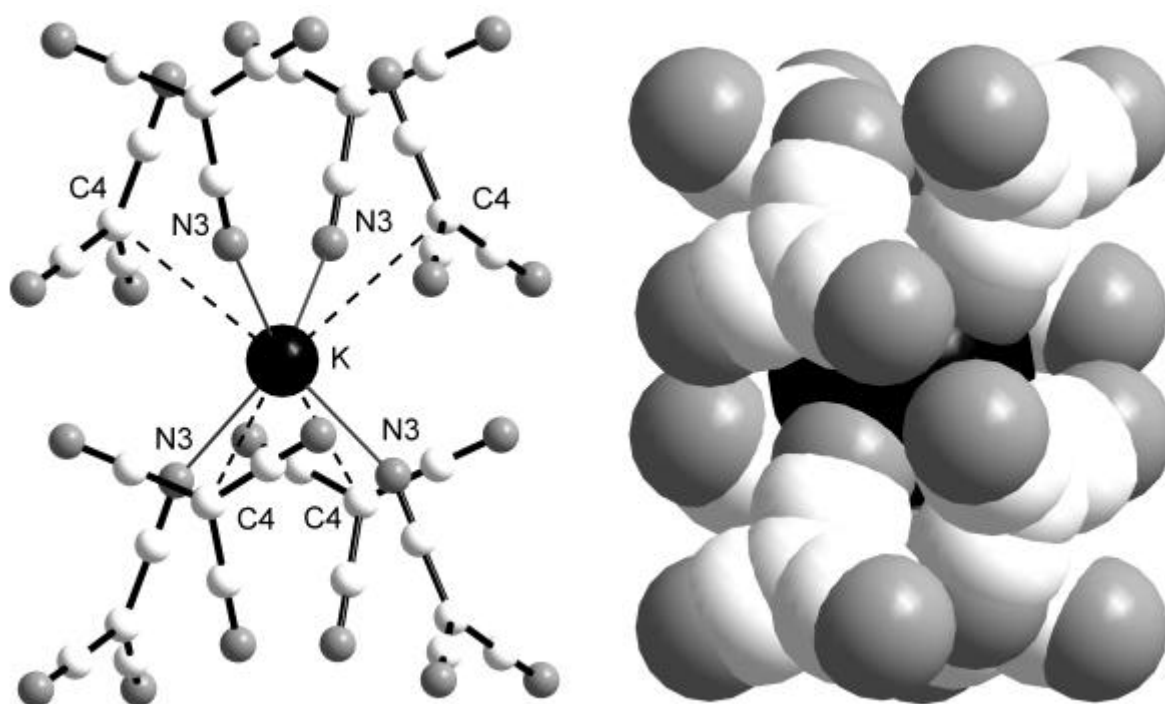
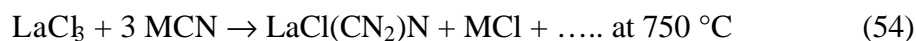


Figure 33. Environment around the K^+ ion with 4 + 4 tcm ions, shown as a ball and stick (left) and as a space-filling model (right). Colour of the atoms are same as in Figure 31.

4. 6. Reaction between LaCl_3 and MCN with $\text{M} = \text{Na, K}$

The reaction between InBr and NaCN led to two different carbodiimides, $\text{In}_{2.24}(\text{CN}_2)_3$ and $\text{NaIn}(\text{CN}_2)_3$ instead of expected InCN [7]. So the reaction between LaCl_3 and KCN or NaCN was performed to know whether $\text{La}_2(\text{CN}_2)_3$ could be synthesised by this route. The stoichiometric 1:3 reaction mixture of LaCl_3 and KCN have yielded $\text{LaCl}(\text{CN}_2)\text{N}$ along with KCl and LaOCl at $750\text{ }^\circ\text{C}$ in one day. The formation of KCl was only identified from powder pattern at $350\text{ }^\circ\text{C}$. At higher temperature of $750\text{ }^\circ\text{C}$, the reflections from the powder pattern were indexed to the known $\text{LaCl}(\text{CN}_2)\text{N}$. The obtained $\text{LaCl}(\text{CN}_2)\text{N}$ was black in colour, may be due to the formation of graphite as a side product.

The reaction between 1:3 LaCl_3 and NaCN at $500\text{ }^\circ\text{C}$ for one week was also carried out in the presence of LiCl/KCl flux for better reactivity. $\text{LaCl}(\text{CN}_2)$ was the product obtained along with KCl .



4. 7. Reaction between LaCl_3 and $\text{Li}_2(\text{CN}_2)$ in the presence of metal

4. 7. 1. Reaction between LaCl_3 , $\text{Li}_2(\text{CN}_2)$ and Li

The metallothermic reduction reaction between LaCl_3 and $\text{Li}_2(\text{CN}_2)$ was performed with Li to get metal-rich compounds similar to that known from $\text{LaCl}_3/\text{Li}_3(\text{BN}_2)$ system in the presence of Li [79].

The reactions were carried out in different stoichiometries and reaction conditions. At higher temperatures of above $800\text{ }^\circ\text{C}$, black LaN was formed along with LiCl . When the reaction mixture was heated at $750\text{ }^\circ\text{C}$ for one week, good crystals of $\text{LaCl}(\text{CN}_2)\text{N}$ were obtained along with LiCl . Hence the presence of Li may serve as a melt to the crystallisation of $\text{LaCl}(\text{CN}_2)\text{N}$. The similar situation of Li acts as a melt was reported in the synthesis of $\text{Li}_2(\text{CN}_2)$ from Li_2C_2 and Li_3N [4].

4. 7. 2. Reaction between LaCl_3 , $\text{Li}_2(\text{CN}_2)$ and Ca

The metallothermic reduction reactions between LaCl_3 and $\text{Li}_2(\text{CN}_2)$ were performed with calcium dendrites at different stoichiometries and reaction conditions. The reaction was carried out in the temperature range of 650-950 °C. In all the reactions performed, the obtained products were the mixture of good yellow crystalline Ca_2NCl , $\text{Ca}(\text{CN}_2)$, black LaN and LiCl .

4. 8. Synthesis and structure of $\text{Pr}_3\text{O}_4\text{Br}$

4. 8. 1. Synthesis of $\text{Pr}_3\text{O}_4\text{Br}$

The well developed greenish yellow plate like single crystals of $\text{Pr}_3\text{O}_4\text{Br}$ were synthesised while pursuing reactions for $\text{Pr}_2\text{Br}(\text{CN}_2)\text{N}$ from a stoichiometric 2:1:1 molar ratio of PrBr_3 , $\text{Li}_2(\text{CN}_2)$, and Li_3N respectively. The reaction mixture was reacted at 850 °C in a quartz sealed copper ampoule for one week and cool down slowly to room temperature. Due to the presence of oxide bromide impurity in PrBr_3 , $\text{Pr}_3\text{O}_4\text{Br}$ was formed besides $\text{Pr}_2\text{Br}(\text{CN}_2)\text{N}$. The crystal structure of $\text{Pr}_3\text{O}_4\text{Br}$ was determined by single-crystal X-ray diffraction. In the crystal structure of $\text{Pr}_3\text{O}_4\text{Br}$, the bromide ion position is refined at 88% only.

4. 8. 2. Crystal structure of $\text{Pr}_3\text{O}_4\text{Br}$

Suitable greenish yellow plate-like single crystals of $\text{Pr}_3\text{O}_4\text{Br}$ for single crystal X-ray diffraction studies were selected under a microscope and mounted on the tip of glass fibers. Some important crystallographic data are shown in Table 18. The atomic positions are given in Table 19. A summary of selected bond lengths is given in Table 20. The crystal structure of $\text{Pr}_3\text{O}_4\text{Br}_{0.88}$ was found to be isotypic to $\text{Eu}_3\text{O}_4\text{Br}$. The unit cell of $\text{Pr}_3\text{O}_4\text{Br}$ is shown in Figure 35.

The crystal structure contains layers of edge bridged Pr_4O tetrahedra with bromide ion and another oxide ion situated in between these layers as shown in Figure 36. The Pr1 is seven coordinated in a distorted pentagonal bipyramidal fashion and Pr2 is nine coordinated in a distorted tricapped trigonal prismatic geometry. The layered arrangement of Pr_4O tetrahedra in $\text{Pr}_3\text{O}_4\text{Br}$ has similarities to the previously described structure of layered $\text{LaCl}(\text{CN}_2)$.

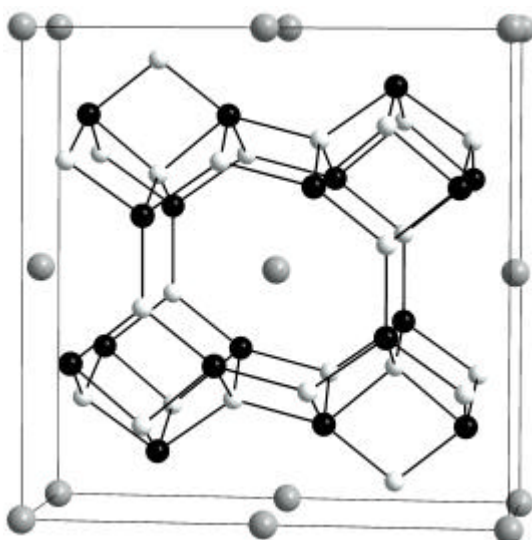


Figure 34. Unit cell of $\text{Pr}_3\text{O}_4\text{Br}$. Praseodymium atoms are shown black, oxygen atoms light grey and bromine atoms dark grey.

Table 18. Some of the crystallographic data of $\text{Pr}_3\text{O}_4\text{Br}$.

Space group (no.), Z	$\text{Cmcm}(63)$, 4
Unit cell dimension (in \AA)	$a = 4.2650(4)$, $b = 12.3300(9)$, $c = 12.119(1)$
Cell volume (in \AA^3)	637.31(9)
Molecular weight (g. mol^{-1})	1043.28
Crystal appearance	Greenish yellow plates
Crystal size (in mm^3)	0.16 x 0.2 x 0.08
μ (mm^{-1})	27.980
Unique reflections	447
Collected reflections ($F_0 > 2\sigma(F_0)$)	3585
Parameters refined	31 (all atoms refined anisotropically)
R indices (all data)	$R1^a = 0.0224$, $wR2^b = 0.0527$
Final R indices ($I > 2\sigma(I)$)	$R1^a = 0.0214$, $wR2^b = 0.0521$
Res. peak: max.; min. ($\text{e}/\text{\AA}^3$)	1.399, -1.863

$$^a R1 = \frac{\sum ||F_o| - |F_c||}{\sum |F_o|}; ^b wR2 = \left[\frac{\sum w(F_o^2 - F_c^2)^2}{\sum w(F_o^2)^2} \right]^{1/2}$$

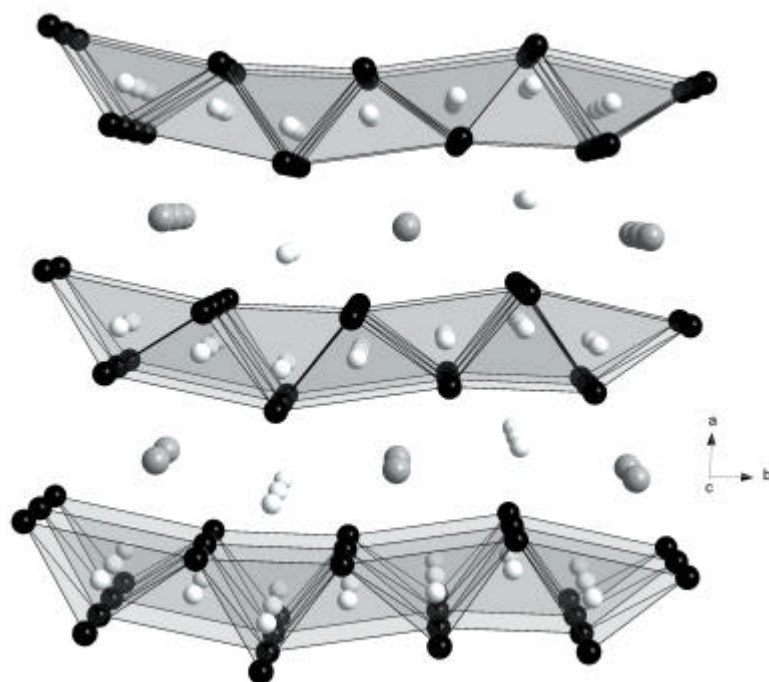


Figure 35. Perspective view of the crystal structure of $\text{Pr}_3\text{O}_4\text{Br}$. Colour of the atoms are same as in Figure 34.

Table 19. Atomic coordinates for $\text{Pr}_3\text{O}_4\text{Br}$

Atom	position	x	y	z
Pr(1)	4c	1/2	0.6744(1)	0.4005(1)
Pr(2)	8f	0	0,8767(1)	1/4
Br(1)	4a	0	1/2	1/2
O(1)	8f	-1/2	0.8001(5)	1/4
O(2)	4c	0	0.7641(4)	0.4108(3)
O(3)	4c	0	0.0611(5)	1/4

Table 20. Bond distances (in Å) in $\text{Pr}_3\text{O}_4\text{Br}$.

Pr(1)–O(3)	2.319(4)
Pr(1)–O(2)	2.389(2)
Pr(1)–O(1)	2.369(4)
Pr(2)–O(3)	2.275(7)
Pr(2)–O(2)	2.392(4)
Pr(2)–O(1)	2.332(3)
Pr(1)–Br(1)	3.2843(3)
Pr(1)–Pr(2)	3.7295(4)

4. 8. 3. Isotypic compounds in this structure type

The orthorhombic $\text{Ln}_3\text{O}_4\text{X}$ ($\text{Ln}_3\text{O}_4\text{Cl}$, $\text{Ln} = \text{Dy, Ho, Er, Tm, Yb, Lu}$ and the $\text{Ln}_3\text{O}_4\text{Br}$, $\text{Ln} = \text{Pr, Sm, Eu, Yb}$) compounds also exist in $\text{Eu}_3\text{O}_4\text{Br}$ type. The layers of edge bridged (Ln_4O) tetrahedra are characteristic for compounds crystallising with this structure type. The cell parameters of isotypic compounds are listed in Table 21.

Table 21. Cell parameters (in Å) of compounds isotypic to $\text{Eu}_3\text{O}_4\text{Br}$ structure with space group Cmcm .

Compound	<i>a</i>	<i>b</i>	<i>c</i>	Reference
$\text{Dy}_3\text{O}_4\text{Cl}$	4.0648(5)	11.662(2)	11.573(2)	[80]
$\text{Ho}_3\text{O}_4\text{Cl}$	4.041(2)	11.636(6)	11.557(5)	[80]
$\text{Er}_3\text{O}_4\text{Cl}$	4.011(1)	11.539(3)	11.525(3)	[81]
$\text{Tm}_3\text{O}_4\text{Cl}$	3.996(1)	11.459(4)	11.450(3)	[81]
$\text{Yb}_3\text{O}_4\text{Cl}$	4.041(2)	11.406(2)	11.316(1)	[80]
$\text{Lu}_3\text{O}_4\text{Cl}$	4.03(1)	11.35(2)	11.33(2)	[81]
$\text{Pr}_3\text{O}_4\text{Br}$	4.2650(4)	12.3300(9)	12.119(1)	This work
$\text{Sm}_3\text{O}_4\text{Br}$	4.141(1)	12.049(3)	11.507(4)	[82]
$\text{Eu}_3\text{O}_4\text{Br}$	4.124(5)	11.986(2)	11.854(2)	[82]
$\text{Yb}_3\text{O}_4\text{Br}$	4.010(1)	11.507(4)	11.406(3)	[82]

4. 9. Synthesis and structure of $\text{La}_2\text{O}(\text{CN}_2)_2$

4. 9. 1. Synthesis and structure of known $\text{Ln}_2\text{O}_2(\text{CN}_2)$ with $\text{Ln} = \text{La, Ce, Pr, Nd, Sm, Eu, and Gd}$

$\text{Ln}_2\text{O}_2(\text{CN}_2)$ was originally synthesised by treating La_2O_3 with flowing NH_3 at 950°C for 12 hours in a graphite boat. The source for carbon in the CN_2^{2-} unit was claimed to be from the graphite boat [35]. There is a large group of compounds of composition $\text{Ln}_2\text{O}_2\text{X}$ with $\text{X} = \text{S}$ [83], Se [84], Te [85], and so on. Their structure is closely related to that of the high-temperature form of La_2O_3 in which third O takes a position between the $[\text{La}_2\text{O}_2]^{2+}$ layers [83]. In addition, $\text{La}_2\text{O}_2\text{CO}_3$ [86] also takes a similar structure to $\text{La}_2\text{O}_2\text{X}$ in which CO_3^{2-} ions are located between the $[\text{La}_2\text{O}_2]^{2+}$ layers. In these compounds, the $[\text{La}_2\text{O}_2]^{2+}$ layers are perpendicular to the *c*-axis, and anions are held between these layers. The crystal structure is

tetragonal in the case of X = Se, Te, and CO₃. Regardless of the kind of anions, their a-parameters are about 4 Å because of rigidity of the [La₂O₂]²⁺ layers, but the c-parameters vary remarkably depending on the size of anions which are located at the interlayers. The crystal structures of La₂O₂(CN₂) were found to be tetragonal for La and trigonal for Ce, Pr, Nd, Sm, Eu, and Gd according to the literature [35]. The unit cell parameters of these compounds are tabulated in the appendix. The tetragonal form consist of [La₂O₂]²⁺ layers with disordered (CN₂)²⁻ ions inserted perpendicular to the c-axis and the trigonal Ln₂O₂(CN₂) (Ln = Ce, Pr, Nd, Sm, Eu, and Gd) contain [Ln₂O₂]²⁺ layers with linear (CN₂)²⁻ ions inserted parallel to the c-axis. There is no single crystal available till todote and the structures were solved from the powder pattern by rietveld refinements. The unit cell of tetragonal La₂O₂(CN₂) and trigonal Pr₂O₂(CN₂) are shown in Figure 37.

The CN₂²⁻ unit is a cyanamide in the tetragonal form and a carbodiimide in the trigonal form of oxide cyanamides. Some bond distances and angles of tetragonal La₂O₂(CN₂) and trigonal Pr₂O₂(CN₂) are summarized in Table 22.

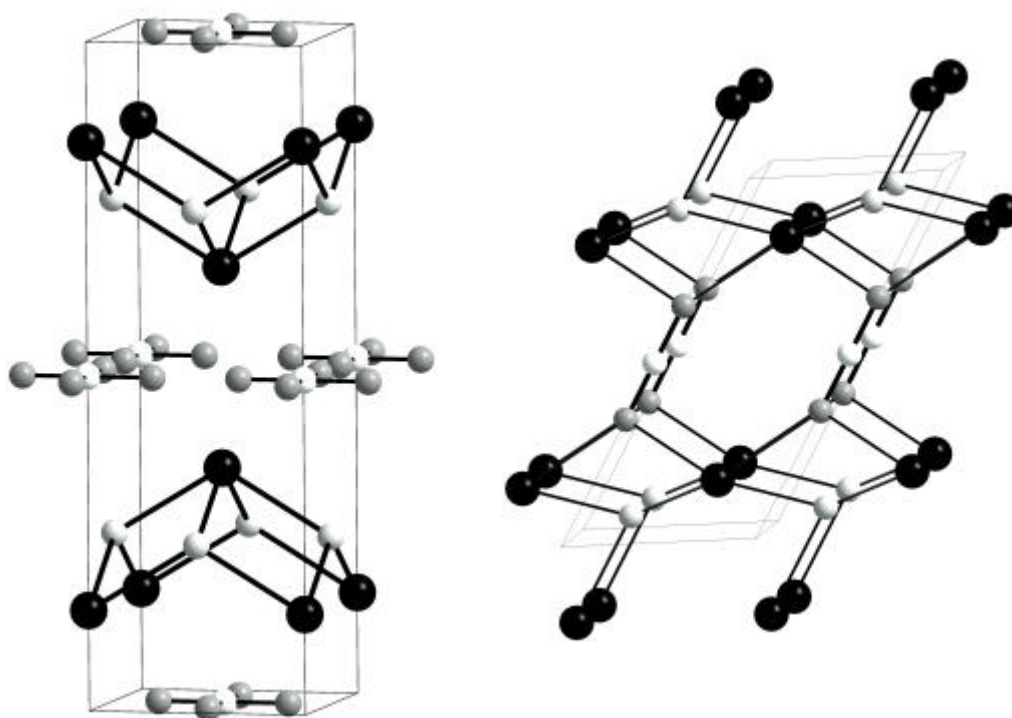


Figure 36. Unit cell of tetragonal La₂O₂(CN₂) (left) and trigonal Pr₂O₂(CN₂) (right). The (CN₂) unit in the tetragonal structure is disordered owing to two orientations. Metal atoms are shown black, oxygen atoms light grey, nitrogen atoms dark grey, and carbon atoms white.

Table 22. Some of the bond distances (in Å) and angles (°) from the literature.

Bond	La ₂ O ₂ (CN ₂)	Pr ₂ O ₂ (CN ₂)
Ln–O	2.390	2.699
Ln–N	2.88	2.610; 2.657
C–N	1.23	1.283
N–C–N	90	179.9

4. 9. 2. Reaction between LaCl₃, LaOCl and Li₂(CN₂)

The stoichiometric 1:1:2 reaction mixture of LaCl₃, LaOCl, Li₂(CN₂) respectively was reacted at 650 °C to yield a light brownish white powder, later known to be La₂O(CN₂)₂.

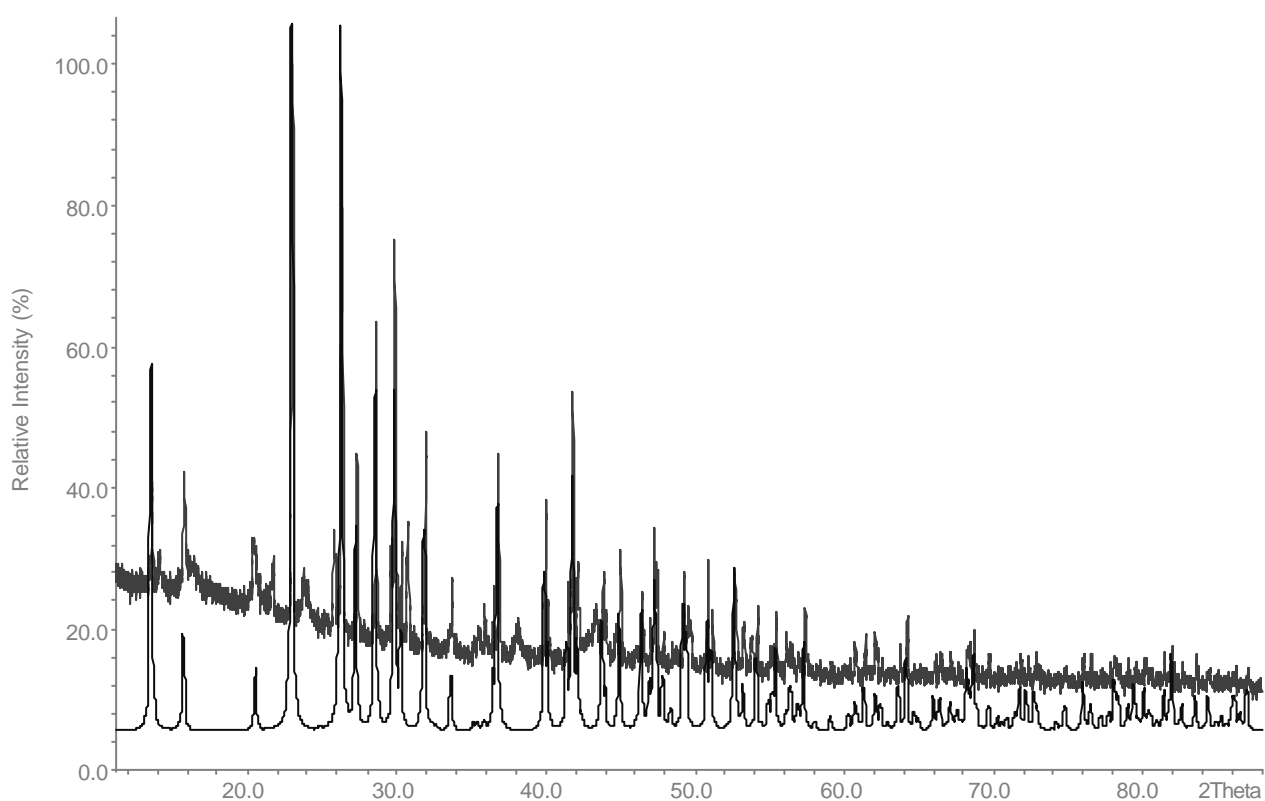
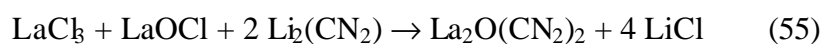
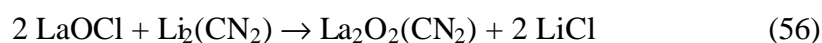


Figure 37. The calculated powder pattern from single crystal data (below) is compared with the measured X-ray powder pattern (above).

The stoichiometry of the compound was obtained from the X-ray powder diffraction studies. The studies were performed for the phase obtained more often as a side product, when LaCl_3 containing oxide impurities and $\text{Li}_2(\text{CN}_2)$ was reacted in a quartz ampoule in the temperature range of 500 - 650 °C in different stoichiometries. The powder pattern was indexed using Louer's algorithm (DICVOL) consistent with a monoclinic cell ($a = 13.507(2)$ Å, $b = 6.2432(9)$ Å, $c = 6.1002(7)$ Å, $\beta = 104.833(8)$, $V = 497.3(2)$ Å³) for 75 selected peaks. The number of single indexed lines obtained was 54 with a figure of merit of 88. The measured powder pattern is in agreement with the calculated pattern as shown in Figure 37. Although the positions of light atoms were difficult to refine, the composition was predicted to be $\text{La}_2\text{O}(\text{CN}_2)_2$ with some degree of uncertainty. Later on, well developed plate-like white crystals with very light brownish tint was obtained by flux route as shown in the reaction 55. In the presence of LiCl-KCl flux (29mg), stoichiometric reaction mixture (225 mg) according to reaction 54 was heated at the rate of 0.4 °C/min to 600 °C and allowed to dwell at this temperature for ten days in a quartz sealed copper ampoule before cool down slowly to 300 °C first and then to room temperature. The compound $\text{La}_2\text{O}(\text{CN}_2)_2$ is air as well as water stable and so the side product and flux can be washed with water before drying it in an oven to obtain the major phase.

After $\text{La}_2\text{O}_2(\text{CN}_2)$ is known for a decade, $\text{La}_2\text{O}(\text{CN}_2)_2$ is the second compound in this system. The synthesis route employed here to obtain $\text{La}_2\text{O}(\text{CN}_2)_2$ may be also considered for the synthesis of (doped) $\text{La}_2\text{O}_2(\text{CN}_2)$ compounds as shown in (56), instead of the reported one where graphite serves as a carbon source for the $(\text{CN}_2)^{2-}$ formation.



This synthesis may also be helpful for a reinvestigation of the crystal structure of $\text{La}_2\text{O}_2(\text{CN}_2)$, so as to take a closer look at the reported disorder of NCN groups in this structure.

4. 9. 3. Crystal structure of $\text{La}_2\text{O}(\text{CN}_2)_2$

The suitable white plate-like single crystals of $\text{La}_2\text{O}(\text{CN}_2)_2$ were selected under the microscope and mounted on the tip of glass fibers for single crystal X-ray diffraction studies. Some selected crystallographic data of the measurement and the structure refinement are shown in Table 23. The atomic positions and isotropic-equivalent displacement parameters

are given in Table 24. A summary of selected bond lengths and bond angle are given in Table 25.

The crystal structure of $\text{La}_2\text{O}(\text{CN}_2)_2$ shown in Figure 38 may occur complicated on the first glance. However the arrangements of La^{3+} and $(\text{CN}_2)^{2-}$ ions can be well derived from the positions of cations and anions in a NaCl type structure. In addition, the oxygen atoms of $\text{La}_2\text{O}(\text{CN}_2)_2$ occupy the 1/4 of the tetrahedral voids created by the La^{3+} ions. Such relations with NaCl structure type are frequently used to explain the structures of cubic pyrite (FeS_2) or of cubic CaC_2 . A comparison of a section of the $\text{La}_2\text{O}(\text{CN}_2)_2$ structure with the cubic pyrite (FeS_2) [87] structure having S_2^{2-} ions similar to linear CN_2^{2-} ions in $\text{La}_2\text{O}(\text{CN}_2)_2$ is illustrated in Figure 39. For better understanding of the structure, the lanthanum atoms are connected with carbon instead of nitrogen atoms of the $(\text{CN}_2)^{2-}$ units in the Figures 38 and 39.

In a different view, the crystal structure of $\text{La}_2\text{O}(\text{CN}_2)_2$ contains one-dimensional chains composed of edge sharing $[\text{OLa}_{4/2}]$ tetrahedra running along the c -axis. A perspective view of the carbodiimide ions being situated in between the chains of tetrahedra is shown in Figure 40. In literature, N species, hydride and K ions of $\text{K}_5(\text{CN}_2)_2\text{H}$ [88] form rocksalt type slabs with linear carbodiimide units stacked with in the layers.

The $(\text{N-C-N})^{2-}$ unit in $\text{La}_2\text{O}(\text{CN}_2)_2$ has two different crystallographic positions for the nitrogen atoms. However, the calculated C–N distances of 1.227(6) Å and 1.233(6) Å do not differ significantly from each other. Hence the $(\text{N-C-N})^{2-}$ unit is clearly closer to a carbodiimide than to a cyanamide, even though the N–C–N angle was refined at 176.1(5)°. The average La–O bond distance of 2.428(5) Å in $\text{La}_2\text{O}(\text{CN}_2)_2$ is slightly longer than the corresponding value of 2.39 Å in $\text{La}_2\text{O}_2(\text{CN}_2)$.

The IR spectra of $\text{La}_2\text{O}(\text{CN}_2)_2$ also suggested the presence of carbodiimide with strong characteristic absorption peak of $\nu_{\text{as}}(\text{CN}_2)^{2-}$ around 1979 cm^{-1} and strong $\nu(\text{CN}_2)^{2-}$ peaks around 661 and 684 cm^{-1} . The corresponding characteristic IR peaks of 1950 cm^{-1} and 670 cm^{-1} were reported for $\text{La}_2\text{O}_2(\text{CN}_2)$.

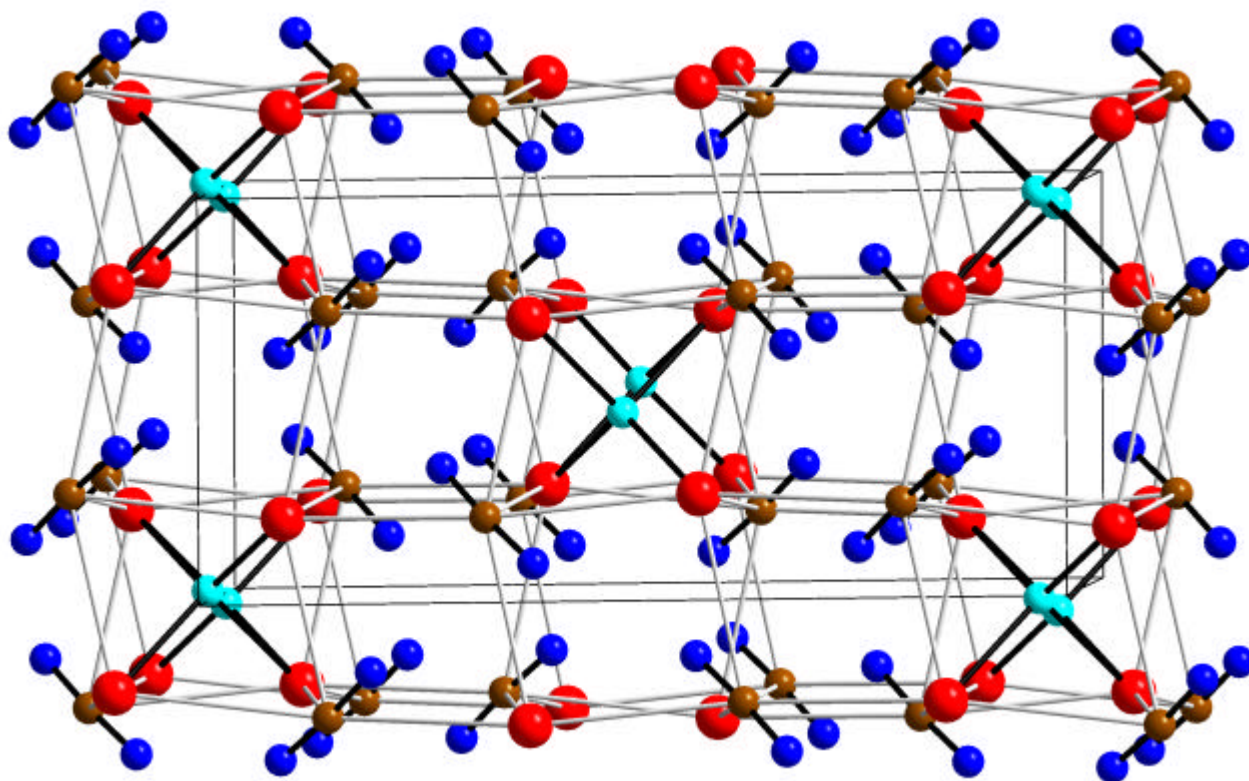


Figure 38. Unit cell of $\text{La}_2\text{O}(\text{CN}_2)_2$. Lanthanum atoms are shown red, carbon atoms brown, nitrogen atoms blue, and oxygen atoms cyan.

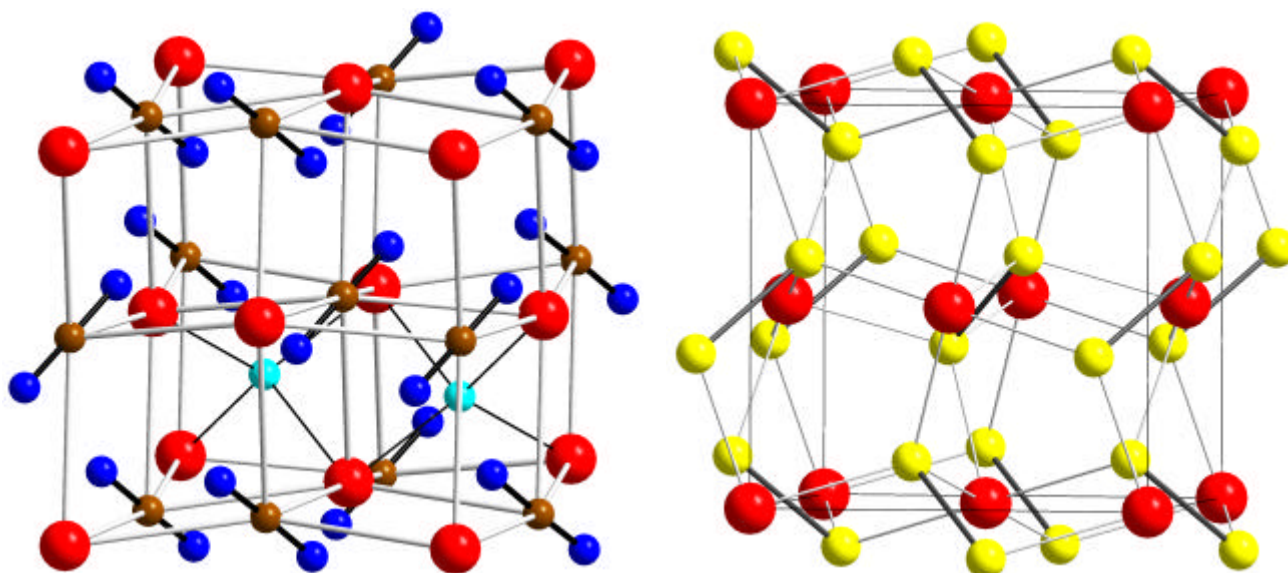


Figure 39. Relation of cubic FeS_2 (Pyrite, above) with the substructure of $\text{La}_2\text{O}(\text{CN}_2)_2$ (below) in which oxide ions occupy 1/4 of the tetrahedral voids. Atom colours are the same as in Figure 38 with iron atoms in red and sulphur atoms in yellow.

Table 23. Crystallographic details of $\text{La}_2\text{O}(\text{CN}_2)_2$.

Space group (no.), Z	$C2/c$ (15), 4
Unit cell dimension (in Å)	$a = 13.530(2)$, $b = 6.250(1)$, $c = 6.1017(9)$, $\hat{a} = 104.81(2)$
Cell volume (in Å ³)	498.89(14)
Density calc. (g. cm ⁻³)	4.978
Molecular weight (g.mol ⁻¹)	373.88
Crystal appearance	Transparent white plates
Crystal size (in mm ³)	0.1 x 0.04 x 0.04
Diffractometer	STOE, IPDS
Radiation, Temperature	Mo-K α ($\lambda = 71.073$ pm), Graphite Monochromator, 293(2) K
Range: θ	5.27 to 30.35°
Range: h, k, l	$-19 \leq h \leq 19$, $-8 \leq k \leq 8$, $-8 \leq l \leq 8$
Data correction	Lorentz, polarisation and absorption
μ (mm ⁻¹)	16.78
Unique reflections	734
Collected reflections ($F_0 > 2\sigma(F_0)$)	4289
Parameters refined	42 (all atoms refined anisotropically)
R indices (all data)	R1 = 0.0266, wR2 = 0.0283
Final R indices [$I > 2\sigma(I)$]	R1 = 0.0671, wR2 = 0.0679
GooF (all reflections)	1.141
Res. peak: max.; min. (e/Å ³)	3.17, -1.19

$$^a R1 = \frac{\sum ||F_o| - |F_c||}{\sum |F_o|}; ^b wR2 = \left[\frac{\sum w(F_o^2 - F_c^2)^2}{\sum w(F_o^2)^2} \right]^{1/2}$$

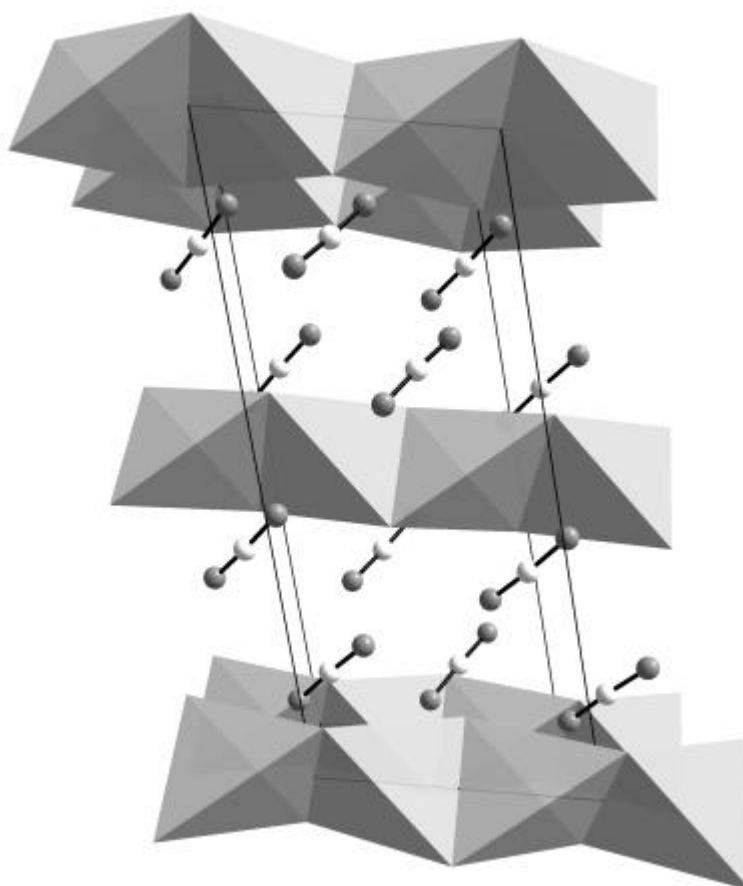


Figure 40. Perspective view of edge shared [OLa₄] tetrahedral chains along the c-axis.

Table 24. Atomic coordinates and isotropic-equivalent displacement parameters (\AA^2) for $\text{La}_2\text{O}(\text{CN}_2)_2$.

Atom	multiplicity, x symmetry	x	y	z	U_{eq}^a
La1	8 f	0.10072(2)	0.21443(3)	0.07542(4)	0.0096(1)
O1	4 e	0	0.0260(6)	0.75	0.0118(8)
N1	8 f	0.2915(3)	0.3423(7)	0.2473(6)	0.0143(6)
N2	8 f	0.0923(3)	0.6174(6)	0.9698(6)	0.0133(7)
Cl	8 f	0.1530(3)	0.2739(6)	0.6112(8)	0.0111(8)

^a U_{eq} is defined as one-third of the trace of the orthogonalized U_{ij} tensor.

The La atom is eight coordinated in a distorted square antiprismatic fashion with four cyanamide ions from one side and two cyanamide ions as well as two oxide ions from the other side. The two different nitrogen atoms (3 N1 and 3 N2) bonded to lanthanum are shown

in Figure 41. The symmetrical coordination environment with three lanthanum ions on both sides of the carbodiimide unit is also shown in Figure 41.

Table 25. Bond distances (in Å) and bond angle (in °) in $\text{La}_2\text{O}(\text{CN}_2)_2$.

La1–O1	2.409(2)
La1–O1	2.448(2)
La1–N1	2.650(4)
La1–N1	2.756(3)
La1–N1	2.811(4)
La1–N2	2.595(4)
La1–N2	2.655(3)
La1–N2	2.762(4)
C1–N1	1.227(6)
C1–N2	1.233(6)
N1–C–N2	176.1(5)

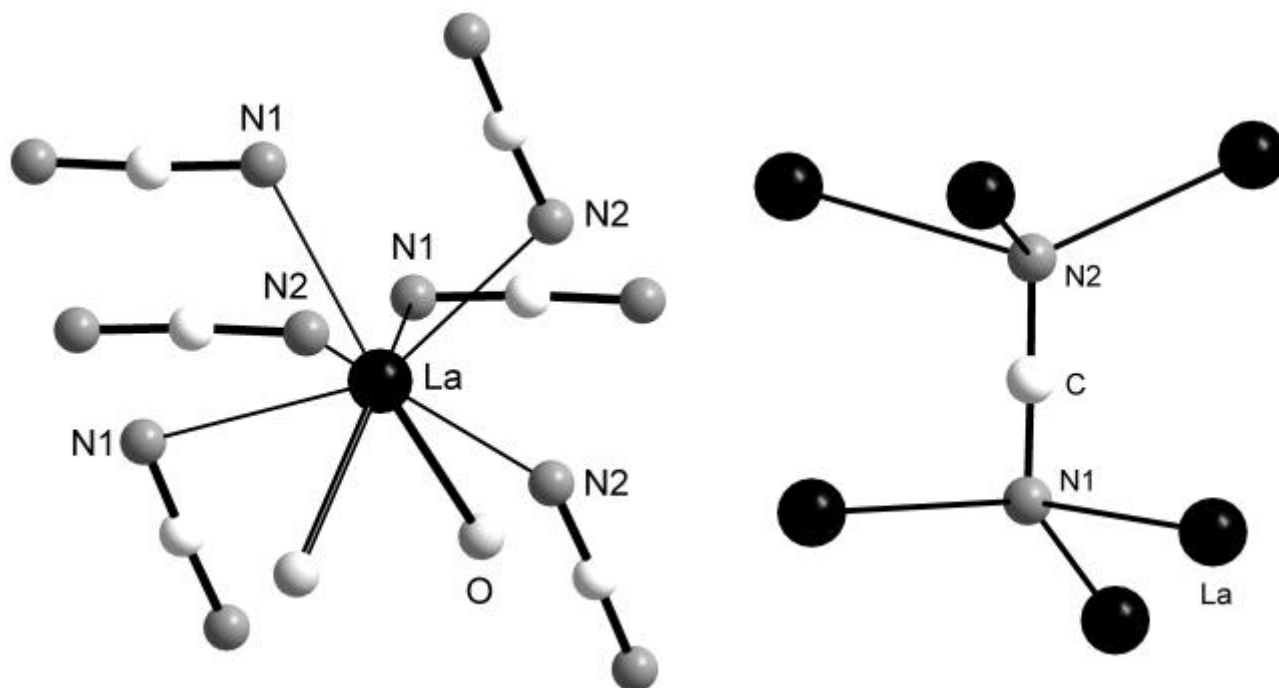


Figure 41. Coordination environment around the lanthanum (left) and carbodiimide ion (right) in $\text{La}_2\text{O}(\text{CN}_2)_2$.

4. 9. 4. Reaction between LaOCl and Li₂(CN₂)

The stoichiometric 2:1 reaction between LaOCl and Li₂(CN₂) was carried out to synthesise La₂O₂(CN₂) as shown in the reaction 56.

LaOCl remained unreacted even after heating the reaction mixture to 800 °C. So in order to get better reactivity, LiCl-KCl flux was introduced along the reaction mixture of LaOCl and Li₂(CN₂). La₂O(CN₂)₂ was obtained from the above reaction after treated to 650 °C for one week. The powder pattern was indexed using Louer's algorithm (DICVOL) consistent with a monoclinic cell ($a = 13.501(5) \text{ \AA}$, $b = 6.249(2) \text{ \AA}$, $c = 6.101(3) \text{ \AA}$, $\hat{a} = 104.82(2)$, $V = 497.6(5) \text{ \AA}^3$) for 39 selected peaks. The number of single indexed lines obtained was 35.

Tetragonal La₂O₂(CN₂) was obtained only as a side product along with LaOCl and an other unknown phase, when LaOCl containing LaCl₃ was reacted with Li₂(CN₂) at 800 °C for four days in a tantalum ampoule. Hence attempts to synthesise single crystal of La₂O₂(CN₂) or pure powder was not successful with flux and without flux at different temperatures ranging from 600 - 950 °C in different stoichiometries.

4. 9. 5. Reaction between CeOCl and Li₂(CN₂)

Hexagonal Ce₂O₂(CN₂) [35] was obtained when CeOCl containing CeCl₃ was reacted with Li₂(CN₂) at 900 °C for four days in a quartz sealed tantalum container. The major phase from the X-ray powder pattern was indexed to the similar cell parameters of known Ce₂O₂(CN₂) by omitting some unidentified reflections as shown in Figure 42. The powder pattern was indexed using werner's algorithm consistent with a hexagonal cell ($a = 3.9471(2) \text{ \AA}$, $c = 8.3579(6) \text{ \AA}$, $V = 112.77(1) \text{ \AA}^3$) for 44 selected peaks. The number of single indexed lines obtained was 34 with a figure of merit of 106.

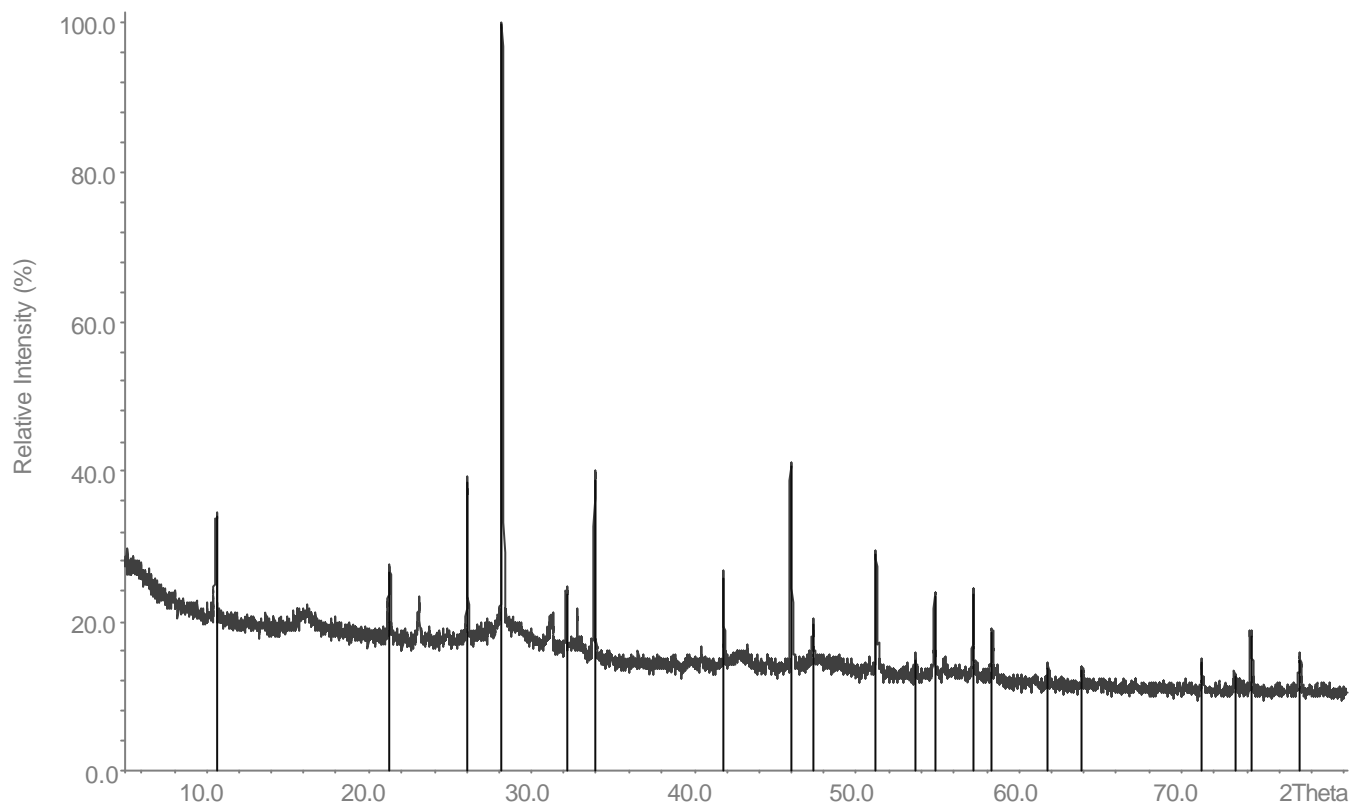


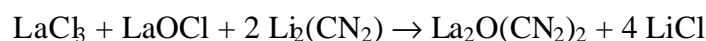
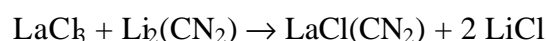
Figure 42. The powder pattern obtained from the reaction between CeCl_3 , CeOCl and $\text{Li}_2(\text{CN}_2)$. Lines in black indicate the indexed lines for $\text{Ce}_2\text{O}_2(\text{CN}_2)$.

5. 0. Summary and Outlook

5. 1. Summary

The synthesis of molecular precursors with controlled element composition has become a highly demanding subject due to its potential applications in the area of materials science. In earlier studies of cyanamide or carbodiimide containing compounds, the directed approach of synthesis using appropriate ligands was not studied in detail. Many new carbodiimide or cyanamide compounds with novel structural features from the literature were synthesised rather accidentally. For example, $\text{Ca}_4\text{N}_2(\text{CN}_2)$ and $\text{Ca}_{11}\text{N}_6(\text{CN}_2)_2$ compounds were discovered while pursuing the reactions for the nitride phase ‘ Ca_{11}N_8 ’ with the source of carbon believed to be from the container material.. Also $\text{In}_{2.24}(\text{CN}_2)_3$ and $\text{NaIn}(\text{CN}_2)_2$ were synthesised while pursuing the synthesis of indium cyanides.

The original aim of this work is to investigate the synthesis and structure of new compounds in the system of lanthanide halides and lithium carbodiimide by the aid of solid state metathesis route. The motivation for adopting the solid state metathesis route was from the synthesis of lanthanide nitridoborates at comparatively lower temperatures. The solid state metathesis route is successfully applied to synthesise the following stoichiometric compounds.



With the use of LiCl/KCl flux route, $\text{LaCl}(\text{CN}_2)$ and $\text{La}_2\text{O}(\text{CN}_2)_2$ were crystallised under comparatively low temperature conditions at 650 °C. The utility of AlCl_3 as a chemical transport agent for purification is utilised for the synthesis of lanthanide chloride cyanamides [53].

With the obtained results, the reactivity in the system of $\text{LaCl}_3/\text{Li}_2(\text{CN}_2)$ is understood. The reactivity studies revealed that the $(\text{CN}_2)^{2-}$ ions remain intact at least up to 650 °C, when

LaCl_3 is heated with $\text{Li}_2(\text{CN}_2)$ in a sealed quartz ampoule with either 1:1 or 2:3 molar ratios [53]. The syntheses of $\text{La}_2\text{Cl}(\text{CN}_2)\text{N}$ were performed from three different starting mixtures: (a) $2 \text{LaCl}_3 + \text{Li}_3\text{N} + \text{Li}_2(\text{CN}_2)$, (b) $2 \text{La}_2\text{NCl}_3 + \text{Li}_2(\text{CN}_2)$, and (c) $2 \text{LaCl}_3 + 3 \text{Li}_2(\text{CN}_2)$, all of them varied in stoichiometry and reacted at 750 °C or higher. In reaction (a), La_2NCl_3 is being formed from $2 \text{LaCl}_3 + \text{Li}_3\text{N}$ near 500 °C and is an intermediate that can react further with $\text{Li}_2(\text{CN}_2)$ to yield $\text{La}_2\text{Cl}(\text{CN}_2)\text{N}$ at above 750 °C, as obtained according to (b). A fragmentation reaction of the $(\text{CN}_2)^{2-}$ ion is necessary in reaction (c) to yield $\text{La}_2\text{Cl}(\text{CN}_2)\text{N}$ at around 800 °C [53].

The formation of $\text{LaCl}(\text{CN}_2)$ has been obtained in reactions similar to (c) from approximate 1:1 molar reactions of LaCl_3 and $\text{Li}_2(\text{CN}_2)$ at 600 °C. According to the thermal decomposition, layered $\text{LaCl}(\text{CN}_2)$ may be suspected to transform into 3-D network $\text{La}_2\text{Cl}(\text{CN}_2)\text{N}$ under the release of cyanuric chloride. On the other hand, when Li_3N was used along with the 1:1 molar $\text{LaCl}_3/\text{Li}_2\text{CN}_2$ mixture at 650 °C for one week, $\text{La}_2\text{Cl}(\text{CN}_2)\text{N}$ was obtained as the product without any $\text{LaCl}(\text{CN}_2)$. Hence the reactivity between LaCl_3 and Li_2CN_2 is clearly influenced by the presence and absence of Li_3N [53].

The structure of layered $\text{LaCl}(\text{CN}_2)$ has close structural relations to the PbFCl type LaOCl and hence can be considered as a *Sillen* X_2 -type compound. $\text{La}_2\text{Cl}(\text{CN}_2)\text{N}$ has a novel structure pattern with M_6X_8 cluster type $[\text{La}_6(\text{CN}_2)_4\text{N}_4]$ basic building units interconnected by bridging carbodiimide units to form a 3-D network structure containing channels occupied by chloride ions. The analogous bromide and iodide compounds were also synthesised and structurally characterised.

The crystal structure of lanthanum oxide dicyanamide is determined for the first time. It's novel structure pattern contains a distorted ccp arrangement of lanthanide ions and cyanamide ions with similarities to cubic pyrite. In addition, the oxide ions are occupying one fourth of the tetrahedral holes formed by lanthanum.

The first tricyanomethanide compound of lanthanum, $\text{KLa}[\text{C}(\text{CN})_3]_4 \cdot \text{H}_2\text{O}$ was synthesised from the aqueous solution of nitrate salt in a simple way. The crystal structure contains tridentate planar tricyanomethanide ions bridging both lanthanum and potassium. The lanthanum atoms are coordinated by eight nitrogen atoms from the tricyanomethanide ion to form a beautiful flower like arrangement.

5. 2. Outlook

The focus of the work reported herein has been targeted on the synthesis and characterisation of C–N containing lanthanide compounds. A more general extension of this work would be using transition metal chlorides or non-metal halides like $C_3N_3Cl_3$ to synthesise new types of cyanamide or carbodiimide compounds of transition metal or $(CN)_x$ polymers by low temperature flux routes. The use of chemical transport agents like $AlCl_3$ can also be encountered to synthesise new cyanamide or carbodiimide compounds with different structural possibilities in transition metal chemistry. These reactions also indicate the possibility of synthesising nano level controlled carbon nitrides using the spacer ligands like cyanamide or carbodiimide units. Further on, this type of reactions involving metal halides can also be extended to boron containing cyanamide/carbodiimide compounds or non metal boron containing carbon nitrides in non metal chemistry.

The scope of these compounds may be with their luminescence properties in the presence of dopants like Eu or other lanthanide.

Similar to tricyanomethanide ligand, the other poly cyano ligands like $K[B(CN)_4]$ can be used in solution route to synthesise new lanthanide or other metal compounds. Structures with $[C(CN)_3]^-$ ions show promise in the design of magnetic materials because of their conjugated π resonance structures, which may provide coupling pathways for magnetic interactions between paramagnetic lanthanide or even mixed lanthanide–transition metal centers.

6. Appendix

The compounds from the literature present in the system Metal/O/C/N with their crystal system, space group, unit cell parameters and the typical structure unit is tabulated in Table 26.

Table 26. Compounds in Metal/O/C/N system known from the literature (metal cyanides are excluded)

Compound	Crystal system, Space group (no.)	Unit cell a, b, c in Å $\hat{a}, \hat{b}, \hat{c}$ in °	Typical structure units	Reference
H ₂ N-CN	Orthorhombic, Pbca (61)	6.856(1), 6.625(1), 9.147(1)	bent cyanamide (CN ₂) ²⁻ ion	22
Li ₂ (CN ₂)	Tetragonal I4/mmm (139)	3.687(3), 8.668(5)	linear isolated carbodiimide (CN ₂) ²⁻ ion	4
Na ₂ (CN ₂)	Monoclinic C2/m (12)	5.0456(3), 5.0010(3), 5.5359(3), 110.078(5)	linear isolated carbodiimide (CN ₂) ²⁻ ion	4
K ₂ (CN ₂)	Monoclinic C2/m (12)	5.7877(1), 5.7030(1), 5.7857(2), 109.016(1)	linear isolated carbodiimide (CN ₂) ²⁻ ion	4
Na(HCN ₂)	Orthorhombic, Pbcm (57)	3.531, 10.358, 6.486	(HNCN) ⁻ anion	4
Na ₅ H(CN ₂) ₃	Cubic, Im-3m (229)	7.2449(9)	linear isolated carbodiimide (CN ₂) ²⁻ ion	89

Na[C(NH ₂) ₃][C(NCN) ₃]	Trigonal, P-3 (147)	8.942(2), 6.576(4)	planar (C ₄ N ₆) ²⁻ anion	17
Na ₃ (C ₆ N ₉)	Monoclinic P2 ₁ /n (14)	11.0482(1), 23.3806(3), 3.51616(3), 97.9132(9)	planar (C ₆ N ₉) ³⁻ ring	18
Na ₃ (C ₆ N ₉)•3H ₂ O	Hexagonal P- 62c (190)	10.2358(8), 6.5085(15)	planar (C ₆ N ₉) ³⁻ ring	90
K(HCN ₂)	Orthorhombic P2 ₁ 2 ₁ 2 ₁ (19)	7.087, 9.090, 9.014	(HNCN) ⁻ anion	91
K ₅ (CN ₂) ₂ H	Tetragonal, P4/ncc (130)	9.0953(3), 11.0291(6)	linear isolated carbodiimide (CN ₂) ²⁻ ion	88
K ₅ H(CN ₂) ₃	Cubic, I4-3m (229)	7.9568(7)	linear isolated carbodiimide (CN ₂) ²⁻ ion	92
K ₃ (C ₆ N ₉)	Monoclinic P2 ₁ /c (14)	3.7382(1), 11.9248(5), 25.004(1), 101.406(3)	planar (C ₆ N ₉) ³⁻ ring	18
K ₃ (C ₆ N ₉)•H ₂ O	Triclinic P1 (1)	3.7291(2), 8.0920(5), 10.1222(5), 71.209(2), 80.524(3), 86.653(3)	planar (C ₆ N ₉) ³⁻ ring	93
Rb(HCN ₂)	Orthorhombic P2 ₁ 2 ₁ 2 ₁ (19)	7.299(1), 9.435(1), 9.420(1)	(HNCN) ⁻ anion	94
Rb ₃ (C ₆ N ₉)	Monoclinic P2 ₁ /c (14)	3.8993(2), 12.2606(6)	planar (C ₆ N ₉) ³⁻ ring	18

	P2 ₁ /c (14)	12.2606(6), 25.475(1), 98.741(5)	(C ₆ N ₉) ³⁻ ring	
Rb ₃ (C ₆ N ₉)•H ₂ O	Triclinic P1 (1)	3.9317(1), 8.2648(2), 10.3628(3), 70.798(1), 81.872(2), 87.504(1)	planar (C ₆ N ₉) ³⁻ ring	93
RbH ₂ (C ₆ N ₉)•1/2H ₂ O	Monoclinic C2/c (15)	20.074(3), 5.122(1), 21.680(4), 111.66(2)	planar (C ₆ N ₉) ³⁻ ring	95
Mg(CN ₂)	Trigonal R-3m (166)	3.2734(1), 14.1282(5)	linear isolated carbodiimide (CN ₂) ²⁻ ion	5
Ca(CN ₂)	Rhombohedral R-3m (166)	5.347	linear isolated carbodiimide (CN ₂) ²⁻ ion	3
Ca ₄ N ₂ (CN ₂)	Orthorhombic, Pnma (62)	11.439(2), 3.5772(7), 13.844(3)	linear isolated carbodiimide (CN ₂) ²⁻ ion	29
Ca ₁₁ N ₆ (CN ₂) ₂	Tetragonal P4 ₂ nm (102)	11.4532(16), 3.6083(6)	linear isolated carbodiimide (CN ₂) ²⁻ ion	29
Ca _{4-x} Sr _x (CN ₂)N ₂ (x = 0.80)	Orthorhombic Pnma (62)	11.677(1), 3.6470(4), 13.911(1)	bent isolated cyanamide (CN ₂) ²⁻ ion	96

$\acute{\alpha}$ -Sr(CN ₂)	Orthorhombic, Pnma (62)	12.410(2), 3.963(2), 5.389(2)	Bent isolated cyanamide (CN ₂) ²⁻ ion	5
$\hat{\alpha}$ -Sr(CN ₂)	Trigonal R-3m (166)	3.9799(1), 14.9407(7)	Linear isolated carbodiimide (CN ₂) ²⁻ ion	97
Sr ₄ N ₂ (CN ₂)			linear isolated carbodiimide (CN ₂) ²⁻ ion	98
Sr ₂ (CN ₂)(CN) ₂	Hexagonal P6 ₃ /mmc (194)	10.3591(1), 6.6423(1)	linear isolated carbodiimide (CN ₂) ²⁻ ion	99
Ba(CN ₂)	Trigonal R-3c (167)	15.282(2), 7.013(2)	bent isolated cyanamide (CN ₂) ²⁻ ion	5
Ba ₂ Na(CN ₂)(CN) ₃	Cubic Fd-3m (227)	15.188(3)	linear isolated carbodiimide (CN ₂) ²⁻ ion	100
Ba ₂ (CN ₂)(CN) ₂	Hexagonal P6 ₃ /mmc (194)	10.6652(5), 6.9682(3)	linear isolated carbodiimide (CN ₂) ²⁻ ion	99
Ba ₉ (NbN ₄) ₂ O(CN ₂)	Triclinic P-1 (2)	7.9905(2), 9.6261(2), 12.6438(4), 75.859(1), 85.745(1), 87.8621(8)	bent isolated cyanamide (CN ₂) ²⁻ ion	101

$(\text{Ba}_6\text{N})_2(\text{MoN}_4)(\text{CN}_2)_6$	Cubic, Pn-3 (201)	11.228(1)	(Ba_6N) octahedra and (MoN_4) tetrahedra with isolated cyanamide ion	102
$\text{Ba}_8(\text{WN}_4)(\text{CN}_2)_5$	Monoclinic, $\text{P2}_1/\text{a}$ (14)	11.746(1), 14.947(2), 11.526(3), 94.21(1)	(WN_4) tetrahedra with isolated cyanamide ion	102
$\text{Co}(\text{NCNH}_2)_4\text{Cl}_2$	Cubic Im-3m (229)	12.663(2)	neutral cyanamide	28
$\text{Ni}(\text{NCNH}_2)_4\text{Cl}_2$	Cubic Im-3m (229)	12.593(2)	neutral cyanamide	28
$\text{Cu}(\text{NCNH}_2)_4\text{Cl}_2$	Cubic Im-3m (229)	12.443(2)	neutral cyanamide	28
$\text{Ag}_2(\text{CN}_2)$	Monoclinic, $\text{P2}_1/\text{c}$ (14)	7.315(1), 6.010(1), 6.684(1), 102.29(1)	bent cyanamide $(\text{CN}_2)^{2-}$ ion	6
$\text{Zn}(\text{CN}_2)$	Tetragonal I-42d (122)	8.8047(2), 5.4329(2)	bent cyanamide $(\text{CN}_2)^{2-}$ ion	6
$\text{Cd}(\text{CN}_2)$	Trigonal R-3m (166)	3.317(1), 14.5558(4)	bent cyanamide $(\text{CN}_2)^{2-}$ ion	6
$\text{Hg}(\text{CN}_2)$	Orthorhombic, Pbca (61)	10.4851(1), 6.5138(1), 6.8929(1)	bent cyanamide $(\text{CN}_2)^{2-}$ ion	6
$\text{Hg}(\text{CN}_2)$	Monoclinic $\text{P2}_1/\text{a}$ (14)	6.8521(4), 6.9797(4),	bent cyanamide	6

		5.5515(4), 113.212(4)	(CN ₂) ²⁻ ion	
Hg ₂ (CN ₂)Cl ₂	Monoclinic P2 ₁ /c (14)	8.067(1), 9.071(2), 7.880(1), 106.446(3)	Linear isolated carbodiimide (CN ₂) ²⁻ ions	31
Hg ₃ (CN ₂) ₂ Cl ₂	Orthorhombic Pca2 ₁ (29)	7.020(2), 10.785(2), 10.503(2)	linear carbodiimide and bent cyanamide (CN ₂) ²⁻ ions	31
In _{2.24} (CN ₂) ₃	Rhombohedral R-3c (161)	6.0609(4), 28.844(2)	Linear isolated carbodiimide (CN ₂) ²⁻ ions	7
NaIn(CN ₂) ₂	Orthorhombic Cmcm (63)	9.6130(6), 7.1684(5), 6.0365(4)	Linear isolated carbodiimide (CN ₂) ²⁻ ions	7
â-Si(CN ₂) ₂	Cubic Pn-3m (224)	6.1885(1)	linear carbodiimide (CN ₂) ²⁻ ions	30
Si ₂ CN ₄	Orthorhombic Aba2 (41)	5.44, 13.58, 4.81	linear carbodiimide (CN ₂) ²⁻ ions	30
(CH ₃) ₃ Si(CN ₂)Si(CH ₃) ₃	Monoclinic P2 ₁ /c (14)	9.71(2), 11.11(1), 11.88(2), 102.3(2)	Linear carbodiimide (CN ₂) ²⁻ ions	103
[(CH ₃) ₃ Si(CN ₂)] ₄	Monoclinic P2 ₁ /c (14)	10.508(3), 9.326(2), 11.608(3), 114.35(2)	Linear carbodiimide (CN ₂) ²⁻ ions	104

[Mes ₂ Ge(CN ₂) ₃ Mes = mesityl group	Triclinic, P-1 (2)	13.193(5), 15.729(5), 15.923(5), 107.32(6), 112.61(5), 105.76(6)	linear carbodiimide (CN ₂) ²⁻ ions	105
[Mes ₂ Ge(CN ₂) ₄ Mes = mesityl group	Tetragonal, I-4 (82)	20.779(5), 8.615(3)	linear carbodiimide (CN ₂) ²⁻ ions	105
Cl ₄ Sb(CN ₂)Si(CH ₃) ₃	Monoclinic P2 ₁ /c (14)	6.383(3), 9.722(5), 20.346(9), 92.17(4)	linear carbodiimide (CN ₂) ²⁻ ions	106
Pb(CN ₂)	Orthorhombic Pnma (62)	5.5566(4), 3.8677(2), 11.7350(8)	bent cyanamide (CN ₂) ²⁻ ion	7
La ₂ O ₂ (CN ₂)	Tetragonal I4/mmm (139)	4.0964(2), 12.333(1)	bent cyanamide (CN ₂) ²⁻ ion	35
La ₂ O(CN ₂) ₂	Monoclinic C2/c (15)	13.530(2), 6.250(1), 6.1017(9), 104.81(2)	bent cyanamide (CN ₂) ²⁻ ion	107
Pr ₂ O ₂ (CN ₂)	Trigonal P-3m1 (64)	3.9139(10), 8.3324(15)	linear carbodiimide (CN ₂) ²⁻ ions	35
Nd ₂ O ₂ (CN ₂)	Trigonal P-3m1 (64)	3.8840(7), 8.3106(12)	linear carbodiimide (CN ₂) ²⁻ ions	35
Sm ₂ O ₂ (CN ₂)	Trigonal P-3m1 (64)	3.8276(9), 8.2666(15)	linear carbodiimide (CN ₂) ²⁻ ions	35

$\text{Eu}_2\text{O}_2(\text{CN}_2)$	Trigonal P-3m1 (64)	3.8049(6), 8.2515(9)	linear carbodiimide $(\text{CN}_2)^{2-}$ ions	35
$\text{Eu}(\text{CN}_2)$	Orthorhombic Pnma (62)	12.3241(9), 3.9526(3), 5.3943(4)	linear carbodiimide $(\text{CN}_2)^{2-}$ ions	32
$\text{LiEu}_2(\text{CN}_2)_3\text{I}_3$	Cubic Fd-3m (227)	15.1427(17)	linear carbodiimide $(\text{CN}_2)^{2-}$ ions	33
$\text{LiSr}_2(\text{CN}_2)_3\text{I}_3$	Cubic Fd-3m (227)	15.2312(13)	linear carbodiimide $(\text{CN}_2)^{2-}$ ions	108
$\text{LiEu}_4(\text{CN}_2)_3\text{I}_3$	Hexagonal P6 ₃ /mmc (194)	10.6575(11), 6.8232(10)	linear carbodiimide $(\text{CN}_2)^{2-}$ ions	33
$\text{LaCl}(\text{CN}_2)$	Monoclinic P2 ₁ /m (11)	5.330(1), 4.0305(8), 7.545(1), 100.75(2)	bent cyanamide $(\text{CN}_2)^{2-}$ ion	53
$\text{CeCl}(\text{CN}_2)$	Monoclinic P2 ₁ /m (11)	5.322(3), 4.022(2), 7.530(5), 100.75(4)	bent cyanamide $(\text{CN}_2)^{2-}$ ion	53
$\text{PrCl}(\text{CN}_2)$	Monoclinic P2 ₁ /m (11)	5.296(2), 3.934(1), 7.460(2), 100.43(1)	bent cyanamide $(\text{CN}_2)^{2-}$ ion	53
$\text{La}_2\text{Cl}(\text{CN}_2)\text{N}$	Orthorhombic Cmmm (65)	13.3914(8), 9.6345(7), 3.9568(2)	linear carbodiimide $(\text{CN}_2)^{2-}$ ions	55
$\text{Ce}_2\text{Cl}(\text{CN}_2)\text{N}$	Orthorhombic Cmmm (65)	13.334(1), 9.5267(8), 3.9402(5)	linear carbodiimide $(\text{CN}_2)^{2-}$ ions	55

$C_2N_4H_4$	Monoclinic C2/c (15)	15.00, 4.44, 13.12, 115°20'	$(C_2N_3)^-$ anion	109
$NH_4(N(CN)_2)$	Monoclinic P2 ₁ /c (14)	3.7867(6), 12.409(3), 9.1184(14), 91.488(18)	$(C_2N_3)^-$ anion	110
\acute{a} -Na(N(CN) ₂)	Monoclinic P2 ₁ /n (14)	6.477(1), 14.948(3), 3.5725(7), 93.496(1)	$(C_2N_3)^-$ anion	16
\hat{a} -Na(N(CN) ₂)	Orthorhombic Pbnm(62)	6.5015(5), 14.951(2), 3.6050(3)	$(C_2N_3)^-$ anion	16
\acute{a} -K(N(CN) ₂)	Orthorhombic Pbcm (57)	8.3652(1), 6.469(1), 7.2127(1)	$(C_2N_3)^-$ anion	16
\hat{a} -K(N(CN) ₂)	Monoclinic P2 ₁ /n (14)	7.2692(1), 15.9634(2), 3.87037(5), 111.8786(6)	$(C_2N_3)^-$ anion	16
\tilde{a} -K(N(CN) ₂)	Orthorhombic Pnma (62)	8.5540(3), 3.8780(1), 12.5273(4)	$(C_2N_3)^-$ anion	16
\acute{a} -Rb(N(CN) ₂)	Orthorhombic Pbcm (57)	8.5609(1), 6.61711(7), 7.65067(9)	$(C_2N_3)^-$ anion	16
\hat{a} -Rb(N(CN) ₂)	Monoclinic C2/c (15)	13.8156(2), 10.0002(1), 14.4328(2), 116.8963(6)	$(C_2N_3)^-$ anion	16

$\text{Cs}(\text{N}(\text{CN})_2)$	Monoclinic C2/c (15)	9.385(5), 12.702(9), 8.261(5), 110.94(4)	$(\text{C}_2\text{N}_3)^-$ anion	16
$\text{NaCs}_2(\text{N}(\text{CN})_2)_3$	Hexagonal P6 ₃ /m (176)	7.0001(4), 14.4929(7)	$(\text{C}_2\text{N}_3)^-$ anion	16
$\text{Ca}(\text{N}(\text{CN})_2)_2$	Monoclinic C2/c (15)	12.4455(3), 6.0797(1), 7.8981(1), 98.864(2)	$(\text{C}_2\text{N}_3)^-$ anion	111
$\text{Mg}(\text{N}(\text{CN})_2)_2$	Orthorhombic Pnmm (58)	6.1714(3), 7.1697(3), 7.4035(5)	$(\text{C}_2\text{N}_3)^-$ anion	111
$\text{Sr}(\text{N}(\text{CN})_2)_2$	Monoclinic C2/c (15)	12.7963(2), 6.24756(8), 8.1756(1), 99.787(1)	$(\text{C}_2\text{N}_3)^-$ anion	111
$\text{Ba}(\text{N}(\text{CN})_2)_2$	Orthorhombic Pnma (62)	13.6868(7), 4.2907(7), 12.2626(2)	$(\text{C}_2\text{N}_3)^-$ anion	111
$\text{Co}(\text{N}(\text{CN})_2)_2$	Orthorhombic Pnmm (58)	5.9985(15), 7.0711(18), 7.4140(19)	bridging $(\text{C}_2\text{N}_3)^-$ anion	19
$\text{Ni}(\text{N}(\text{CN})_2)_2$	Orthorhombic Pnmm (58)	5.97357(25), 7.03196(28), 7.29424(22)	bridging $(\text{C}_2\text{N}_3)^-$ anion	19
$\text{Cu}(\text{N}(\text{CN})_2)_2$	Orthorhombic Pnmm (58)	7.340(1), 6.1218(8), 7.1815(6)	bridging $(\text{C}_2\text{N}_3)^-$ anion	19
$\text{Ag}(\text{N}(\text{CN})_2)$	Trigonal P3121 (152)	3.601(2), 22.868(22)	$(\text{C}_2\text{N}_3)^-$ anion	112
$\text{Ag}(\text{N}(\text{CN})_2)$	Orthorhombic Pnma (62)	16.133(8), 3.612(2),	$(\text{C}_2\text{N}_3)^-$ anion	113

		5.983(3)		
Zn(N(CN) ₂) ₂	Orthorhombic Pnma (62)	7.6209(4), 7.5958(4), 12.0477(7)	(C ₂ N ₃) ⁻ anion	114
á-Cd(N(CN) ₂) ₂	Orthorhombic Pnmm (58)	6.2462(5), 7.5292(6), 7.6830(7)	(C ₂ N ₃) ⁻ anion	115
â-Cd(N(CN) ₂) ₂	Monoclinic P2 ₁ /n (14)	6.2160(3), 7.4876(4), 7.7021(5), 91.784(3)	(C ₂ N ₃) ⁻ anion	115
Pb(N(CN) ₂) ₂	Orthorhombic Pnma (62)	13.5045(10), 3.9989(4), 11.9939(11)	(C ₂ N ₃) ⁻ anion	116
Cu[C(CN) ₃] ₂	Orthorhombic Pmna (53)	7.212(5), 5.452(7), 10.696(7)	[C(CN) ₃] ⁻ anion	76
Mn[C(CN) ₃] ₂	Orthorhombic Pmna (53)	7.742(5), 5.411(6), 10.561(6)	[C(CN) ₃] ⁻ anion	76
Cr[C(CN) ₃] ₂	Orthorhombic Pmna (53)	7.313(1), 5.453(1), 10.640(1)	[C(CN) ₃] ⁻ anion	76
BeCN ₂			Carbide nitride	117
Y ₆ I ₉ C ₂ N	Hexagonal P6 (168)	20.275(2), 13.025(7)	2 octahedral [Y ₁₀ (C ₂) ₂] connected to Y ₆ N ₂ double tetrahedra	37
Y ₇ I ₁₂ C ₂ N	Triclinic P-1 (2)	9.7124(7), 10.3038(7), 16.7353(11),	Y ₆ C ₂ ⁻ octahedra, (Y ₄ N) ⁻	38

		101.366(5), 92.758(5), 112.799(5)	double tetrahedra.	
$\acute{\alpha}$ -La ₄ I ₆ CN	Tetragonal P4 ₂ /mmm (136)	13.953(3), 9.811(3)	La ₆ I ₁₄ C ₂ - octahedra connected to La ₄ N- tetrahedra	37
$\acute{\alpha}$ -Gd ₄ Br ₆ CN	Tetragonal P4 ₂ /mmm (136)	12.719(1), 9.099(6)	Gd ₆ Br ₁₄ C ₂ - octahedra connected to Gd ₄ N- tetrahedra	37
$\acute{\alpha}$ -Gd ₄ I ₆ CN	Tetragonal P4 ₂ /mmm (136)	13.578(1), 9.313(2)	Gd ₆ I ₁₄ C ₂ - octahedra connected to Gd ₄ N- tetrahedra	37
$\hat{\alpha}$ -Gd ₄ I ₆ CN	Hexagonal P6 (168)	40.804(6), 9.232(5)	2 octahedral [Gd ₁₀ (C ₂) ₂] connected to Gd ₆ N ₂ double tetrahedra	37
Ho ₇ I ₁₂ C ₂ N	Triclinic P-1 (2)	9.688(3), 10.287(3), 16.678(5), 101.31(2), 92.78(2), 112.80(1)	Ho ₆ C ₂ - octahedra, (Ho ₄ N)- double tetrahedra.	38

7. List of Publications

[1]. K. Gibson, M. Ströbele, B. Blaschkowski, J. Glaser, M. Weisser, R. Srinivasan, H.-J. Kolb, H.-J. Meyer: Solid State Metathesis Reactions in Various Applications, *Z. Anorg. Allg. Chem.* **2003**, 629, 1863.

[2]. R. Srinivasan, M. Ströbele, H.-J. Meyer: Chains of [RE₆] Octahedra Coupled by (NCN) Links in the Network Structure of RE₂Cl(CN₂)N: Synthesis of Two Novel Rare Earth Chloride Carbodiimide Nitrides with Structures Related to the RE₂Cl₃ Type, *Inorg. Chem.* **2003**, 42, 3406.

[3]. R. Srinivasan, J. Glaser, S. Tragl, H.-J. Meyer: LnCl(CN₂) with Ln = La, Ce, and Pr: Synthesis and Structure of a New Lanthanum Chloride Cyanamide Related to the PbFCl Type Structure, *Z. Anorg. Allg. Chem.* **2004** (in press).

[4]. R. Srinivasan, S. Tragl, H.-J. Meyer: Synthesis and Structure of the new compound La₂O(CN₂)₂ possessing an interchanged anion proportion compared to the parent La₂O₂(CN₂), *Z. Anorg. Allg. Chem.* **2004** (in press).

[5]. R. Srinivasan, S. Tragl, H.-J. Meyer: Synthesis and Crystal Structure of KLa[C(CN)₃]₄•H₂O containing a shielded Potassium Ion, *Z. Anorg. Allg. Chem.* **2004** (in press).

8. Literature

- [1] (a) H. Hartmann, W. Eckelmann, *Z. Anorg. Allg. Chem.* **1948**, 257, 183. (b) H. Hartmann, G. Dobek, *Z. Anorg. Allg. Chem.* **1953**, 271, 138.
- [2] M. Pavlov, N. A. Sokolov, Yu. I. Dergunov, V. G. Golov, *Trudy Khim. i Khim. Tekhnol.*, **1973**, 2, 27.
- [3] N. G. Vannerberg, *Acta Chem. Scand.* **1962**, 16, 2263.
- [4] (a) A. Harper, P. Hubberstey, *J. Chem. Res.(S)* **1989**, 7, 194. (b) M. G. Barker, A. Harper, P. Hubberstey, *J. Chem. Res.(S)* **1978**, 11, 432. (c) M. Becker, J. Nuss, M. Jansen, *Z. Anorg. Allg. Chem.* **2000**, 626, 2505. (d) M. G. Down, M. J. Haley, P. Hubberstey, R. J. Pulham, A. E. Thunder, *J. Chem. Soc., Dalton Trans.* **1978**, 10, 1407. (e) M. G. Down, M. J. Haley, P. Hubberstey, R. J. Pulham, A. E. Thunder, *Chem. Commun.* **1978**, 2, 52. (f) M. Becker, M. Jansen, *Sol. State Sciences.* **2000**, 2, 711.
- [5] U. Berger, W. Schnick, *J. Alloys Comp.* **1994**, 206, 179.
- [6] (a) F. P. Bowden, H. M. Montagu-Pollock, *Nature* **1961**, 191, 556. (b) M. Becker, J. Nuss, M. Jansen, *Z. Naturforsch.* **2000**, 55, 383. (c) K. M. Adams, M. J. Cooper, M. J. Sole, *Acta Crystallogr.* **1964**, 17, 1449. (d) S .K. Deb, A. D. Yoffe, *Trans. Faraday Soc.* **1958**, 55, 106. (e) M. Becker, M. Jansen, *Acta Crystallogr.* **2001**, C57, 347. (f) G. Baldinozzi, B. Malinowska, M. Rakib, G. Durand, *J. Mat. Chem.* **2002**, 12, 268. (g) M. Becker, M. Jansen, *Z. Anorg. Allg. Chem.* **2000**, 626, 1639. (h) X. Liu, P. Müller, P. Kroll, R. Dronskowski, *Inorg. Chem.* **2002**, 41, 4259.
- [7] (a) R. Dronskowski, *Z. Naturforsch.* **1995**, 50, 1245. (b) X. Liu, A. Decker, D. Schmitz, R. Dronskowski, *Z. Anorg. Allg. Chem.* **2000**, 626, 103.
- [8] J. A. Bauer, J.-F. Halet, J.-Y. Saillard, *Coord. Chem. Rev.* **1988**, 178-180, 723.
- [9] R. J. Cava, H. Takagi, H. W. Zandbergen, J. J. Krajewski, W. F. Peck, T. Siegrist, B. Batlogg, R. B. Van Dover, R. J. Fekler, *Nature.* **1994**, 367, 252.
- [10] (a) E. Tominez, E. Alleno, P. Berger, M. Bohn, C. Mazumdar, C. Gordart, *J. Solid. State. Chem.* **2000**, 154, 114. (b) J. F. Halet, J. Y. Saillard, *J. Less-Common Met.* **1990**, 158, 239.

- [11] H. Mattausch, A. Simon, C. Felser, R. Dronskowski, *Angew. Chem.* **1996**, *108*, 1805; *Angew. Chem. Int. Ed. Eng.* **1996**, *35*, 1685.
- [12] B. Blaschkowski, H. Jing, H.-J. Meyer, *Angew. Chem.* **2002**, *114*, 3468; *Angew. Chem. Int. Ed. Eng.* **2002**, *41*, 3322.
- [13] B. Blaschkowski, H.-J. Meyer, *Z. Anorg. Allg. Chem.* **2003**, *629*, 129.
- [14] H. J. Verweel, J. M. Bijvoet, *Z. Kristallogr.* **1938**, *100*, 210.
- [15] (a) P. Andersen, B. Klewe, *Nature* **1963**, *200*, 464. (b) P. Andersen, B. Klewe, E. Thorn, *Acta Chim. Scand.* **1967**, *21*, 1530. (c) J. R. Witt, D. Britton, *Acta Crystallogr.* **1971**, *B27*, 1835.
- [16] (a) I. Elisabeth, J. Barbara, W. Schnick, *Chem. Eur. J.* **2001**, *7(24)*, 5372. (b) P. Starynowicz, *Acta Crystallogr.* **1991**, *C47(10)*, 2198. (c) B. Juergens, W. Milius, P. Morys, W. Schnick, *Z. Anorg. Allg. Chem.* **1998**, *624(1)*, 91.
- [17] P. R. Subrayan, A. H. Anthony, J. W. Kampf, P. G. Rasmussen, *Chem. Mater.* **1995**, *7*, 2213.
- [18] B. Juergens, E. Irran, J. Schneider, W. Schnick, *Inorg. Chem.* **2000**, *39*, 665.
- [19] (a) J. L. Manson, C. R. Kmety, Q. Z. Huang, J. W. Lynn, G. M. Bendele, S. Pagola, P. W. Stephens, L. M. Liable-sands, A. L. Rheingold, A. J. Epstein, J. S. Miller, *Chem. Mater.* **1998**, *10*, 2552. (b) S. R. Batten, P. Jensen, B. Moubaraki, K. S. Murray R. Robson, *Chem. Commun* **1998**, 439.
- [20] O Reckeweg, **1999**, Universität Tübingen, Dissertation No. 1331.
- [21] B. Blaschkowski, **2003**, Universität Tübingen, Dissertation No. 1604.
- [22] L. Denner, P. Luger, J. Buschmann, *Acta Cryst.* **1988**, *C44*, 1979.
- [23] O. Lichtenberger, J. Woltersdorf, N. Hering, R. Riedel, *Z. Anorg. Allg. Chem.* **2000**, *626*, 1881.
- [24] A. Williams, I. T. Ibrahim, *Chem. Rev.* **1981**, *81*, 589.
- [25] T. Schimzu, N. Sehi, H. Taka, N. Kamigata, *J. Org. Chem.* **1996**, *61*, 6013.

- [26] J. Pump, E. G. Rochow, *Z. Anorg. Allg. Chem.* **1964**, 330, 101.
- [27] A. Kienzle, A. Obermeyer, R. Riedel, F. Aldinger, A. Simon, *Chem. Ber.* **1993**, 126, 2569.
- [28] (a) X. Liu, P. Kroll, R. Dronskowski, *Z. Anorg. Allg. Chem.* **2001**, 627, 1682. (b) R. Dronskowski, X. Liu, *Z. Kristallogr.* **2002**, 217, 118.
- [29] O. Reckeweg, F. J. DiSalvo, *Angew. Chem.* **2000**, 112, 397; *Angew. Chem. Int. Ed. Eng.* **2000**, 39, 412.
- [30] R. Riedel, A. Greiner, G. Miehe, W. Dreßler, H. Fueß, J. Bill, F. Aldinger, *Angew. Chem.* **1997**, 109, 657; *Angew. Chem. Int. Ed.* **1997**, 36, 603.
- [31] X. Liu, R. Dronskowski, *Z. Naturforsch.* **2002**, 57, 1108.
- [32] O. Reckeweg, F. J. DiSalvo, *Z. Anorg. Allg. Chem.* **2003**, 629, 177.
- [33] W. Liao, C. Hu, R. Kremer, R. Dronskowski, *Inorg. Chem.* **2004**, 43, 5884.
- [34] (a) M. S. Zaworotko, *Chem. Commun.* **2001**, 1, . (b) B. Holliday, C. Mirkin, *Angew. Chem. Int. Ed.* **2001**, 40, 2022. (c) A. K. Cheetham, G. Ferey, T. Loiseau, *Angew. Chem. Int. Ed.* **1999**, 38, 3268.
- [35] (a) Y. Hashimoto, M. Takahashi, S. Kikkawa, F. Kanamaru, *J. Solid State Chem.* **1995**, 114, 592. (b) Y. Hashimoto, M. Takahashi, S. Kikkawa, F. Kanamaru, *Chem. Lett.* **1994**, 10, 1963. (c) Y. Hashimoto, M. Takahashi, S. Kikkawa, F. Kanamaru, *J. Solid State Chem.* **1996**, 125, 37.
- [36] (a) E. Säilynoja, M. Lastusaari, J. Hölsä, P. Porcher, *J. Luminescence* **1997**, 72-74, 210. (b) J. Hölsä, R. -J. Lamminmäki, M. Lastusaari, E. Säilynoja, P. Porcher, *Spectrochim. Acta* **1998**, A(54), 2065. (c) M. Takahashi, Y. Hashimoto, S. Kikkawa, H. Kobayashi, *Zairyo*, **2000**, 49, 1230.
- [37] H. Mattausch, H. Borrmann, R. Eger, R. K. Kremer, A. Simon, *Z. Anorg. Allg. Chem.* **1994**, 620, 1889.
- [38] H. Mattausch, H. Borrmann, R. Eger, R. K. Kremer, A. Simon, *Z. Naturforsch.* **1995**, 50b, 931.

- [39] A. Perret, A.M. Krawczynski, *Helv. Chim. Acta* **1932**, *15*, 1009.
- [40] (a) J. L. O'Loughlin, C. H. Wallace, M. S. Knox, R. B. Kaner, *Inorg. Chem.* **2001**, *40*, 2240. (b) E. G. Gillan, R. B. Kaner, *Chem. Mat.* **1996**, *8*, 333. (c) I. P. Parkin, *Chem. Soc. Rev.* **1996**, *25*, 199. (d) E. G. Gillan, R. B. Kaner, *Inorg. Chem.* **1994**, *33*, 5693. (e) I. P. Parkin, A. M. Nartowski, *Polyhedron* **1998**, *17*, 2617.
- [41] H. Jing, B. Blaschkowski, H. -J. Meyer, *Z. Anorg. Allg. Chem.* **2002**, *628*, 1955.
- [42] G. M. Sheldrick, SHELX-97, Univ-Göttingen, **1997**.
- [43] A. Altomare, M.C. Burla, M. Camalli, G. Cascarano, C. Giacovazzo, A. Guagliardi, A.G.G. Moliterni, R. Rizzi, EXPO: a program for full powder pattern decomposition and crystal structure solution, *J. Appl. Crystallogr.* **1998**, *32*, 339
- [44] T. Roisnel, J. Rodríguez-Carvajal, WinPLOTR: a Windows tool for powder diffraction patterns analysis, Materials Science Forum, Proceedings of the Seventh European Powder Diffraction Conference (EPDIC 7), Barcelona, Eds. R. Delhez and E.J. Mittemeijer **2000**, 118.
- [45] (a) G. Meyer,; P. Ax, *Mat. Res. Bull.* **1986**, *17*, 1447. (b) G. Meyer, T. Staffel, S. Doetsch, T. Schleid, *Inorg. Chem.* **1985**, *24*, 3504. (c) G. Meyer, *Inorg. Synth.* **1989**, *25* 146. (d) F. L. Carter, J. F. Murray, *Mat. Res. Bull.* **1972**, *7*, 519. (e) G. Meyer, L. R. Morss, *Synthesis of Lanthanide and Actinide Compounds*, **1990**, Kluwer Academic Publishers.
- [46] (a) H. Gunsilius, W. Urland, R. Kremer, *Z. Anorg. Allg. Chem.* **1987**, *550*, 35. (b) Z. C. Wang, L. S. Wang, *Inorg. Chem.* **1997**, *36*, 1536. (c) G. N. Papatheodorou, G. H. Kucera, *Inorg. Chem.* **1979**, *18*, 385. (d) D. Hake, W. Urland, *Z. Anorg. Allg. Chem.* **1990**, *586*, 99.
- [47] (a) G. Meyer, S. Doetsch, T. Staffel, *J. Less-Com. Met.* **1987**, *127*, 155. (b) D. Hake, W. Urland, *Z. Anorg. Allg. Chem.* **1992**, *613*, 45. (c) M. Schulze, W. Urland, *Eur. J. Solid State Inorg. Chem.* **1991**, *28*, 571.
- [48] (a) M. D. Taylor, C. P. Carter, *J. Inorg. Nucl. Chem.* **1962**, *24*, 387. (b) F. L. Carter, J. F. Murray, *Mat. Res. Bull.* **1972**, *7*, 519.
- [49] H. Jing, H.-J. Meyer, *Z. Anorg. Allg. Chem.* **2002**, *628*, 1548.

- [50] S. Uhrlandt, G. Meyer, *J. Alloys Comp.* **1995**, 225, 171.
- [51] K. Gibson, M. Ströbele, B. Blaschkowski, J. Glaser, M. Weisser, R. Srinivasan, H.-J. Kolb, H.-J. Meyer, *Z. Anorg. Allg. Chem.* **2003**, 629, 10, 1863.
- [52] A. L. Hector, I. P. Parkin, *Chem. Mater.* **1995**, 7, 1728.
- [53] R. Srinivasan, J. Glaser, S. Tragl, H. -J. Meyer, *Z. Anorg. Allg. Chem.* **2004** (in press).
- [54] E. Korin, L. J. Soifer, *J. Thermal Analysis* **1997**, 50, 3, 347.
- [55] R. Srinivasan, M. Ströbele, H. -J. Meyer, *Inorg. Chem.* **2003**, 42, 3406.
- [56] O. Reckeweg, A. Simon, *Z. Naturforsch.* **2003**, 58, 1097.
- [57] (a) D. H. Templeton, C. H. Dauben, *J. Am. Chem. Soc.* **1953**, 75, 6069. (b) G. Meyer, T. Schleid, *Z. Anorg. Allg. Chem.* **1986**, 533, 181. (c) H. Haeuseler, M. Jung, *Mat. Res. Bull.* **1986**, 21, 1291. (d) I. Mayer, S. Zolotov, F. Kassierer, *Inorg. Chem.* **1965**, 4, 1637.
- [58] (a) T. Schleid, H. Grossholz, *Z. Anorg. Allg. Chem.* **2001**, 627, 2693. (b) T. Schleid, *Z. Anorg. Allg. Chem.* **1999**, 625, 1700. (c) T. Schleid, *Z. Anorg. Allg. Chem.* **2000**, 626, 2429.
- [59] T. Schleid, H. Z. Grossholz, *Z. Anorg. Allg. Chem.* **2002**, 628, 1012.
- [60] J. M. Haschke, *Inorg. Chem.* **1974**, 13, 1812.
- [61] L. G. Sillén, *Z. Anorg. Allg. Chem.* **1939**, 242, 41.
- [62] L. G. Sillén, *Svensk. Kem. Tidskr.* **1941**, 53, 39.
- [63] (a) W. Nieuwenkamp, J. M. Bijvoet, *Z. Kristallogr.* **1932**, 82, 157. (b) W. Nieuwenkamp, J. M. Bijvoet, *Z. Kristallogr.* **1932**, 81, 469.
- [64] E. Garcia, J. D. Corbett, J. E. Ford, W. J. Vary, *Inorg. Chem.* **1985**, 24, 494.
- [65] Hj. Mattausch, A. Simon, *Z. Kristallogr.* **1996**, 211, 398.
- [66] Hj. Mattausch, J. B. Hendricks, R. Eger, J. D. Corbett, A. Simon, *Inorg. Chem.* **1980**, 19, 2128.
- [67] H.-J. Meyer, N. N. Jones, J. D. Corbett, *Inorg. Chem.* **1990**, 28, 2635.

- [68] R. D. Shannon, *Acta Cryst.* **1976**, A32, 751.
- [69] R. L. Collin, *Acta Cryst.* **1952**, A5, 431. (b) B. Vonnegut, B. E. Warren, *J. Am. Chem. Soc.* **1936**, 58, 2459. (c) O. Shimomura, K. Takemura, Y. Fujii, S. Minomura, *Phys. Rev.* **1978**, B18, 715.
- [70] G. A. Landrum, R. Dronskowski, R. Niewa, F. DiSalvo, *Chem. Eur. J.* **1999**, 5, 515.
- [71] Y. Gu, L. Chen, L. Shi, J. Ma, Z. Yang, Y. Qian, *Carbon* **2003**, 41, 13, 2674.
- [72] R. Srinivasan, S. Tragl, H.-J. Meyer, *Z. Anorg. Allg. Chem.* **2004** (in press).
- [73] (a) J. Kohout, L. Jaeger, M. Hvastijova, J. Kozisek, *J. Coord. Chem.* **2000**, 51, 169. (b) J. Malecka, A. Kochel, J. Mrozinski, *Materials Science* **2002**, 20, 91.
- [74] (a) P. Andersen, B. Klewe, *Nature* **1963**, 200, 464. (b) P. Andersen, B. Klewe, E. Thorn, *Acta Chim. Scand.* **1967**, 21, 1530. (c) J. R. Witt, D. Britton, *Acta Crystallogr.* **1971**, B27, 1835.
- [75] J. Konnert, D. Britton, *Inorg. Chem.* **1966**, 5, 1193.
- [76] (a) J. L. Manson, E. Ressouche, J. S. Miller, *Inorg. Chem.* **2000**, 39, 1135. (b) J. L. Manson, C. Campana, J. S. Miller, *Chem. Commun.* **1998**, 2, 251. (c) R. Feyerherm, A. Loose, S. Landsgesell, J. L. Manson, *Inorg. Chem.* **2004**, 43, 6633. (d) P. Jensen, D. J. Price, S. R. Batten, B. Moubaraki, K. S. Murray, *Chem-Eur. J.* **2000**, 6, 3186. (e) H. Hoshino, K. Iida, T. Kawamoto, T. Mori, *Inorg. Chem.* **1999**, 38, 4229. (f) S. R. Batten, B. F. Hoskins, R. Robson, *Inorg. Chem.* **1998**, 37, 3432. (g) S. R. Batten, B. F. Hoskins, R. Robson, *Chem. Commun.* **1991**, 6, 445. (h) K. Brodersen, J. Hofmann, *Z. Anorg. Allg. Chem.* **1992**, 609, 29. (i) M. Hvastijova, J. Kohout, J. Kozisek, L. Jaeger, J. Mrozinski, *Z. Anorg. Allg. Chem.* **1998**, 624, 349.
- [77] V. V. Skopenko, A. A. Kapshuk, *Ukr. Khim. Zh.* **1979**, 45, 920.
- [78] Y. Morioka, K. Toriumi, T. Ito, A. Saito, I. Nakagawa, *J. Phys. Soc. Japan* **1985**, 54, 2184, and literature referenced therein.
- [79] H. Jing, B. Blaschkowski, H.-J. Meyer, *Z. Anorg. Allg. Chem.* **2002**, 628, 1955.
- [80] E. Garcia, J. D. Corbett, J. E. Ford, W. J. Vary, *Inorg. Chem.*, **1985**, 24, 4, 494.

- [81] S. Finklea, L. Cathey, E. Amma, *Acta Cryst.* **1976**, A32, 529.
- [82] (a) H. Bärnighausen, *Angew. Chem.* **1963**, 75, 1109. (b) H. Bärnighausen, G. Brauer, N. Schultz, *Z. Anorg. Allg. Chem.* **1965**, 338, 250. (c) J. Strähle, *Z. Anorg. Allg. Chem.* **1973**, 402, 47.
- [83] A. F. Wells, "Structural Inorganic Chemistry", 5th ed. pp. 1271-1272. Clarendon Press, Oxford, 1984.
- [84] H. A. Eick, *Acta Crystallogr.* **1960**, 13, 161.
- [85] R. Ballestracci, C. R. Seances, *Acad. Sci. Ser.* **1967**, B264, 1736.
- [86] J. O. Sawyer, P. Caro, L. Eyring, *Monatsh. Chem.* **1971**, 102, 333.
- [87] S. Finklea, L. Cathey, E. Amma, *Acta Cryst.* **1976**, A32, 529.
- [88] R. Niewa, P. Hohn, R. Kniep, A. Weiske, H. Jacobs, *Z. Kristallogr.* **2001**, 216, 335.
- [89] M. Becker, M. Jansen, *J. Chem. Res.(S)*. **1998**, 2, 86.
- [90] B. Jurgens, W. Milius, P. Morys, W. Schnick, *Z. Anorg. Allg. Chem.* **1998**, 624, 1, 91.
- [91] W. Schnick, H. Huppertz, *Z. Anorg. Allg. Chem.* **1995**, 621, 10, 1703.
- [92] M. Becker, M. Jansen, A. Lieb, W. Milius, W. Schnick, *Z. Anorg. Allg. Chem.* **1998**, 624, 1, 113.
- [93] I. Elisabeth; B. Jurgens, W. Schnick, *Solid State Sciences* **2002**, 4, 10, 1305.
- [94] M. Becker, M. Jansen, *Z. Naturforsch.* **1999**, 54, 11, 1375.
- [95] B. Jurgens, H. A. Hoppe, W. Schnick, *Z. Anorg. Allg. Chem.* **2004**, 630, 1, 35.
- [96] P. Hohn, R. Niewa, R. Kniep, *Z. Kristallogr.* **2000**, 215, 3, 323.
- [97] (a) B. Wißmann, **2001**, Universität Tübingen, Dissertation No. 1496. (b) W. Liao, R. Dronskowski, *Acta Cryst.* **2004**, E60, 10, 124.
- [98] R. Niewa, R. Kniep, *Z. Kristallogr.* **2000**, NCS 215, 323.

- [99] U. Berger, W. Milius, W. Schnick, *Z. Anorg. Allg. Chem.* **1995**, 621, 12, 2075.
- [100] U. Berger, W. Schnick, *Z. Naturforsch.* **1996**, 51, 1, 1.
- [101] O. Reckeweg, F. J. DiSalvo, *Z. Naturforsch.* **2003**, 58, 201.
- [102] P. Höhn, R. Kniep, *Z. Anorg. Allg. Chem.* **2002**, 628, 2173.
- [103] M. Jansen, H. Juengermann, *Z. Kristallogr.* **1994**, 209, 9, 779.
- [104] A. Obermeyer, A. Kienzle, J. Weidlein, R. Riedel, A. Simon, *Z. Anorg. Allg. Chem.* **1994**, 620, 8, 1357.
- [105] M. Dahrouch, M. Riviere-Baudet, J. Satge, M. Mauzac, C. J. Cardin, J. H. Thorpe, *Organometallics*, **1998**, 17, 4, 623.
- [106] G. Rajca, W. Schwarz, J. Weidlein, *Z. Naturforsch.* **1984**, 39B, 9, 1219.
- [107] R. Srinivasan, S. Tragl, H.-J. Meyer, *Z. Anorg. Allg. Chem.* **2004** (in press).
- [108] W. Liao, J. V. Appen, R. Dronskowski, *Chem. Commun.* **2004**, 20, 2302.
- [109] E. Hughes, *J. Am. Chem. Soc.* **1940**, 62, 1258.
- [110] B. Jurgens, H. Hoppe, E. Irran, W. Schnick, *Inorg. Chem.* **2002**, 41, 19, 4849.
- [111] B. Jurgens, E. Irran, W. Schnick, *J. Solid State Chem.* **2001**, 157, 2, 241.
- [112] D. Britton, Y. M. Chow, *Acta Crystallogr.* **1977**, B33, 3, 697.
- [113] D. Britton, *Acta Crystallogr.* **1990**, C46, 12, 2297.
- [114] M. L. Jamie, D. W. Lee, A.L. Rheingold, J. S. Miller, *Inorg. Chem.* **1998**, 37, 23, 5966.
- [115] B. Jurgens, E. Irran, H. Hoppe, W. Schnick, *Z. Anorg. Allg. Chem.* **2004**, 630, 2, 219.
- [116] B. Jurgens, H. Hoppe, W. Schnick, *Solid State Sciences* **2002**, 4, 6, 821.
- [117] A. G. Petukhov, W. R. L. Lambrecht, B. Segall, *Phy. Rev.* **1994**, 49, 7, 4549.

Meine akademischen Lehrer waren:

N. S. Subramanian, D. Jeyakar Chellaraj, T. Venkatachalam, E. R. Chelladurai, Rajendran, Princie Merlin, S. Rajam, S. Lydia, N. Prabavathy, S. Padmavathi, N. Balasubramanian.

T. V. Antony, S. Paulraj, S. Peter, N. Mathiyalagan, S. Durairaj, N. Xavier, K. V. Raman, S. Raja, S.J. Selvaraj, J. Rosario.

R. Manoharan, G. A. Pathenjali, B. Krishnamoorthy, B. R. Jagirdar.

H.-J. Meyer, J. Strähle, E. Schweda, L. Wesemann, B. Speiser, H. Oberhammer.

Lebenslauf

Radhakrishnan Srinivasan, geboren am 19. Februar 1977 in Trichy, Süd Indien

Staatsangehörigkeit	indisch
Familienstand	ledig
Eltern	Venkatraman Radhakrishnan Radhakrishnan Annapoorani

Schulbildung

Juni 1982 - Sri Bala Gurukulam Middle School, Srirangam, Indien.
April 1987 (Grundschule, Classes I - V)

Juni 1987 - E. R. Hr. Sec. School, Trichy, Indien.
März 1994 (Gymnasium, Classes VI - XII)

Hochschulausbildung

1994 - 1997 Studium der Chemie, Physik, und Mathematik an der
Bharathidasan University (Bishop Heber College), Trichy,
Indien.

April 1997 Bachelor of Science (Zwischenprüfung, Hauptfach: Chemie).

1997 - 1999 Studium der Chemie, Bharathidasan University (St. Joseph's
College), Trichy, Indien.

April 1999 Master of Science (Abschlußprüfung, Fach: Chemie).

Juni 1999 - Research Assistant, Department of Inorganic and Physical
April 2001 Chemistry, Indian Institute of Science, Bangalore.

Juni 2001 - Anfertigung einer Dissertation am Institut für Anorganische
Dezember 2004 Chemie, Universität Tübingen zum Thema: „Synthesen,
Strukturen und Reaktionswege von C–N-haltigen Lanthanoid-
Verbindungen“ unter der Anleitung von Prof. Dr. H.-Jürgen
Meyer.